Modeling, Simulation and Performance Evaluation of Parabolic Trough Solar Collector Power Generation System

By

Mekuannint Mesfin

A thesis submitted to the School of Graduate Studies of Addis Ababa University in partial fulfillment of the requirements of the Degree of Masters of Science in Mechanical Engineering (Thermal Engineering Stream)

Advisor

Dr.-Ing. Abebayehu Assefa

Department of Mechanical Engineering

Addis Ababa University

September 2009

Abstract

Parabolic troughs are one of the low cost solar electric power options available today and have significant potential for further cost reduction. Parabolic trough power plants use concentrated sunlight, in place of fossil fuels, to provide the thermal energy required to drive a conventional power plant. These plants use a large field of parabolic trough collectors which track the sun during the day and concentrate the solar radiation on a receiver tube located at the focus of the parabolic shaped mirrors. A heat transfer fluid passes through the receiver and is heated to temperatures required to generate steam and drive a conventional Rankine cycle steam power plant.

In this thesis paper model of a parabolic trough power plant, taking into consideration the different losses associated with collection of the solar irradiance and other thermal losses is presented. MATLAB software is used to model the power plant at reference state and TRNSYS software is used to simulate the performance of the model at off design weather conditions.

MATLAB modeling of the power plant is used to find the different reference values which are used as inputs for the TRNSYS modeling and simulation of the power plant. The reference values include the solar field area, the heat transfer fluid (HTF) and steam/water mass flow rates, overall heat transfer coefficients of the different heat exchangers, etc.

The TRNSYS modeling and simulation are used to determine the net power, initial steam temperature, the inlet and outlet heat transfer fluid temperatures out of the solar field and steam and HTF mass flow rates in hourly basis for representative days of year 2001.

The cost and financial analysis is made for the power plant. Solar Advisor Model is used to make this analysis under Addis Ababa weather condition. This analysis is used to determine the different costs associated with the power plant. The cash flow for the 30 years of operation of the power plant is also shown.

Acknowledgments

I am very grateful to my advisor Dr.-Ing. Abebayehu Assefa for sharing his time and providing valuable comments and suggestions during this thesis paper. Without his valuable comments and encouragements this paper would not have been complete in time.

I am also grateful to my family and friends for their support and concern which fills me with extra motivation and energy.

TABLE OF CONTENTS

CHAPTER 5

COST AND FINANCIAL ANALYSIS OF THE POWER PLANT 95

List of Figures

List of Tables

Nomenclature

a	Accommodation coefficient of annulus gas
A	Coefficient
A_{eff}	Solar field aperture area [m^2]
b	Interaction coefficient of annulus gas
B	Coefficient
C	Coefficient
C, m, n	Constants
$\dot{C}_c$	Capacitance rate of the cold side fluid (steam) [kW/K]
$\dot{C}_H$	Capacitance rate of the hot side fluid (HTF) [kW/K]
C_{min}	The smaller capacitance rate between the steam and the HTF [kW/K]
C_{max}	The bigger capacitance rate between the steam and the HTF [kW/K]
$C_{p,HTF}$	Average specific heat of HTF between inlet and outlet [kJ/kg-K]
$C_{p,steam}$	Average specific heat of steam between inlet and outlet [kJ/kg-K]
C_r	The ratio of C_{min} to C_{max}
D	Coefficient
D_2	Inside diameter of absorber pipe [m]
D_3	Outside diameter of absorber pipe [m]
D_4	Inside diameter of glass envelope [m]
D_5	Outside diameter of glass envelope [m]
D_h	Hydraulic diameter of absorber pipe [m]
D_{HCE}	Diameter of the steel absorber tube [m]
E	Equation of time E (in minutes)
EFF	Effectiveness
EXP_UA	Power law exponent to UA
f	Focal length [m]
$FLBI$	Condensate inlet mass flow rate [kg/s]
$FLBO$	Hot side outlet flow rate [kg/s]
$FLCI$	Cold side inlet flow rate [kg/s]

FLCO	Cold side outlet flow rate [kg/s]
FLHDM	Demanded hot inlet flow rate [kg/s]
FLWREF	Cold side reference flow rate [kg/s]
FPL	Florida power & light company
g	Gravitational constant, 9.81 [m/s^2]
h_{12}	Convection heat transfer coefficient between the HTF and the inside of absorber tube [W/m^2-K]
h_{34}	Convection heat transfer coefficient of annulus gas at T_{34} [W/m^2-K]
h_{56}	Convection heat transfer coefficient of air at T_{56} [W/m^2-K]
$h_{Feedwater}$	Enthalpy of the feedwater [kJ/kg]
h_{HTF}	Enthalpy of HTF [kJ/kg]
h_{steam}	Enthalpy of steam [kJ/kg]
HBI	Condensate inlet enthalpy [kJ/kg]
HBO	Hot side outlet enthalpy [kJ/kg]
HHI	Hot side inlet enthalpy [kJ/kg]
I_{ext}	Extraterrestrial radiation [W/m^2]
I_{sc}	Solar constant [W/m^2]
K	Incident angle modifier
k_1	Thermal conductance of HTF at T_1 [W/m-K]
k_{23}	Thermal conductance of absorber wall at T_{23} [W/m-K]
k_{34}	Thermal conductance of annulus gas at T_{34} [W/m-K]
k_{56}	Thermal conductance of air at T56 [W/m-K]
k_{std}	Thermal conductance of annulus gas at standard temperature and pressure [W/m.K]
L_{LOC}	The longitude of the location in question [^{o}]
L_{SCA}	Length of one solar collector assembly loop [m]
$L_{spacing}$	Distance between the collector rows [m]
L_{ST}	The standard meridian for the local time zone [^{o}]
M_{SF}	Mass of the HTF in the solar field [kg/s]
$\dot{m}_{steam,HTF}$	Mass flow rate of steam, HTF [kg/s]
n	Number of feedwater heaters

N	Day of the year
N_{SCA}	Number of SCA loops in the solar field
$\overline{Nu}_{D2}$	Nusselt number of HTF based on D_2
$\overline{Nu}_{D5}$	Nusselt number of air based on D_5
Pa	Annulus gas pressure [mmHg]
Pr_1	Prandtl number of HTF evaluated at T_1
Pr_2	Prandtl number of HTF evaluated at T_2
Pr_{34}	Prandtl number of annulus gas at T_{34}
Pr_5	Prandtl number of air at T_5
Pr_{56}	Prandtl number for air at T_{56}
Pr_6	Prandtl number of air at T_6
PFW	Cold side inlet pressure
PHI	Hot side inlet pressure
$\dot{q}'_{12}$	Convection heat transfer rate between the heat transfer fluid and inside wall of the absorber pipe per unit receiver length [W/m]
$\dot{q}'_{23cond}$	Conduction heat transfer rate through the absorber pipe wall per unit receiver length [W/m]
$\dot{q}'_{34conv}$	Convection heat transfer rate between the outer surface of the absorber pipe to the inner surface of the glass envelope per unit receiver length [W/m]
$\dot{q}'_{34rad}$	Radiation heat transfer rate between the outer surface of the absorber pipe to the inner surface of the glass envelope per unit receiver length [W/m]
$\dot{q}'_{45cond}$	Conduction heat transfer rate through the glass envelope per unit receiver length [W/m]
$\dot{q}'_{56conv}$	Convection heat transfer rate between the outer surface of the glass envelope to the atmosphere per unit receiver length [W/m]
$\dot{q}'_{57rad}$	Radiation heat transfer rate between the outer surface of the glass envelope to the sky per unit receiver length [W/m]
$\dot{Q}$	Actual heat transfer between HTF and steam/water [W]

$\dot{Q}_{abs}$	Absorbed energy [W]
$\dot{Q}_{dot}$	Transferred power [W]
$\dot{Q}_{Expansionvessel}$	Expansion vessel heat losses [W]
$\dot{Q}_{\max}$	Maximum heat transfer between HTF and steam/water [W]
$\dot{Q}_{pipe}$	Piping system and expansion vessel heat losses [W]
$\dot{Q}_{piping}$	Piping system heat losses [W]
$\dot{Q}_{net}$	Net heat transfer between HTF and steam/water [W]
Ra_{D3}	Rayleigh number of annulus gas based on D_3
Ra_{D4}	Rayleigh number of annulus gas based on D_4
Ra_{D5}	Rayleigh number of air based on D_5
Re_{D2}	Reynolds number of HTF based on D_2
Re_{D5}	Reynolds number of air based on D_5
T_1	Mean (bulk) temperature of the HTF [^{o}C]
T_2	Absorber pipe inner surface temperature [^{o}C]
T_{23}	Average absorber wall temperature, (T2 + T3)/2 [^{o}C]
T_3	Absorber pipe outer surface temperature [^{o}C]
T_{34}	Average temperature of annulus gas, (T_3+T_4)/2 [^{o}C]
T_4	Glass envelope inner surface temperature [^{o}C]
T_5	Glass envelope outer surface temperature [^{o}C]
T_{56}	Average temperature of air, (T_5 + T_6)/2 [^{o}C]
T_6	Atmosphere temperature [^{o}C]
T_7	Estimated effective sky temperature [^{o}C]
T_{amb}	Ambient temperature [^{o}C]
T_{avg}	Average temperature of the HTF in the solar field [^{o}C]
T_B	Saturation temperature of the boiler [^{o}C]
T_C	Condenser temperature [^{o}C]

TCI	Cold side inlet temperature [^oC]
TCO	Cold side outlet temperature [^oC]
$T_{Deaerator}$	Temperature of the Deaerator [^oC]
$T_{Hpheater\_1}$	Temperature of the high pressure CFWH one [^oC]
$T_{Hpheater\_2}$	Temperature of the high pressure CFWH two [^oC]
$T_{Hpheater\_1}$	Temperature of the high pressure CFWH one [^oC]
T_{HTF}	Temperature of the HTF [^oC]
$T_{Lpheater}$	Low pressure preheater temperature [^oC]
T_{SAT}	Hot side outlet temperature [^oC]
T_{steam}	Temperature of the steam [^oC]
UA	Overall heat transfer coefficient [W/K]
UA_{REF}	Reference overall heat transfer coefficient [W/K]
W	Collector aperture width [m]

Acronyms:

CF	Capacity factor
CFWH	Closed feedwater heater
CL	Cleanness
CPC	Cold side specific capacity
CR	Clean reflectivity
CSP	Concentrating solar power
DNI	Direct normal insolation [W/m^2]
DSCR	Debt service coverage ratio
EL	End loss
EPW	Energy plus weather
HCE	Heat collecting elements
HTF	Heat transfer fluid
IOU	Investor owned utility
IPP	Independent power producer
IRR	Internal rate of return
ITC	Investment tax credit

LCOE	Levilized cost of energy [$/kWh]
MACRS	Modified accelerated cost recovery system
NIP	Normal incidence Pyrheliometer
NPV	Net present value
NTU	Number of transfer units
PPA	Power purchase agreement
PTSEGS	Parabolic trough solar electrics generation systems
RS	Row shading
SAM	Solar advisor model
SCA	Solar collecting assembly
SEGS	Solar electric generation systems
TES	Thermal energy storage
TMY	Typical Metrological Year
WACC	Weighted average cost of capital
WS	Wind speed [m/s]

Greek Letters:

α	Solar altitude angle [^{o}]
α_1	Thermal diffusivity of HTF [m^2/s]
α_{56}	Thermal diffusivity of air at T_{56} [m^2/s]
β	Volumetric thermal expansion coefficient [1/K]
γ	Solar azimuth angle [^{o}]
γ	Ratio of Specific heats for the annulus gas
δ	Declination angle [^{o}]
ΔT	Average fluid temperature [^{O}C]
$\Delta T_{in}, \Delta T_{out}$	Difference between inlet and outlet temperature of the HTF from the solar field and ambient temperature [^{O}C]
ΔT_{opt}	Optimum temperature difference between CFWHs [^{O}C]
ε	Effectiveness
ε_3	Emissivity of absorber selective coating

ε_4	Emissivity of inner surface of glass envelope
ε_{45}	Emissivity of outer surface of glass envelope
η	Efficiency [%]
η_{SF}	Efficiency of the solar field [%]
η_{SF}	Efficiency of the solar field [%]
η_{pump}	Isentropic Efficiency of the pump [%]
$\eta_{turbine}$	Isentropic Efficiency of the turbine [%]
θ	Incidence angle [^{o}]
θ_Z	Solar zenith angle [^{o}]
λ	Mean free-path between collisions of a molecule [cm]
ν_1	Kinematic viscosity of the HTF [m^2/s]
ν_{56}	Kinematic viscosity of air at T_{56} [m^2/s]
ρ	Density [kg/m^3]
σ	Stefan-Boltzman constant [$W/m^2\text{-}K^4$]
ϕ	Altitude angle [^{o}]
ω	The hour angle [^{o}]

CHAPTER 1

INTRODUCTION

Parabolic troughs are currently the most used means of power generation option of solar sources. Solar electric generation systems (SEGS) employ solar collectors to track the sun and use its energy to produce steam. These plants replace the boiler part of a conventional Rankine Cycle power plant with solar fields that are used to increase the temperature of HTFs (heat transfer fluids). The solar field area must however be wide enough to satisfy the power demand. Heat exchangers are used to transfer heat energy from the HTF to steam coming from the feedwater heaters.

To date, all SEGS are hybrid solar/fossil plants. The power plants have a backup fossil-fired capability that can be used to supplement the solar output during periods of low solar radiation. The fossil backup can also be used to produce rated electric output during overcast or nighttime periods.

1.1 Current Status of the SEGS Plants

Nine solar power plants in Mojave Desert, California, where insolation is among the best available in the United States are built from1984 to 1991. FPL (Florida Power & Light Company) Energy operates and partially owns the plants. SEGS III–VII (150 MW) are located at Kramer Junction, SEGS VIII–IX (160 MW) at Harper Lake, and SEGS I–II (44 MW) at Daggett respectively.

The plants altogether have a 354 MW installed capacity, making them the largest installation of solar plants of any kind in the world. By comparison, the largest photovoltaic plant, which is in Spain, produces 60 MW, although a 62 MW PV installation (Moura photovoltaic power station) is under construction in Portugal and a 154 MW PV Solar power station in Victoria, Australia, is planned. The average gross solar output for all nine plants at SEGS is around 75 MWe a capacity factor of 21%. In addition, the turbines can be utilized at night by burning natural gas.

FPL claims that the solar plants power 232,500 homes and displace 3,800 tons of pollution per year that would have been produced if the electricity had been provided by fossil fuels.

The facilities have a total of 936,384 mirrors and cover more than 1,600 acres (6.5 km^2). Lined up, the parabolic mirrors would extend over 229 miles (370 km).

The SEGS power plants were built by Luz Industries, and commissioned between 1984 and 1991. Kramer Junction employs about 95 people and 45 people work at Harper Lake [26].

Table 1-1 Characteristics of SEGS I through IX [24]

SEGS Plant	1st Year of Operation	Net Output (MWe)	Solar Field Outlet Temp. (ºC)	Solar Field Area (m^2)	Solar Turbine Eff. (%)	Fossil Turbine Eff. (%)	Annual Output (MWh)
I	1985	13.8	307	82,960	31.5	-	30,100
II	1986	30	316	190,338	29.4	37.3	80,500
III & IV	1987	30	349	230,300	30.6	37.4	92,780
V	1988	30	349	250,500	30.6	37.4	91,820
VI	1989	30	390	188,000	37.5	39.5	90,850
VII	1989	30	390	194,280	37.5	39.5	92,646
VIII	1990	80	390	464,340	37.6	37.6	252,750
IX	1991	80	390	483,960	37.6	37.6	256,125

1.2 Benefits of SEGS plants

SEGS have a benefit of providing lowest cost source of solar generated electricity available. The plants are expected to continue to be the least-cost solar option for another 5-10 years depending on the rate of development and acceptance of other solar technologies.

SEGS provide peak power at daytime when the demand is high. Integrated natural gas hybridization and thermal storage have allowed the plants to provide firm power even during non-solar and cloudy periods.

SEGS plants reduce operation of higher-cost, cycling fossil generation that would be needed to meet peak power demands during sunny afternoons at times when the most photochemical smog, which is aggravated by NO_x emissions from power plants, is produced.

The construction and operation of trough plants typically have a positive impact on the local economy. A large portion of material during construction can generally be supplied locally. Also trough plants tend to be fairly labor-intensive during both construction and operation, and much of this labor can generally be drawn from local labor markets [24].

1.3 Problem with SEGs plants

Despite its many benefits, solar thermal power is still employed on a very limited basis. The technology is still relatively new, and there are disadvantages to solar thermal power that have delayed its growth. Primarily, the efficiency of these plants is relatively low compared to that of traditional fossil fuel plants, and their equipment and maintenance costs are higher due to the complexity and vulnerability of the technology.

Many of the problems lie with the receiver tubes, which absorb the intensified solar radiation reflected from the parabolic mirrors. A typical receiver tube consists of a stainless steel absorber pipe which carries the heat transfer fluid, and a cylindrical glass envelope that is concentric to and surrounds the absorber pipe. The annular space between the two serves as a barrier to convective heat losses, and the absorber pipe is coated with a solar-selective material that maintains a high absorptance while minimizing the emittance of infrared radiation.

After serving for some year hydrogen will permeate through the stainless steel pipe and leaks into the annulus of the receiver tubes. The high conductivity of the hydrogen creates high heat transfer that alters functionality of the receivers and must either be punctured to release the hydrogen or be completely replaced.

Damage to the glass envelopes is likely the most common problem in the field. The glass envelopes are relatively fragile, and can break easily when exposed to severe weather conditions or when pieces of the reflecting mirrors break off and fall onto the receiver tubes.

With a broken envelope, the absorber tube may be fully exposed to the ambient air, greatly increasing thermal losses. The replacement of these highly expensive and easily damaged components upon failure greatly increases the cost of operating and maintaining a SEGS solar field [2].

1.4 Background to the Study

In the currently ever increasing cost of fossil fuels, renewable energy sources are the primary solution for energy demand of the world. Using renewable energy sources has advantage of no pollution, no greenhouse gas generation and there is no danger on the security of the energy resource.

Solar thermal power plants are one of the most interesting options for renewable electricity production. Ethiopia has a huge potential in solar energy particularly in the Southwest where the deserts have some of the best solar resource levels in the world. This sets parabolic trough power plants as an option for power production in the country.

Parabolic trough power plants are one of the low cost solar electric power options available today and have significant potential for further cost reduction. The plants have been designed to use solar energy as the primary energy source to produce electricity. They can operate at full rated power using solar energy alone given sufficient solar input. During clear days, the plants can operate for 10 to 12 hours at full-rated electric output. However, to date, all SEGS plants have a backup fossil-fired capability that can be used to supplement the solar output during periods of low solar radiation.

Although additional benefits are considered when typical power plant is selected; the primary consideration taken is the cost and efficiency of the plant. This requires a careful modeling and optimization of the model. In addition simulation of the model must be made to determine the annual performance of a typical configuration.

Currently Ethiopian Electric Power Corporation (EEPCo) provides 721.MW from 8 hydro, 13 diesels and one geothermal power plant. EEPCo also provides electric power from the self contained systems (SCS) that consists of three small hydro power plants and several diesel power plants. Generation in this system is mainly by diesel power plants having an aggregate capacity of 31.7 MW. The contribution from the small hydropower plants is only 6.15 MW [6]. Accordingly replacing the diesel generators with SEGS is very beneficial with increased cost of fossil fuels.

Today the hydropower plants installed in the country are experiencing severe difficulties to operate at rated figures due to lack of water in their dams. The main reasons for these difficulties are the increased demand and delayed rainfall. Therefore studying parabolic trough as an option for power production is very essential and timely.

1.5 Objective of the Thesis

This thesis has the following main objectives.

1. To properly design and model a parabolic trough power plant, taking into consideration the different losses associated with collection of the solar irradiance and other thermal losses;

2. To simulate the model using the proper simulation software (e.g. TRNSYS, EES, MATLAB) and make performance evaluation;

3. To make cost and financial analysis of the power plant using the appropriate software (solar advisor model (SAM)).

1.6 Methodology

First literature review of relevant materials on parabolic trough collectors and power production from steam using Rankine cycle is conducted. The literatures available are from electronic media, journals, and books. Secondary data are referred from previous and related research studies, existing statistical data, etc.

Necessary weather data are collected from available sources. Next the power plant is modeled using MATLAB and TRNSYS. MATLAB code is written to model the power plant at reference weather condition of Addis Ababa. TRNSYS software is used to simulate the power plant at weather conditions different from the reference values. This software is selected than similar software's for its simplicity and flexibility. Cost and financial analysis is also made using Solar Advisor Model (SAM). Finally conclusion and recommendation are made.

1.7 Outline of the Thesis

This thesis has six chapters. The first chapter deals with the introduction part. The second chapter deals with the solar field model. In this chapter different solar associated terms and the different heat losses from the parabolic troughs are discussed briefly. The third chapter is used to model the power plant. This chapter includes modeling of the different components in the power plant. The fourth chapter is used to simulate the power plant at weather conditions off reference values. In this chapter TRNSYS software is used. The results of the simulation are also given in this chapter. Cost and financial analysis of the power plant is made using solar advisor model (SAM) in the fifth chapter. The different costs associated with parabolic trough solar electric generation systems and the different financial terms are briefly discussed. The final chapter is used to present the different conclusions and recommendations derived from the thesis work.

CHAPTER 2

SOLAR FIELD MODEL

2.1 Introduction

The solar filed is composed of mainly solar collecting elements, HTF pumps, tubes and, valves. The main purpose of the solar field is to increase the cold heat transfer fluid (HTF) temperature that flows into the collector loop at one end by the absorbed energy of the sun. The hot HTF leaves the collector at the other end.

Figure 2-1 Solar field [21]

The hot HTF of every collector merges in a central header, which is connected to the power plant. In the power plant, the heat energy of the merged hot HTF is used to heat a working fluid, which is water or steam. After transferring its thermal energy to the power plant, the cold HTF leaves the power plant in a central header that feeds the collectors in the field with the cold fluid.

The objective of this chapter is to present the major components of the solar field. The different solar terms that are related with absorbing solar energy using parabolic troughs are also described. Heat transfer in the parabolic trough collectors are also discussed briefly. Finally linear regression models (found from the experimental setups) for the heat transfer process in the collectors are presented.

2.2 Solar Collecting Assembly (SCA)

The basic component of the solar field is the solar collector assembly (SCA). Each SCA is an independently tracking parabolic trough solar collector made up of parabolic reflectors (mirrors), the metal support structure, the receiver tubes, and the tracking system that includes the drive, sensors, and controls. Table 2-1 shows the design characteristics of the Acurex, single axis tracking M.A.N., and three generations of Luz SCAs. The general trend was to build larger collectors with higher concentration ratios (collector aperture divided by receiver diameter) to maintain collector thermal efficiency at higher fluid outlet temperatures.

Table 2-1 Solar collector characteristics [24]

Collector	Acurex 3001	M.A.N M480	Luz LS-1	Luz LS-2		Luz LS-3
Year	1981	1984	1984	1985	1988	1989
Area (m^2)	34	80	128	235		545
Aperture (m)	1.8	2.4	2.5	5		5.7
Length (m)	20	38	50	48		99
Receiver Diameter (m)	0.051	0.058	0.042	0.07		0.07
Concentration Ratio	36:1	41:1	61:1	71:1		82:1
Optical Efficiency	0.77	0.77	0.734	0.737	0.767	0.8
Receiver Absorptivity	0.96	0.96	0.94	0.94	0.99	0.96
Mirror Reflectivity	0.93	0.93	0.94	0.94	0.94	0.94
Receiver Emittance	0.27	0.17	0.3	0.24	0.19	0.19
@ Temperature (^oC)			300	300	350	350
Operating Temp.(^oC)	295	307	307	349	390	390

The LS-3 collector was the last collector design produced by Luz and was used primarily at the larger 80 MW plants. The LS-3 collector represents the current state-of-the-art in parabolic trough collector design and is the collector that would likely be used in the next parabolic trough plant built. A more detailed description of the LS-3 collector and its components follows.

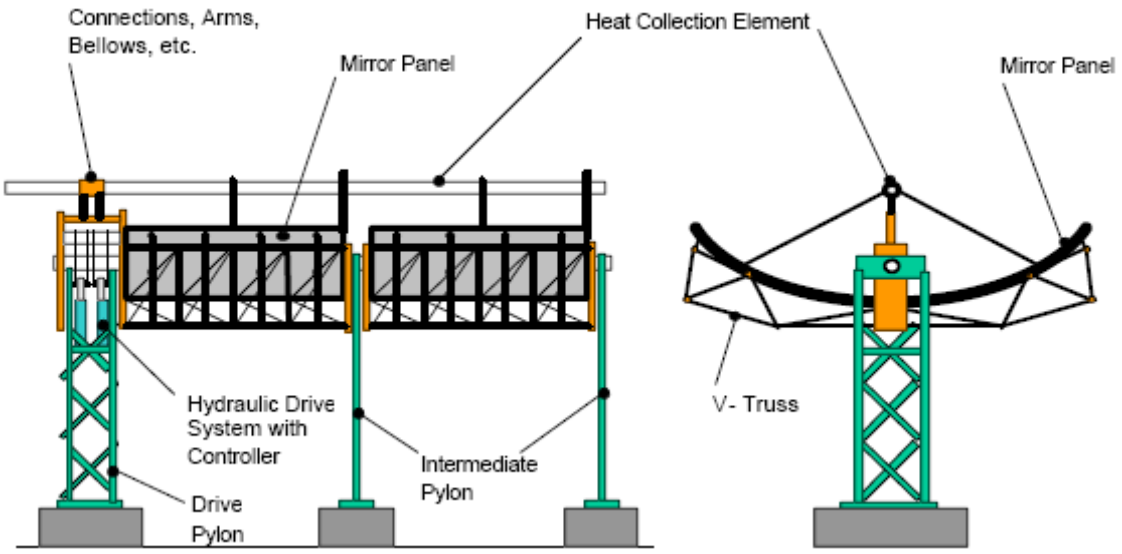

Figure 2-2 Luz System Three Solar Collector Assembly [22]

Figure 2-2 shows a diagram of the LS-3 collector. The LS-3 reflectors are made from hot-formed mirrored glass panels, supported by the truss system that gives the SCA its structural integrity. The aperture or width of the parabolic reflectors is 5.76 m and the overall SCA length is 95.2 m (net glass). The mirrors are made from a low iron float glass with a transmissivity of 98% that is silvered on the back and then covered with several protective coatings. The mirrors are heated on accurate parabolic molds in special ovens to obtain the parabolic shape. Ceramic pads used for mounting the mirrors to the collector structure are attached with a special adhesive. The high mirror quality allows 97% of the reflected rays to be incident on the linear receiver.

The SCAs rotate around the horizontal north/south axis to track the sun as it moves through the sky during the day. The axis of rotation is located at the collector center of mass to minimize the required tracking power. The drive system uses hydraulic rams to position the collector. A closed loop tracking system relies on a sun sensor for the precise alignment required to focus the sun on

the HCE during operation to within +/- 0.1 degrees. The tracking is controlled by a local controller on each SCA. The local controller also monitors the HTF temperature and reports operational status, alarms, and diagnostics to the main solar field control computer in the control room. The SCA is designed for normal operation in winds up to 25 mph (40 km/h) and somewhat reduced accuracy in winds up to 35 mph (56 km/h).The SCAs are designed to withstand a maximum of 70 mph (113 km/h) winds in their stowed position (the collector aimed 30º below eastern horizon).

The SCA structure on earlier generations of Luz collectors was designed to high tolerances and erected in place in order to obtain the required optical performance. The LS-3 structure is a central truss that is built up in a jig and aligned precisely before being lifted into place for final assembly. The result is a structure that is both stronger and lighter. The truss is a pair of V-trusses connected by an endplate. Mirror support arms are attached to the V-trusses [24].

2.3 Heat Collecting Elements (HCEs)

The linear receiver also referred to as a heat collection element (HCE), is one of the primary reasons for the high efficiency of the Luz parabolic trough collector design.

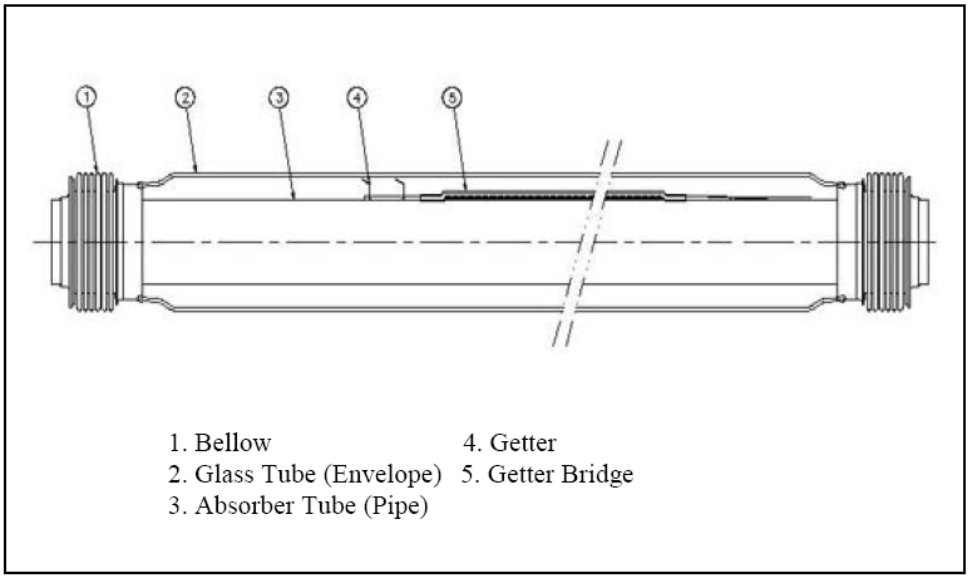

Figure 2-3 Heat Collecting Element [10]

The HCE consists of a 70 mm external diameter of steel tube with a Cermet selective surface, surrounded by an evacuated glass tube. The selective coating has a high absorptance for radiation in the solar energy spectrum, and low emittance in the long wave energy spectrum to reduce thermal radiation losses.

The HCE incorporates glass-to-metal seals and metal bellows to achieve the vacuum-tight enclosure. The vacuum enclosure serves primarily to protect the selective surface and to reduce heat losses at the high operating temperatures. The vacuum in the HCE is maintained at about 0.0001 mm Hg (0.013 Pa).

The cermet coating is sputtered onto the steel tube to give it excellent selective heat transfer properties with an absorptivity of 0.96 for direct beam solar radiation, and a design emissivity of 0.19 at 350ºC (662ºF). The outer glass cylinder has anti-reflective coating on both surfaces to reduce reflective losses off the glass tube.

The getter bridge installed in the annulus consists of metallic compounds designed to absorb hydrogen – which naturally permeates from the HTF and if left in the annulus would decrease the HCE performance. The getter is a vacuum loss indicator consisting of barium, which turns white when exposed to oxygen.

The bellows provide a glass-to-metal seal and allow thermal expansion between the metal absorber and glass envelope. The bellows also allow the absorber to protrude beyond the glass envelope so that HCEs can be butt welded together to form a continuous receiver. Furthermore, the space between bellows provides a place to attach the HCE support brackets.

2.4 The Heat Transfer Fluids (HTFs)

The solar field heat transfer fluid (HTF) absorbs heat as it circulates through the heat collection elements in the solar field and transports the heat to the power block where it is used to run a turbine. Several types of heat transfer fluid are used for trough systems, including hydrocarbon (mineral) s, synthetic s, silicone s and nitrate salts.

Table 2-2 Heat Transfer Fluids [19]

Name	Type	Min HTF Temp [^{O}C]	Max Operating Temp [^{O}C]	Freeze Point	Comments
Solar Salt	Salt	260	600	220	
Caloria	Mineral Hydrocarbon	-20	300	-40	Used in first Luz trough plant, SEGS I
Hitec XL	Nitrate salt	150	500	120	New generation
Therminol VP-1	Mixture of Biphenyl and Diphenyl Oxide	50	400	12	Standard for current generation HTF systems
Hitec	Nitrate Salt	175	500	140	For high-temperature systems
Dowtherm Q	Synthetic	-30	330	-50	New generation
Dowtherm RP	Synthetic	-20	350	-40	New generation

Current SEGS plants use Therminol VP-1 HTF. Therminol VP-1 liquid/vapor phase heat transfer fluid is a high temperature medium that delivers process heat at temperatures up to 400^{O}C with reliability and precise control.

Therminol VP-1 is a mixture of 73.5% diphenyl oxide/26.5% diphenyl, and as such can be used in existing liquid, or vapor phase systems, for top-up or replacement of heat transfer fluids of the same composition. Vapor phase operation is possible at temperature above 257^{O}C.

Physical properties of Therminol VP-1 in liquid phase are shown by the following interpolated formulas as a function of temperature (^{O}C) [11].

$$\rho(T) = -0.90797T + 0.00078116T^2 - 2.367\times10^{-6}T^3 + 1083.25 \ \left[kg/m^3\right] \qquad (2.1)$$

$$h(T) = 0.002414T + 5.9591\times10^{-6}T^2 - 2.9879\times10^{-8}T^3 + 4.4172\times10^{-11}T^4 + 1498 \quad [kJ/kg] \tag{2.2}$$

$$k(T) = -8.19477\times10^{-5}T - 1.92257\times10^{-7}T^2 + 2.5034\times10^{-11}T^3 - 7.2974\times10^{-15}T^4 + 1.498 \quad [W/m.k] \tag{2.3}$$

2.5 Solar Irradiation and Absorption

2.5.1 Direct Normal Insolation

Because the earth's orbit is slightly elliptical, the intensity of solar radiation received outside the earth's atmosphere varies as the square of the earth-sun distance. Variation of the earth-sun distance leads to variation of extraterrestrial radiation flux in the range of ±3% with the maximum irradiance occurring at the perihelion i.e. earth closest to the sun (January 3-5) and the minimum at the aphelion (July 5). The variation of the extraterrestrial radiation measured on the plane normal to the radiation on the n^{th} day of the year is given by the equation below.

$$I_{ext} = I_{SC}\left[1.0 + 0.033\cos\left(\frac{360N}{365}\right)\right] \quad \left(W/m^2\right) \tag{2.4}$$

Where I_{SC} is the extraterrestrial solar irradiance outside the earth's atmosphere at 1 AU, called the solar constant I_{SC} and has a currently accepted value of 1367 W/m^2 [5]; and N is the day number starting at January 1.

When extraterrestrial radiation passes through the atmospheric some part of it is scatted by air molecules, water, and dust found in the atmosphere. Some part of the extraterrestrial radiation is absorbed by molecules in the atmosphere such as O_3, H_2O, and CO_2.The radiation that falls on the earth after being scattered in the atmosphere is called diffuse radiation. The remaining part of the extraterrestrial radiation falling on earth without being scattered is called direct or beam radiation. Beam radiation incident on a plane normal to the radiation is called the **direct normal radiation**. The sum of direct and diffuse solar irradiance is called the global or total solar irradiance.

Since diffuse solar irradiance cannot be concentrated, only flat-plate (non-concentrating) solar collectors and some low-temperature types of concentrators (having wide acceptance angles) can collect diffuse solar irradiance. For concentrating systems like the solar trough collector field only the beam radiation or direct normal radiation is used.

The primary instrument used to measure global solar irradiance is the pyrheliometer, which measures the sun's energy coming from all directions in the hemisphere above the plane of the instrument. To measure the direct normal component of the solar irradiance only, an instrument called a normal incidence pyrheliometer or NIP is used. Usually in these pyrheliometers a two-axis tracking mechanism is incorporated to make incident angle near to zero.

2.5.2 Solar angles

The time used in all of the sun-angle relations is the Solar Time. Solar time is a time based on the apparent angular motion of the sun across the sky, with solar noon the time with the sun crosses the meridian of the observer [4].Watch time (Standard time) is described on longitudes and is dependent on the standard meridian for each country. The difference in minutes between solar time and standard time is given by the Equation (2.5).

$$Solar\ time = Standard\ time + 4(L_{st} + L_{Loc}) + E \tag{2.5}$$

Where: - L_{st} is the standard meridian for the local time zone

L_{loc} is the longitude of the location in question

E is equation of time E (in minutes) given by the Equation 2.6

$$E = 229.2(0.000075 + 0.001868\cos B - 0.032077\sin B - 0.014615\cos 2B - 0.04089\sin 2B) \tag{2.6}$$

Where: $B = (N-1)\frac{360}{365}$

Variation of equation of time with day of the year is plotted in Figure 2-4.

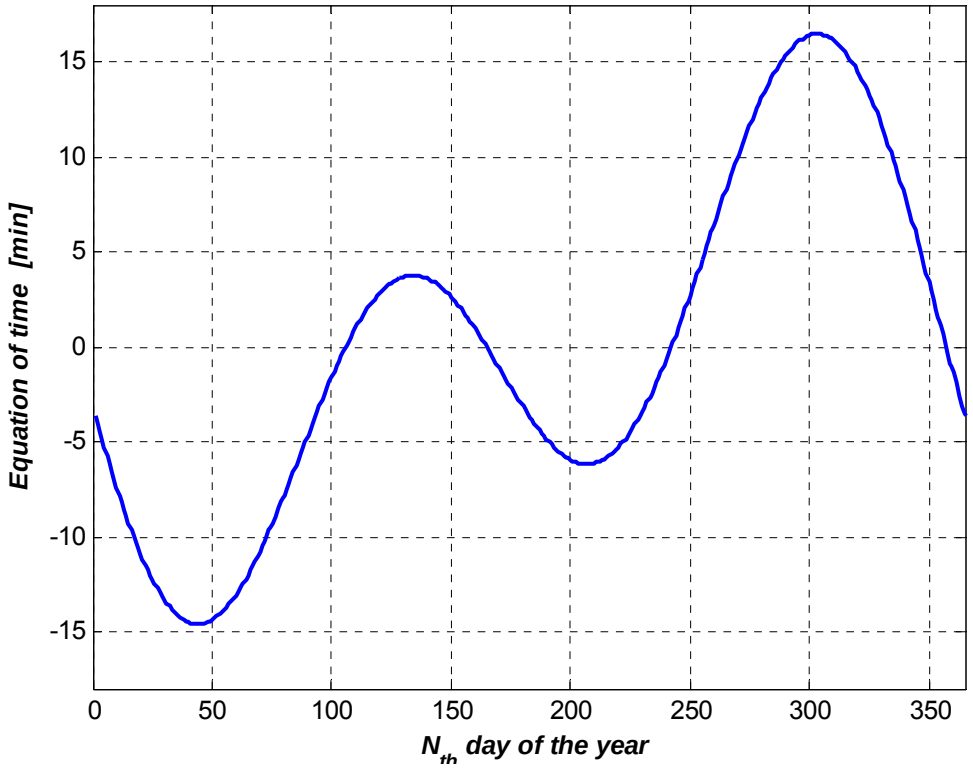

Figure 2-4 Equation of time E in minutes, as a function of time of year

2.5.3 The Hour Angle (ω)

To describe the earth's rotation about its polar axis, we use the concept of the hour angle (ω). As shown in the figure below the hour angle is the angular distance between the meridian of the observer and the meridian whose plane contains the sun. The hour angle is zero at solar noon (when the sun reaches its highest point in the sky). At this time the sun is said to be 'due south' (or 'due north', in the Southern Hemisphere) since the meridian plane of the observer contains the sun. The hour angle increases by 15 degrees every hour.

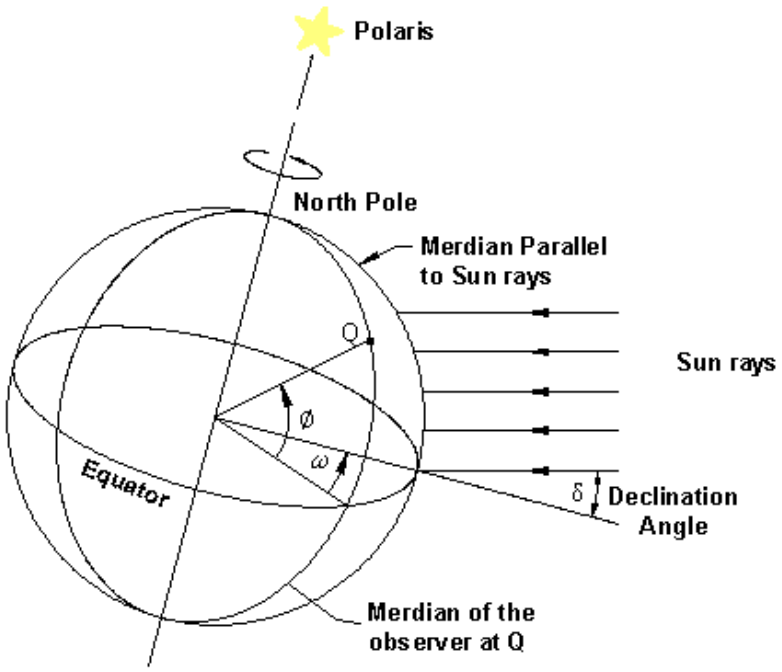

Figure 2-5 The hour angle (ω). This angle is defined as the angle between the meridian parallel to sun rays and the meridian containing the observer [18]

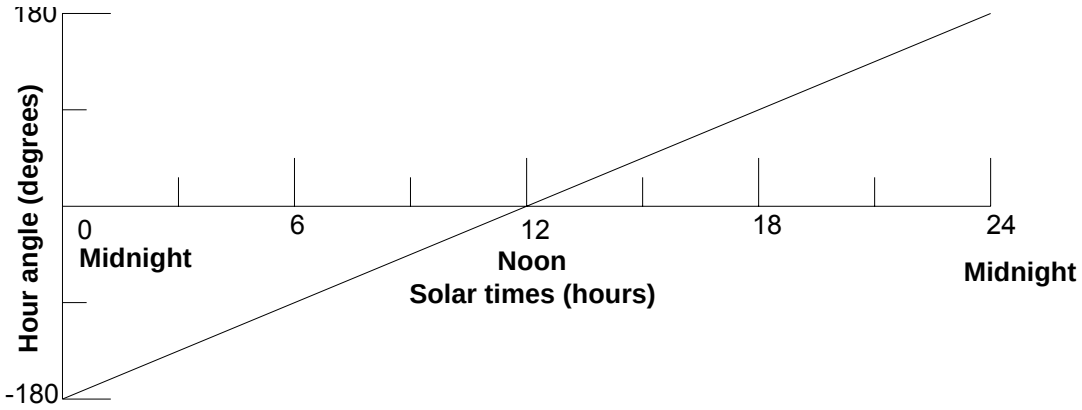

Figure 2-6 Variation of the hour angle in a day [18]

Hour angle is given by the following equation.

$$\omega = (ST - 12) \times 15^{o}, \text{ Where ST is solar time} \qquad (2.7)$$

2.5.4 The Declination Angle (δ)

The plane that includes the earth's equator is called the equatorial plane. If a line is drawn between the center of the earth and the sun, the angle between this line and the earth's equatorial plane is called the declination angle (δ). At the time of year when the northern part of the earth's rotational axis is inclined toward the sun, the earth's equatorial plane is inclined 23.45 degrees to the earth-sun line. At this time (about June 21), we observe that the noontime sun is at its highest point in the sky and the declination angle $\delta = +23.45$ degrees. We call this condition the summer solstice, and it marks the beginning of summer in the Northern Hemisphere.

As the earth continues its yearly orbit about the sun, a point is reached about 3 months later where a line from the earth to the sun lies on the equatorial plane. At this point an observer on the equator would observe that the sun was directly overhead at noontime. This condition is called an equinox since anywhere on the earth, the time during which the sun is visible (daytime) is exactly 12 hours and the time when it is not visible (nighttime) is 12 hours. There are two such conditions during a year; the autumnal equinox on about September 23, marking the start of the fall; and the vernal equinox on about March 22, marking the beginning of spring. At the equinoxes, the declination angle (δ) is zero.

The winter solstice occurs on about December 22 and marks the point where the equatorial plane is tilted relative to the earth-sun line such that the northern hemisphere is tilted away from the sun. We say that the noontime sun is at its "lowest point" in the sky, meaning that the declination angle is at its most negative value (i.e., $\delta = -23.45$ degrees). By convention, winter declination angles are negative. Declination (δ) can be found from the equation

$$\delta = 23.45 \sin\left(360 \frac{284 + N}{365}\right) \tag{2.8}$$

Variation of declination with day of the year is shown in Figure 2-7.

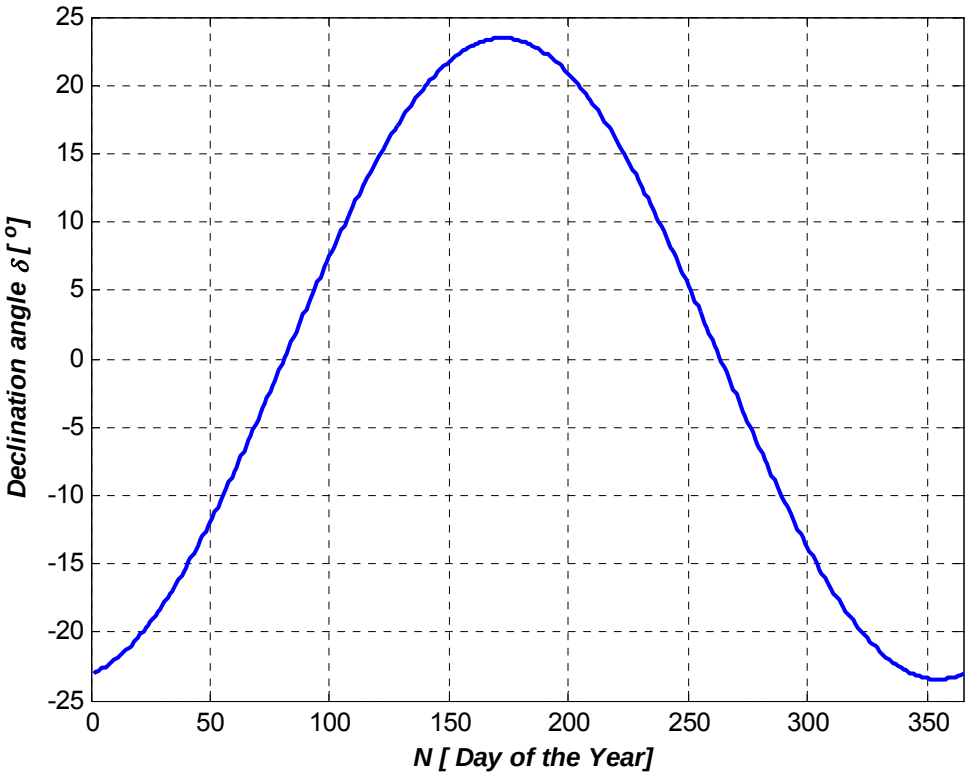

Figure 2-7 Declination angle as a function of day of the year

The **solar altitude angle (α)** is defined as the angle between the central ray from the sun, and a horizontal plane containing the observer as shown in the Figure 2-8. The equation for the solar altitude angle (α) is given in Equation 2.9.

$$\sin\alpha = \sin\delta\sin\phi + \cos\delta\cos\omega\cos\phi \tag{2.9}$$

As an alternative, the sun's altitude may be described in terms of the solar zenith angle (θ_z)which is simply the complement of the solar altitude angle.

$$\theta_Z = 90^o - \alpha \quad \text{(Degrees)} \tag{2.10}$$

This gives the equation for the solar altitude angle to be

$$\cos\theta_Z = \sin\delta\sin\phi + \cos\delta\cos\omega\cos\phi \tag{2.11}$$

The other angle defining the position of the sun is the **solar azimuth angle (γ).** It is the angle, measured clockwise on the horizontal plane, from the north-pointing coordinate axis to the projection of the sun's central ray. Displacements east of south are negative and west of south are positive.

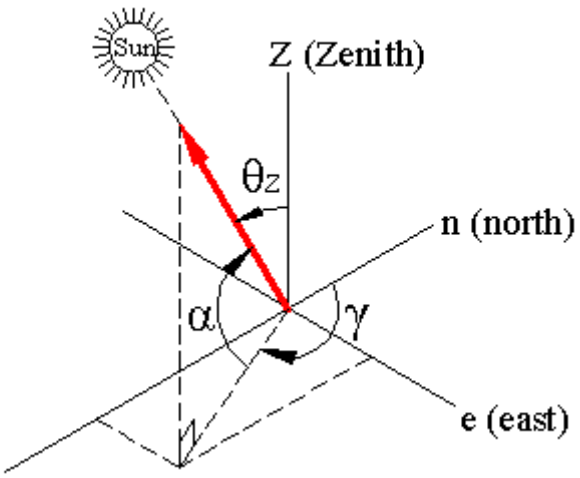

Figure 2-8 Earth surface coordinate system showing the solar azimuth angle zenith angle and Elevation angle

2.5.5 The Angle of Incidence (θ)

The angle between the sun's rays and a vector normal (perpendicular) to the aperture or surface of the collector is the angle of incidence (θ). Knowing this angle is of critical importance to the solar designer, since the maximum amount of solar radiation energy that could reach a collector is reduced by the cosine of this angle.

Certain types of concentrating collector such as parabolic trough collectors are designed to operate with tracking rotation about only one axis to minimize the angle of incidence of beam radiation on their surfaces and thus maximize the incident beam radiation. Here a tracking drive system rotates the collector about an axis of rotation until the sun central ray and the aperture normal are coplanar. The angle of incidence (θ) is also shown in Figure 2.9.

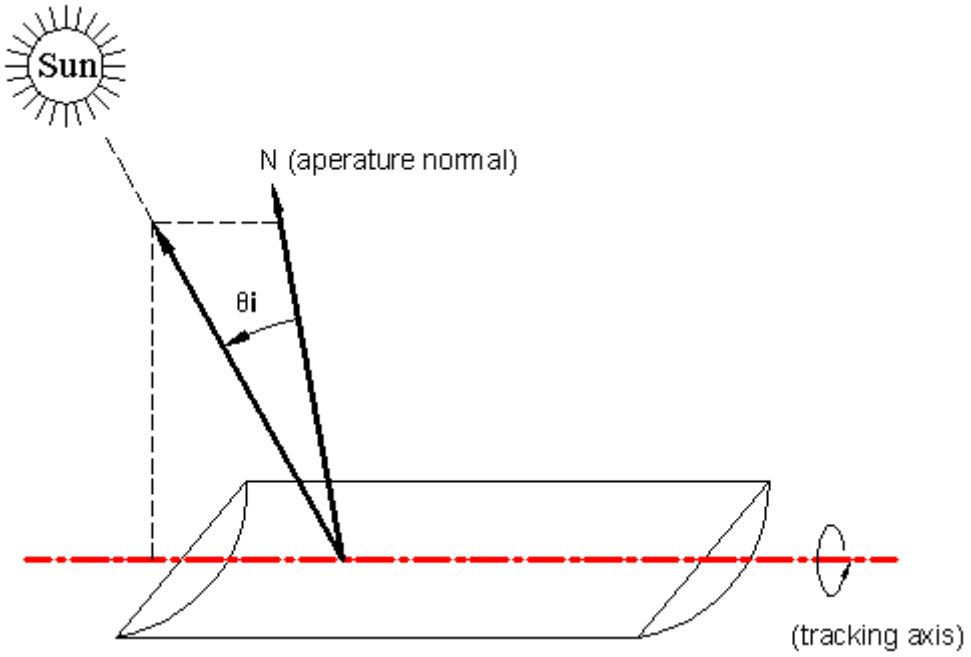

Figure 2-9 A single-axis tracking aperture where tracking rotation is about the tracking axis

For a plane rotated about a horizontal North-South axis with continuous adjustment to minimize the angle of incidence is,

$$\cos\theta = \left(\cos^2\theta_Z + \cos^2\delta\sin^2\omega\right)^{1/2} \tag{2.12}$$

2.6 Incidence angle Modifier

Measured efficiency of a parabolic trough collector decreases as the solar beam incident angle increases. Collector efficiency is at a maximum only when the incident angle is zero. The decrease in collector efficiency with increasing incident angle is caused by cosine foreshortening of the collector aperture as well as other effects, such as the transmissivity of the glass envelope or the absorption of the selective surface as a function of incidence angle.

The incident angle modifier K is the ratio of collector efficiency at any angle of incidence, to that at normal incidence. It is measured experimentally by varying the angle of incidence under noontime solar irradiance conditions with ambient temperature heat transfer fluid passing through the collector. A regression analysis of the data is used to obtain an equation of the form:

$$K = \cos(\theta) - B(\theta) - C(\theta)^2 \tag{2.13}$$

Where: K = Incident angle modifier; value ranges from 0 to1

θ = Solar beam incident angle (0 to 60 degrees)

B = Coefficient for linear term

C = Coefficient for nonlinear term

Test results for SEGS LS-2 SCA yield an incident angle modifier expression as given in equation (2.14) [3]. The equation is applied for temperatures between ambient and 400^{o}C, at any insolation level from 100 to 1100 W/m^2, and at any incident angle from 0 to 60 degrees.

$$K = \cos(\theta) - 0.0003512(\theta) - 0.00003137(\theta)^2 \tag{2.14}$$

2.7 Row Shading

Generally at any solar field the collectors are arranged in parallel rows. The distance between the collector rows is $L_{Spacing}$ = 12.5 m at SEGs VI. Hence, in the morning, at sunrise, when the first sunrays fall on the trough collector field, the first row may be unobstructed, but the following rows are shaded by the first. During the sun's path in the morning, partial shading of the collectors occurs until a particular zenith angle is reached. The shading reduces the effective width of the collector and thus reduces the effective aperture area of the collector on which the solar beam radiation acts. Consequently, the absorbed solar energy is reduced as well. After a certain zenith angle is reached, there is no mutual shading of the collectors anymore. The same phenomenon occurs, of course, in the evening during sunset.

Figure 2-10 Collector tracking through morning, showing digression of collector shading as the day progresses [22]

The row shadow factor is the ratio of the effective mirror aperture width to the actual mirror aperture width. This ratio can be derived from the geometry of the solar zenith angle, the incidence angle, and the layout of the collectors in a field [22]:

$$RS = \frac{L_{Spacing}}{W}\frac{\cos(\theta_Z)}{\cos(\theta)} \tag{2.15}$$

Where: RS = row Shadow factor

$L_{Spacing}$ = length of spacing between troughs

W = collector aperture width (5 [m] for LS-2)

θ_Z = Zenith angle

θ = angle of incidence

Where $RS \in [0; 1]$ A value of 0 for RS means complete shading whereas a value of 1 for RS means no shading of the collector.

$$RS = \min\left[\max\left(0.0; \frac{L_{Spacing}}{W}\frac{\cos(\theta_Z)}{\cos(\theta)}\right); 1.0\right] \tag{2.16}$$

The above equation for row shading is plotted for Addis Ababa of latitude 9.02^0 at summer solstice and the winter solstice.

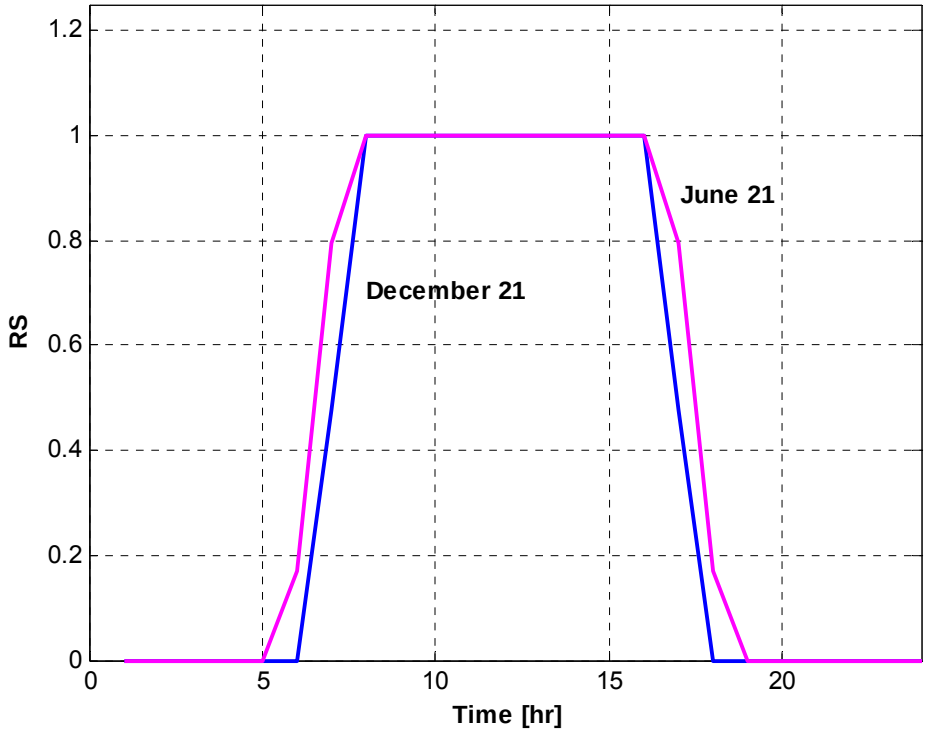

Figure 2-11 Row Shading versus time of day, for June21 and December 21

2.8 End losses

End losses occur at the ends of the HCEs, where, for a nonzero incidence angle, some length of the absorber tube is not illuminated by solar radiation reflected from the mirrors. Figure 2-12 depicts the occurrence of end losses for an HCE with a nonzero angle of incidence.

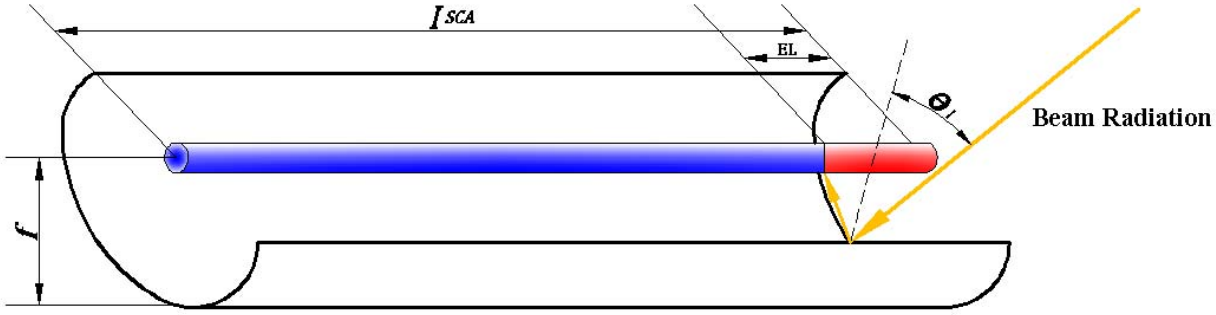

Figure 2-12 End losses from an HCE

The end losses are a function of the focal length of the collector, the length of the collector, and the incident angle [16]:

$$EL = 1 - \frac{f \tan\theta}{L_{SCA}} \tag{2.17}$$

Where: f = focal length of the collectors (5[m] for LS-2 collectors)

θ = incident angle

L_{SCA} = length of a single solar collector assembly (50 [m] for LS-2 Collectors)

2.9 Analytical Heat Loss Model for the Receiver

The following discussion on analytical modeling of the heat transfer loss of the HCEs is based on Forristall [10] and Dudley et al. [4]. The objective of the analytical modeling is to understand the heat transfer phenomena of the collectors.

Figure 2-13 shows the one-dimensional steady-state energy balance for a cross-section of an HCE, without the glass envelope intact, and Figure 2-14 shows the thermal resistance model and subscript definitions.

The effective incoming solar energy (solar energy minus optical losses) is absorbed by the glass envelope $(\dot{q}'_{5SolAbs})$ and absorber selective coating $(\dot{q}'_{3SolAbs})$. Some energy that is absorbed into the selective coating is conducted through the absorber $(\dot{q}'_{23cond})$ and transferred to the HTF by convection $(\dot{q}'_{12conv})$; remaining energy is transmitted back to the glass envelope by convection $(\dot{q}'_{34conv})$ and radiation $(\dot{q}'_{34rad})$ and lost through the HCE support bracket through conduction. The energy from the radiation and convection then passes through the glass envelope by conduction $(\dot{q}'_{45cond})$ and along with the energy absorbed by the glass envelope $(\dot{q}'_{5SolAbs})$ is lost to the environment by convection ($\dot{q}'_{56conv}$) and radiation $(\dot{q}'_{57rad})$. If the glass envelope is missing, the heat loss from the absorber is lost directly to the environment. The model assumes all temperatures, heat fluxes, and thermodynamic properties are uniform around the circumference of the HCE.

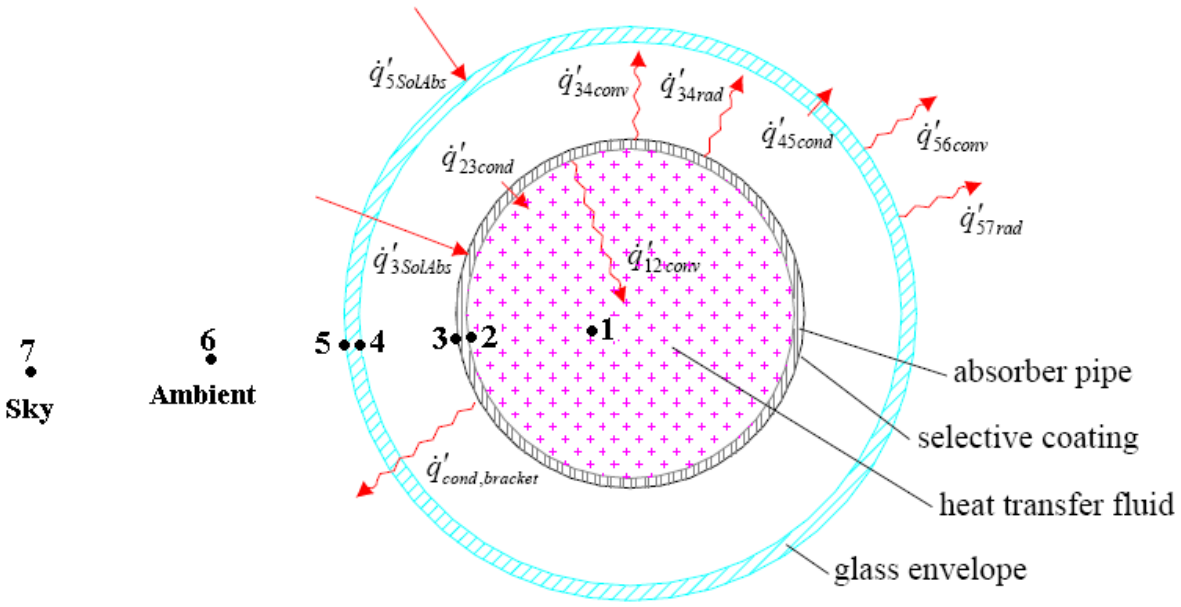

Figure 2-13 One dimensional energy balance

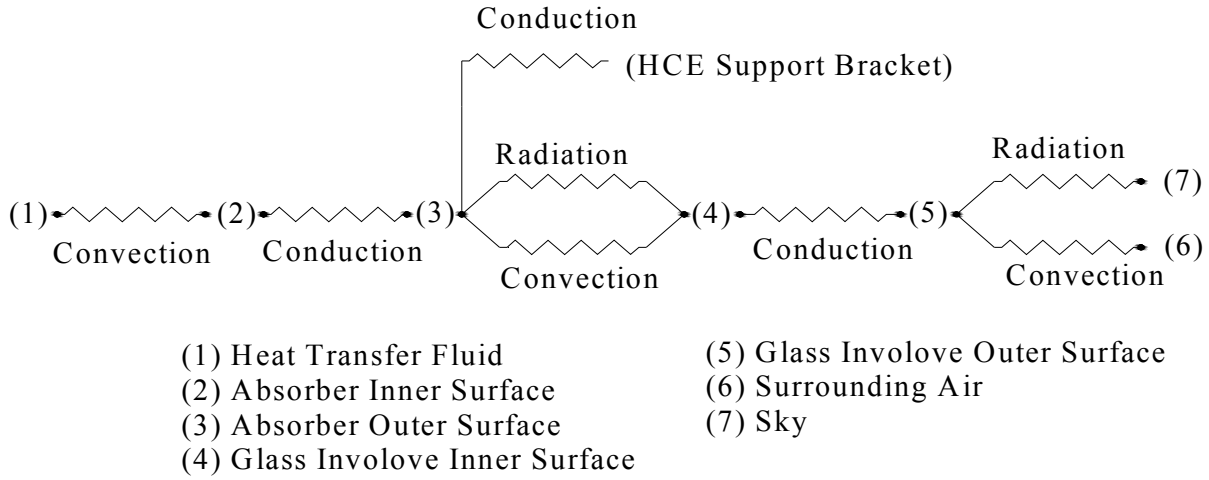

Figure 2-14 Thermal resistance model

2.9.1 Convection Heat Transfer from the Absorber to the HTF

Considering convection for internal flow, the heat transfer per unit length ($\dot{q}'_{12conv}$) is calculated through the Dittus-Boelter equation assuming fully developed (hydro dynamically and thermally)

turbulent flow in a smooth circular tube [12]. Hence, the local Nusselt number (Nu_{D2}) is given by:

$$Nu_{D2} = 0.023(\mathrm{Re}_{D2})^{0.8}(\mathrm{Pr}_1)^n \tag{2.18}$$

Where: n = 0.4 for heating ($T_2 > T_1$) and 0.3 for cooling ($T_2 < T_1$).

The Reynolds number, Re_{D2} for flow in a circular tube, is given by:

$$\mathrm{Re}_{D2} = \frac{4\dot{m}}{\pi D_2 \mu_1} \tag{2.19}$$

With μ_1 as the viscosity of the HTF, the Prandtl number, Pr_1 is determined by

$$\mathrm{Pr}_1 = \frac{\nu_1}{\alpha_1} \tag{2.20}$$

The kinematic viscosity of the HTF, ν_1 is defined by

$$\nu_1 = \frac{\mu_1}{\rho_1} \tag{2.21}$$

and the thermal diffusivity of HTF, α_1, is given by

$$\alpha_1 = \frac{k_1}{\rho_1 C_1} \tag{2.22}$$

In equation (2.22), k_1 is the thermal conductivity of the HTF. The heat transfer coefficient, h_{12} is calculated by using the local Nusselt number, Nu_{D2} through

$$h_{12} = \frac{Nu_{D2} k_1}{D_2} \tag{2.23}$$

Where: D_2 is the inside diameter of the absorber tube. The HTF properties, C_1, k_1, μ_1, and ρ_1 are functions of the HTF film temperature T_f. Finally the absorbed energy per length $\dot{q}'_{12conv}$ becomes:

$$\dot{q}'_{12conv} = h_{12}\pi D_2\left(T_2 - T_1\right) \tag{2.24}$$

2.9.2 Conduction Heat Transfer through the Absorber Wall

Fourier's law of conduction through a hollow cylinder describes the conduction heat transfer through the absorber wall [12]:

$$\dot{q}'_{23cond} = 2\pi k_{23}\left(T_2 - T_3\right)/\ln\left(D_3/D_2\right) \tag{2.25}$$

Where: k_{23} = absorber thermal conductance at the average absorber temperature $(T_2+T_3)/2$ (W/m-K)

T_2 = absorber inside surface temperature (K)

T_3 = absorber outside surface temperature (K)

D_2 = absorber inside diameter (m)

D_3 = absorber outside diameter (m)

In this equation the conduction heat transfer coefficient is constant, and is evaluated at the average temperature between the inner and outer surfaces.

The conduction coefficient depends on the absorber material type. The HCE performance model includes three stainless steels: 304L, 316L, and 321H, and one copper: B42. If 304L or 316L is chosen, the conduction coefficient is calculated with the following equation.

$$k_{23} = \left(0.013\right)T_{23} + 15.2 \tag{2.26}$$

If 321H is chosen,

$$k_{23} = \left(0.0153\right)T_{23} + 14.775 \tag{2.27}$$

If copper is chosen, the conduction coefficient is a constant at 400 W/m-K. Conductive resistance through the selective coating has been neglected.

2.9.2.1 Heat Transfer from the Absorber to the Glass Envelope

Convection and radiation heat transfer occur between the absorber and the glass envelope. The convection heat transfer mechanism depends on the annulus pressure. At low pressures (< ~ 133.3 N/m^2), the heat transfer mechanism is molecular conduction. At higher pressures (> ~ 133.3 N/m^2), the mechanism is free convection.

The radiation heat transfer occurs because of the difference in temperatures between the outer absorber surface and the inner glass envelope surface. The radiation heat transfer calculation is simplified by assuming the glass envelope is opaque to infrared radiation and assuming gray ($\rho = \alpha$) surfaces.

2.9.2.1.1 Convection Heat Transfer

Two heat transfer mechanisms are evaluated to determine the convection heat transfer from the absorber to the glass envelope ($\dot{q}'_{34conv}$), free-molecular and natural convection.

2.9.2.1.2 Convection Heat Transfer for Vacuum in Annulus

When the HCE annulus is under vacuum (pressure < ~133.3 N/m^2), the convection heat transfer between the absorber and glass envelope occurs by free-molecular convection.

$$\dot{q}'_{34conv} = \pi D_3 h_{34} \left(T_3 - T_4\right) \tag{2.28}$$

$$h_{34} = \frac{k_{std}}{\left(\frac{D_3}{2\ln\left(\frac{D_4}{D_3}\right) + b\lambda\left(\frac{D_3}{D_4} + 1\right)} \right)} \tag{2.29}$$

$$b = \frac{(2-a)(9\gamma - 5)}{2a(\gamma + 1)} \tag{2.30}$$

$$\lambda = \frac{2.331E(-20)(T_{34} + 273.15)}{(P_a \delta^2)} \tag{2.31}$$

Where: D_3 = outer absorber surface diameter (m)

D_4 = inner glass envelope surface diameter (m)

h_{34} = convection heat transfer coefficient for the annulus gas at T_{34} (W/m2-K)

T_3 = outer absorber surface temperature (^oC)

T_4 = inner glass envelope surface temperature (^oC)

k_{std} = thermal conductance of the annulus gas at standard temperature and pressure (W/m-K)

b = interaction coefficient

λ = mean-free-path between collisions of a molecule (cm)

a = accommodation coefficient

γ = ratio of specific heats for the annulus gas

T_{34} = average temperature $(T_3 + T_4)/2$ (oC)

P_a = annulus gas pressure (mmHg)

δ = molecular diameter of annulus gas (cm)

This correlation is valid for $Ra_{D4} < (D_4 / (D_4 - D_3))^4$. The molecular diameters of the gases, δ, are shown in Table 2.3. The table also compares the convection heat transfer coefficients (h_{34}) and other parameters that are used in the calculation for each of the three gases included in the HCE performance model.

Table 2-3 Heat transfer coefficients and constants for each annulus gas

Annulus Gas	k_{std} [W/m-K]	b	λ [cm]	γ	δ [cm]	h_{34} [W/m^2-K]
Air	0.02551	1.571	88.67	1.39	3.53E-8	0.0001115
Hydrogen	0.1769	1.581	191.8	1.398	2.4E-8	0.0003551
Argon	0.01777	1.886	76.51	1.677	3.8E-8	0.00007499
T = 300 ^{o}C, Insolation = 940 W/m^2						

2.9.2.1.3 Convection Heat Transfer for Pressure in Annulus

When the HCE annulus loses vacuum (pressure > ~ 133.3 N/m^2), the convection heat transfer mechanism between the absorber and glass envelope occurs by natural convection. Raithby and Holland's correlation for natural convection in an annular space between horizontal cylinders is used for this case [2].

$$\dot{q}'_{34conv} = \frac{2.425 k_{34}(T_3 - T_4)\left(\frac{\mathrm{Pr}_{34}\, Ra_{D3}}{(0.861+\mathrm{Pr}_{34})}\right)^{\frac{1}{4}}}{\left(1+\left(\frac{D_3}{D_4}\right)^{\frac{3}{5}}\right)^{\frac{5}{4}}} \tag{2.32}$$

$$Ra_{D3} = \frac{g\beta(T_3 - T_4)D_3^3}{\alpha\upsilon} \tag{2.33}$$

For an ideal gas

$$\beta = \frac{1}{T_{avg}} \;\; and \;\; \mathrm{Pr}_{34} = \frac{\upsilon_{34}}{\alpha_{34}} \tag{2.34}$$

Where: T_3 = outer absorber surface temperature (^{o}C)

T_4 = inner glass envelope surface temperature (^{o}C)

D_3 = outer absorber diameter (m)

D_4 = inner glass envelope diameter (m)

Pr_{34} = Prandtl number

Ra_{D3} = Rayleigh number evaluated at D_3

β = volumetric thermal expansion coefficient (1/K)

T_{avg}= average temperature, $(T_3 + T_4)/2$ (^oC)

α = thermal diffusivity for the annulus gas

ν = kinematic viscosity for the annulus gas

This correlation assumes long, horizontal, concentric cylinders at uniform temperatures, and is valid for $RaD_4 > (D_4 /(D_4 – D_3))^4$. All physical properties are evaluated at the average temperature $(T_3 + T_4)/2$.

2.9.2.2 Radiation Heat Transfer

The radiation heat transfer from the absorber to the glass envelope ($\dot{q}'_{34rad}$) is estimated with the following equation [12].

$$\dot{q}'_{34rad} = \frac{\sigma \pi D_3 \left(T_3^{\,4} - T_4^{\,4}\right)}{\frac{1}{\varepsilon_3} + \frac{1-\varepsilon_3}{\varepsilon_4}\left(\frac{D_3}{D_4}\right)} \tag{2.35}$$

Where: σ = Stefan-Boltzmann constant (5.670E-8) ($W/m^2\text{-}K^4$)

D_3 = outer absorber diameter (m)

D_4 = inner glass envelope diameter (m)

T_3 = outer absorber surface temperature (K)

T_4 = inner glass envelope surface temperature (K)

ε_3 = Absorber selective coating emissivity

ε_4 = glass envelope emissivity

2.9.3 Conduction Heat Transfer through the Glass Envelope

The conduction heat transfer through the glass envelope uses the same equation as the conduction through the absorber wall described above. The thermal conductance is assumed constant with a value of 1.04 (Pyrex glass).

2.9.4 Heat Transfer from the Glass Envelope to the Atmosphere

The heat will transfer from the glass envelope to the atmosphere by convection and radiation. The convection will either be forced or natural, depending on whether there is wind. Radiation heat loss occurs due to the temperature difference between the glass envelope and sky.

2.9.4.1 Convection Heat Transfer

The convection heat transfer from the glass envelope to the atmosphere ($\dot{q}'_{56conv}$) is the largest source of heat loss, especially if there is a wind. From Newton's law of cooling:

$$\dot{q}'_{56conv} = h_{56} D_5 \pi (T_5 - T_6) \tag{2.36}$$

$$h_{56} = Nu_{D5} \frac{k_{56}}{D_5} \tag{2.37}$$

Where: T_5 = glass envelope outer surface temperature (^oC)

T_6 = ambient temperature (^oC)

h_{56} = convection heat transfer coefficient for air at $(T_5 - T_6)/2$ (W/m^2-K)

k_{56} = thermal conductance of air at $(T_5 - T_6)/2$ (W/m-K)

D_5 = glass envelope outer diameter (m)

Nu_{D5} = average Nusselt number based on the glass envelope outer diameter

The Nusselt number depends on whether the convection heat transfer is natural (no wind) or forced (with wind).

2.9.4.1.1 No Wind Case

If there is no wind, the convection heat transfer from the glass envelope to the environment will be by natural convection. For this case, the correlation developed by Churchill and Chu will be used to estimate the Nusselt number [12].

$$\overline{Nu}_{D5} = \left\{ 0.6 + \frac{0.387 Ra_{D5}^{1/6}}{\left[1 + \left(0.559 / \mathrm{Pr}_{56}\right)^{9/16}\right]^{8/27}} \right\}^2 \tag{2.38}$$

$$Ra_{D5} = \frac{g\beta\left(T_5 - T_6\right)D_5^{\,3}}{\alpha_{56}\nu_{56}} \tag{2.39}$$

$$\beta = \frac{1}{T_{56}} \tag{2.40}$$

$$\mathrm{Pr}_{56} = \frac{\nu_{56}}{\alpha_{56}} \tag{2.41}$$

Where: Ra_{D5} = Rayleigh number for air based on the glass envelope outer diameter, D_5

g = gravitational constant (9.81) (m/s^2)

α_{56} = thermal diffusivity for air at T_{56} (m^2/s)

β = volumetric thermal expansion coefficient (ideal gas) (1/K)

Pr_{56} = Prandtl number for air at T_{56}

ν_{56} = kinematic viscosity for air at T_{56} (m^2/s)

T_{56} = film temperature $(T_5 + T_6)/2$ (K)

This correlation is valid for $10^5 < Ra_{D5} < 10^{12}$, and assumes a long isothermal horizontal cylinder. Also, all the fluid properties are determined at the film temperature, $(T_5 + T_6)/2$.

2.9.4.1.2 Wind Case

If there is wind, the convection heat transfer from the glass envelope to the environment will be forced convection. The Nusselt number in this case is estimated with Zhukauskas' correlation for external forced convection flow normal to an isothermal cylinder [12].

$$\overline{Nu}_{D5} = C\,\mathrm{Re}_{D5}{}^{m}\,\mathrm{Pr}_6{}^{n}\left(\frac{pr_6}{\mathrm{Pr}_5}\right)^{1/4} \tag{2.42}$$

With

Table 2-4 Reynolds number

ReD	C	m
1-40	0.75	0.4
40-1000	0.51	0.5
1000-200000	0.26	0.6
200000-1000000	0.076	0.7

and n = 0.37, for Pr <=10 , n = 0.36, for Pr >10

This correlation is valid for $0.7 < Pr_6 < 500$, and $1 < ReD_5 < 10^6$. All fluid properties are evaluated at the atmospheric temperature, T_6, except Pr_5, which is evaluated at the glass envelope outer surface temperature.

2.9.4.2 Radiation Heat Transfer

The useful incoming solar irradiation is included in the solar absorption terms. Therefore, the infrared radiation transfer between the glass envelope and sky is caused by the temperature difference between the glass envelope and sky. To approximate this, the envelope is assumed to be a small convex gray object in a large blackbody cavity (sky). The net radiation transfer between the glass envelope and sky becomes [12]:

$$\dot{q}'_{57rad} = \sigma \pi D_5 \varepsilon_5 \left(T_5^{\,4} - T_7^{\,4} \right) \tag{2.43}$$

Where: σ = Stefan-Boltzmann constant (5.670E-8) (W/m^2-K^4)

D_5 = glass envelope outer diameter (m)

ε_5 = emissivity of the glass envelope outer surface

T_5 = glass envelope outer surface temperature (K)

T_7 = effective sky temperature (K)

The effective sky temperature is approximated as being 6°C below the ambient temperature [9].

The developed analytical model is validated using experimental setup for LS-2 collectors [4]. From the experimental setup linear regression heat loss model is done after identifying the dominant factors that contribute to the heat loss from the heat transfer fluid through the collector.

These models are shown in Dudley et al. [4]. Lippke [16] has modified these linear regression models considering some neglected terms. Finally these models are updated to be used in TRNSYS Simulation software under STEC libraries [20].

2.10 Dudely Model

A multiple linear regression of calculated heat gain over the range of insolation from zero to 1100 W/m^2, and a temperature from ambient to 400°C produces a heat gain equation of the following form:

$$\dot{q} = A\,(DNI) - B\,(DNI)\,(\Delta T) - C\,(\Delta T) - D\,(\Delta T^2) \quad (2.44)$$

Where: $\dot{q}$ = Operating heat gain (W/m^2) at zero incident angle

ΔT = Average fluid temperature (^OC)

DNI = Direct normal insolation (W/m^2)

In this equation, A accounts for the optical efficiency above ambient air temperature of the trough and the absorbtivity of the selective coating without considering the losses at the end of a collector row. B, C and D describe the heat losses of the HCE dependent on its conditions with ΔT. The above equation is valid only at zero incident angle. An incident angle modifier term must be added to obtain collector heat gain at any other incident angle.

$$\dot{q} = K\,[A\,(DNI) - B\,(DNI)\,(\Delta T)] - C\,(\Delta T) - D\,(\Delta T^2) \quad (2.45)$$

When the heat gain from the above equation is divided by the incident inolation, an efficiency equation for the collector results, which should be valid over the full expected range of operating temperature, insolation, and incident angles.

$$\eta = K\,[A - B\,(\Delta T)] - C\,(\Delta T/DNI) - D\,(\Delta T^2/DNI) \quad (2.46)$$

The above equations are not complete physical models of the collector; rather they are empirical fits to experimental data. The following table summarizes the parameters as they were found in the test results.

Table 2-5 Values of the different coefficients of collector efficiency [16]

	A	B	C	D
Cermet, Vacuum	73.3	-0.007276	-0.496	-0.0691
Cermet, air	73.4	-0.004683	-14.40	-0.0637
Cermet, bare	74.7	-0.042-0.00927*Vwind/K	0	-0.000731*DNI
Black Chrome, Vacuum	73.6	-0.004206	7.44	-0.0958
Black Chrome, air	73.8	-0.006460	-12.16	-0.0641

The figure below illustrates equation of efficiency as derived from the test data for the LS-2 cermet/vacuum receiver, for several values of direct normal inolation.

$$\eta = 73.3\text{-}0.00728(\Delta T) - 0.496(\Delta T/DNI)\text{-}0.0691(\Delta T^2/DNI) \quad (2.47)$$

Where: η =efficiency in percent

ΔT = Temp in degrees C above ambient air temp

DNI = direct Normal Insolation in W/m^2

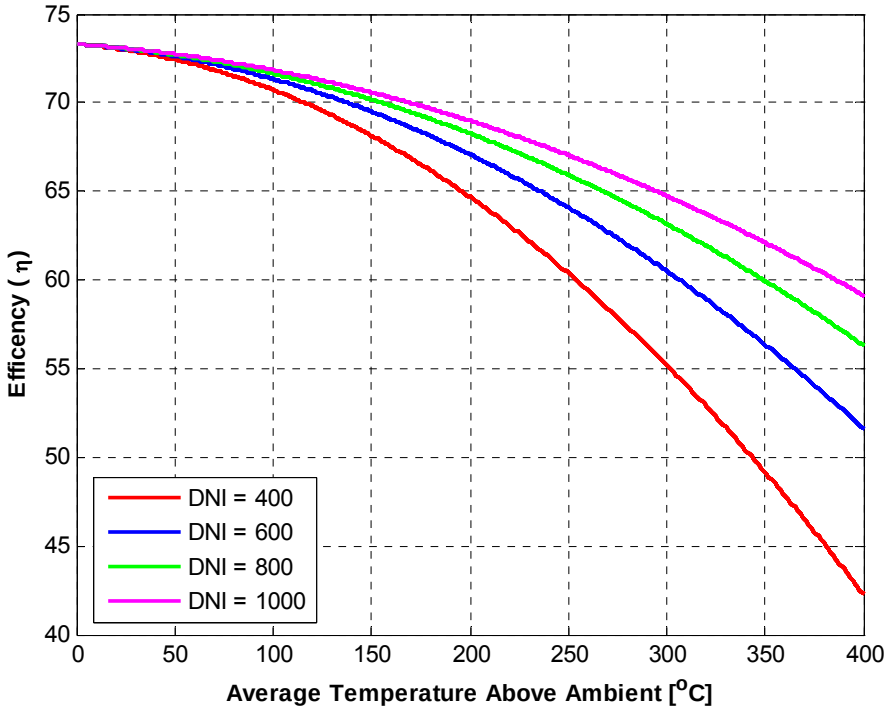

Figure 2-15 Efficiency of LS-2 cermet/vacuum receiver

2.11 Solar Thermal Electric Components (STEC) Model for a Parabolic Trough Collector

This model for a parabolic trough collector which is based on the model of Lippke [16] uses an integrated efficiency equation to account for the different fluid temperature at the field inlet and outlet of the collector field. It calculates the demanded mass flow rate of the heat transfer fluid to achieve a pre-defined outlet temperature Tout by [20]:

$$\dot{M} = \frac{\dot{Q}_{net}}{C_p\left(T_{out} - T_{in}\right)} \tag{2.48}$$

Using

$$\dot{Q}_{net} = \dot{Q}_{abs} - \dot{Q}_{pipe} \tag{2.49}$$

And

$$\dot{Q}_{abs} = A_{eff}.DNI.\eta \tag{2.50}$$

$$\eta = K.EL.RS.\left[A + B.\frac{\Delta T_{out} + \Delta T_{in}}{2.DNI}\right] + \left(C + C_w.WS\right).\frac{\Delta T_{out} + \Delta T_{in}}{2.DNI} + D.\frac{\Delta T_{out}.\Delta T_{in} + \frac{1}{3}\left(\Delta T_{out} + \Delta T_{in}\right)^2}{DNI} \tag{2.51}$$

This is the absorber efficiency model as presented in Lippke. In the above equation the different coefficients are described below.

- The coefficients A, B, C, C_w and D are empirical factors describing the performance of the collector. They can be found for the SEGS LS-2 collector e.g. in [4].
- The factor K is the incident angle modifier, EL considers end losses and RS considers shading of parallel rows. Evaluation of these parameters is described as shown above.
- ΔT_{in} and ΔT_{out} are the difference between collector inlet or outlet temperature and ambient temperature and DNI is the direct normal irradiation. $\dot{Q}_{piping}$ accounts for losses in the piping and expansion vessel using empirical coefficients.

2.12 Piping and Expansion Vessel Heat Losses

In the operation of a distributed Solar Power Plant, the heat losses in all the piping are important and have to be included in the model. Additionally, the heat losses in the expansion vessel, which has a large surface area, should be included in the calculations. Both heat losses are

considered to be temperature dependent. The following dependency was implemented in the model [16]:

$$\dot{Q}_{pipe} = \dot{Q}_{piping} + \dot{Q}_{Expansion\,Vessel} \tag{2.52}$$

$$\dot{Q}_{pipe} = 20\frac{W}{m^2} A_{SF} \frac{T_{avg}}{343^o C} + 2.57 \times 10^6 W \frac{T_{avg}}{275^o C} \tag{2.53}$$

Here, heat losses of all the piping of 20 W per meter square aperture area, A_{eff}, are assumed at full power at a mean solar field temperature above ambient of about T_{avg} = 343^{O}C. The radiation and mixed convection heat losses of the expansion vessel is estimated to be 2.57 MW at 300^{O}C field outlet temperature (275^{O}C mean field temperature) assuming poor insulation conditions [16].

The parabolic trough model of the STEC library is used in the MATLAB modeling of the power plant at full load to calculate the effective area of the solar field and the number of the solar collecting assembly (SCA) needed. The STEC TRNSYS components are used to simulate the power plant at weather conditions off reference conditions.

CHAPTER 3

POWER PLANT MODEL

3.1 Introduction

This is a proposed power plant that operates using Rankine power cycle principle. The power plant uses a solar field replacing a boiler to produce steam. The power plant is designed to produce 10 MWe. The area of the solar field which is necessary to generate the rated capacity is calculated using MATLAB software using reference weather condition of Addis Ababa. The city is chosen because its detailed weather condition can be easily found.

The power plant has two high pressure and three low pressure turbines. Accordingly there are two high and one low pressure closed feed water heaters (CFWHs). Between the high pressure and low pressure feed water heaters a deaerator exists. The complete diagram of the power plant with state points included is shown in Figure 3-1.

Steam flows from the last turbine stage in to the condenser. The condensate is then pumped to low pressure CFWH. Next the feedwater flows through the deaerator. Feed water pump is used to force the feedwater to the two high pressure CFWHs and then finally to the heat exchanger train. The heat exchanger train consists of a superheater, steamgenerator, and feedwater preheater, in series, as well as a reheater in parallel with the other three heat exchangers.

The power cycle begins by collecting the HTF returning from the solar field in an expansion vessel. The expansion vessel serves to compensate for variation in the volume of the heat transfer fluid throughout the day, since the specific volume of the HTF is dependent on temperature. The heat transfer fluid is pumped from the expansion vessel and delivered to the heat exchanger train as the energy source for the power cycle.

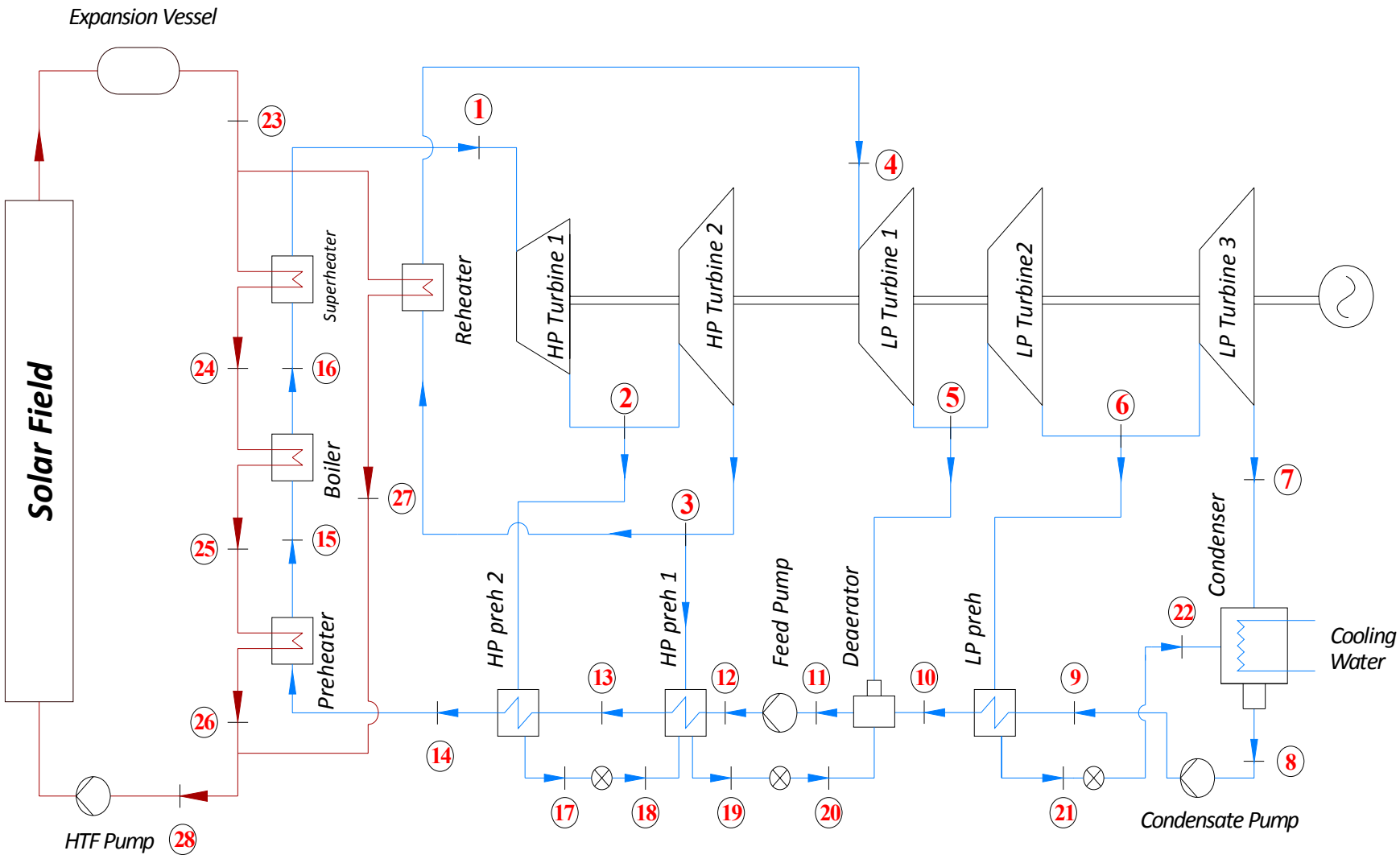

Figure 3-1 Steam power plant

3.2 Initial temperature and pressure of the steam

One way of improving the thermal efficiency of convectional steam power plant is to increase the average temperature at which heat is transferred to the working fluid in the boiler. One way of increasing the average temperature during the heat-addition process is to increase the operating pressure of the boiler, which automatically raises the temperature at which boiling takes place. This, in turn, raises the average temperature at which heat is transferred to the water/steam and thus raises the thermal efficiency of the cycle, [3].

Today, supercritical power plants, pressure greater than the critical pressure of water (P >22.09 Mpa), are common. These power plants are expensive due to metallurgical reasons and are used for nuclear plants.

An important parameter in the optimization of a steam cycle is the temperature difference rating (the "Pinch point") of a boiler, which affects the amount of steam generated. By reducing the pinch point, the rate of energy utilization in a boiler can be influenced within certain limits. However, the surface of the heat exchanger increases exponentially, which quickly sets a limit for the utilization rate [15]. The optimum pinch point considering the effect of surface of the heat exchangers in the boiler and the thermal efficiency is $15^{O}C$.

The initial temperature of steam entering to the first high pressure turbine can be decided by assuming that the inlet temperature of the HTF in to the superheater. Therminol-VP1 stays liquid up to a temperature of 400 ^{O}C. In this designed power plant the inlet HTF temperature is taken to be 390 ^{O}C. Thus the initial temperature of steam entering to the first high pressure turbine cannot be greater than 390 ^{O}C. Thus in the current analysis a temperature equal to T =375 ^{O}C is taken as the initial temperature of steam entering to the first high pressure turbine. The corresponding initial pressure is found by taking the pinch point 15 ^{O}C. A MATLAB code is used to find the initial pressure after giving first guess for the initial pressure and checking the error. This initial pressure is found to be P (1) = 83.434 [bar]. This pressure is found for the HTF outlet temperature from the preheater of 300 ^{O}C.

The outlet temperature of the HTF from the preheater affects the solar field area, the boiler pressure of the steam, and the thermal efficiency. With the increase of this temperature, the solar

field area decreases while the boiler pressure and the thermal efficiency increase. As explained above there is a limit to boiler pressure to be used. Considering this the optimum HTF outlet temperature from the preheater is taken to be $300^{O}C$. Table 3.1 show the effect of this temperature on solar field, boiler pressure, and thermal efficiency. The values in this table are found from the written MATLAB code.

Table 3-1 Effect of the outlet HTF temperature from the Preheater

HTF Outlet Temp. (^{O}C)	Solar Field Area (m^2)	Boiler Pressure (bar)	Thermal Efficiency (%)
290	81913	72.434	37.15
295	81807	77.434	37.38
300	81670	83.434	37.62
305	81589	89.434	37.84
310	81561	95.434	38.04

3.3 Determination of Bled steam Pressures

The pressures at which steam is to be bled from the turbine that will result in the maximum increase in efficiency (or maximum reduction in heat rate) can be obtained accurately by a complete optimization of the cycle which entails large complex and usually not readily available computer programs.

There is, however, a simple approach based on physical reasoning. The role of feedwater heaters is to bring the temperature of the feedwater as close as possible to that of the steam generator before the feedwater enters the steam generator.

Thus the optimum, from an efficiency point of view, of the pressure at which the feedwaters are to be placed is obtained by finding the temperature difference that would divide the temperature difference between the boiler (saturation temperature of the boiler) and the condenser temperature in to equal parts that are equivalent to the number of feedwater heaters [7].

$$\Delta T_{opt} = \frac{T_B - T_C}{n+1} \tag{3.1}$$

Where: ΔT_{opt} = the optimum temperature difference between the feedwater heaters

T_B = the saturation temperature of the boiler

T_C = the condenser temperature, and

n = the number of feedwater heaters

As previously discussed the boiler pressure is equal to 83.434 [bar]. The saturation temperature for this boiler pressure is T_B = 297.96 ^{O}C. The condenser pressure is selected to be equal to 8 kPa. This pressure is selected taking the cooling water inlet temperature equal to atmospheric temperature (near to 25 ^{O}C). In the condenser the cooling water is designed to have a temperature rise of 11.5^{O}C.The terminal temperature difference is selected to be equal to 5^{O}C. This gives the condenser temperature T_C = 41.5^{O}C. The corresponding saturation pressure for this condenser temperature is equal to 8 kPa.

It has been indicated that in this analysis there are three closed feedwater heaters and one open feedwater heater. Thus the total number of feedwater heaters is four. Finally the optimum temperature difference can be calculated as shown below:

$$\Delta T_{opt} = \frac{297.96^{O}C - 41.5^{O}C}{4+1} = 51.29^{O}C$$

The temperature of the low pressure heater becomes:

$$T_{Lpheater} = T_C + 51.29^{O} = 92.8^{O}C$$

The corresponding saturation pressure for this temperature is equal P_6 = 77.983 kPa. Similar analysis is done for the remaining closed feedwater heaters and the deaerator. The results are shown in Table 3-2.

Table 3-2 State point temperature determination

Component	Temperature	P_{Sat}
Lp heater	$T_{Lpheater} = T_C + 51.29^O = 92.8^O C$	77.983 kPa
Deareator	$T_{Deareator} = T_{Lpheater} + 51.29^O = 144.09^O C$	4.0532 bar
Hp heater 1	$T_{Hpheater\_1} = T_{Deareatorr} + 51.29^O = 195.38^O C$	14.1 bar
Hp heater 2	$T_{Hpheater\_2} = T_{Hpheater\_1} + 51.29^O = 246.67^O C$	37.57 bar

The above temperatures are the exit temperatures of the feedwater heaters that are only to be used if ideal cycles are used. In an ideal closed feedwater heater, the feedwater is heated to the exit temperature of the extracted steam, which ideally leaves the heater as a saturated liquid at the extraction pressure. In actual power plants, the feedwater leaves the heater below the exit temperature of the extracted steam because a temperature difference of at least a few degrees is required for any effective heat transfer to take place.

The condensed steam is then either pumped to the feedwater line or routed to another heater or to the condenser through a device called a trap. A trap allows the liquid to be throttled to a lower pressure region but traps the vapor. The enthalpy of steam remains constant during this throttling process, [3]. In this designed power plant the condensed steam is cascaded backwards to another feedwater through a trap.

3.4 Component Modeling

3.4.1 Superheater/Reheater

The superheater and reheater are both shell-and-tube heat exchangers that increase the temperature of the inlet steam (which enters at or near saturated vapor) beyond the saturation temperature corresponding to the prevailing operating pressure. The same model is used for both components. Figure 3-2 shows the flow diagram for the superheater/reheater components.

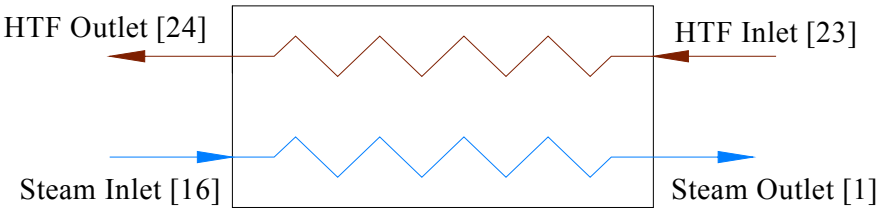

Figure 3-2 Flow diagram of the Superheater with state points shown

The thermal performances of the superheater and reheater are expressed in terms of the effectiveness of each component. Heat exchanger effectiveness is defined as the actual heat transfer realized between streams over the maximum heat transfer possible for the given streams [12]:

$$\varepsilon = \frac{\dot{Q}}{\dot{Q}_{\max}} \tag{3.2}$$

To evaluate $\dot{Q}_{\max}$ it is first necessary to define the heat capacitance of each fluid stream. The heat capacitance of a given stream will equal the mass flow rate of the stream multiplied by the specific heat of the fluid:

$$\dot{C}_c = \dot{m}_{steam}.C_{p,steam} \tag{3.3}$$

$$\dot{C}_H = \dot{m}_{HTF}.C_{p,HTF} \tag{3.4}$$

Where: $\dot{C}_c$ = capacitance rate of the cold side fluid (steam) [kW/K]

$\dot{C}_H$ = capacitance rate of the hot side fluid (HTF) [kW/K]

$\dot{m}_{steam,HTF}$ = mass flow rate of the steam or HTF [kg/s]

$C_{p,steam}$ = average specific heat of steam between inlet and outlet [kJ/kg-K]

$C_{p,HTF}$ = average specific heat of HTF between inlet and outlet [kJ/kg-K]

The average specific heat for each stream is the difference in enthalpy of the stream inlet and exit, divided by the temperature difference between inlet and exit.

$$C_{p,steam} = \frac{h_{steam,out} - h_{steam,in}}{T_{steam,out} - T_{steam,in}} \tag{3.5}$$

$$C_{p,HTF} = \frac{h_{HTF,out} - h_{HTF,in}}{T_{HTF,out} - T_{HTF,in}} \tag{3.6}$$

The maximum heat transfer possible between streams will equal the smaller total heat capacitance of the two fluid streams, multiplied by the difference in inlet temperatures between the streams.

$$\dot{Q}_{\max} = C_{\min}\left(T_{HTF,in} - T_{steam,in}\right) \tag{3.7}$$

Where:

$$C_{\min} = MIN(\dot{C}_C, \dot{C}_H) \tag{3.8}$$

The effectiveness of the heat exchanger is related to two parameters: the capacitance rate ratio of the fluid streams, and the number of transfer units (NTU) for the heat exchanger. The capacitance rate ratio of the fluid streams is the ratio of the smaller total heat capacitance of the two streams to the larger heat capacitance of the streams.

$$C_r = \frac{C_{\min}}{C_{\max}} \tag{3.9}$$

Where:

$$C_{\max} = MAX(\dot{C}_C, \dot{C}_H) \tag{3.10}$$

The NTU is defined as the overall heat transfer conductance-area product (UA) per unit heat capacitance of the smaller capacity fluid.

$$NTU = \frac{UA}{C_{\min}} \tag{3.11}$$

For shell and tube heat exchanger with one shell pass and two tube passes the following relationship determines heat exchanger effectiveness as a function of capacitance ratio and NTU [12]:

$$\varepsilon = 2\left\{1 + C_r + \left(1 + C_r{}^2\right)^{1/2} \times \frac{1 + e^{\left[-NTU\left(1+\left(1+C_r{}^2\right)^{1/2}\right)\right]}}{1 - e^{\left[-NTU\left(1+\left(1+C_r{}^2\right)^{1/2}\right)\right]}}\right\}^{-1} \tag{3.12}$$

Once $\dot{Q}_{\max}$ and the effectiveness have been calculated, the actual heat transfer between fluid streams is determined as:

$$h_{steam,out} = h_{steam,in} + \frac{\dot{Q}}{\dot{m}_{steam}} \tag{3.13}$$

Outlet temperature is determined from the outlet enthalpy and outlet pressure of the steam:

$$T_{steam,out} = \left(h_{steam,Out}, P_{steam,Out}\right) \tag{3.14}$$

The exit enthalpy of the HTF is determined from an energy balance on the fluid:

$$h_{HTF,Out} = h_{HTF,in} + \frac{\dot{Q}}{\dot{m}_{HTF}} \tag{3.15}$$

Continuity requires the mass flow rates of the HTF and steam at the respective outlets to equal the mass flow rates of each steam at their inlet.

$$\dot{m}_{steam,in} = \dot{m}_{steam,Out} \tag{3.16}$$

$$\dot{m}_{HTF,in} = \dot{m}_{HTF,Out} \tag{3.17}$$

The UA for the heat exchanger at the reference state is provided as a parameter to the exchanger model. At partial loads, the UA will decrease with the decreasing flow rates of the streams. The

relationship between the reference UA/flow rate and a reduced UA/flow rate can be derived as follows. The UA of an un-finned, tubular heat exchanger is defined as the total thermal resistance to heat transfer between two fluids [12]:

$$\frac{1}{UA} = \frac{1}{h_i A_i} + \frac{R''_{fi}}{A_i} + \frac{\ln D_o / D_i}{2\pi kL} + \frac{R''_{fo}}{A_o} + \frac{1}{h_o A_o} \tag{3.18}$$

Where: h = convection heat transfer coefficient [W/m^2-K]

A = surface area [m^2]

R'' = fouling factor, per unit area [m^2-K/W]

D = diameter [m]

k = thermal conductivity of the material between the fluids [W/m-K]

L = length of the heat exchanger [m]

i (subscript) = property of the inner surface of the heat exchanger

o (subscript) = property of the outer surface of the heat exchanger

Equation (3.18) can be simplified if it is assumed that there is negligible fouling in the heat exchangers and that the thermal resistance through the tubes can be neglected. With these assumptions, Equation (3.18) reduces to:

$$\frac{1}{UA} = \frac{1}{h_i A_i} + \frac{1}{h_o A_o} \tag{3.19}$$

In Equation (3.19), UA is a function of the inner and outer surface areas of the tubes and the heat transfer coefficient of each fluid. The surface area of the tubes will not change with partial load conditions. The heat transfer coefficients are a function of the Nusselt number:

$$h = \frac{Nu.k_{fluid}}{D} \tag{3.20}$$

Where: Nu = the Nusselt number

k_{fluid} = the thermal conductivity of the fluid

D = the hydraulic diameter

Assuming that the flow for both fluids is fully developed (hydro-dynamically and thermally) and turbulent through smooth circular tubes, the Nusselt number can be expressed as a function of the Reynolds number (Re) and Prandtl number (Pr) by:

$$Nu_D = 0.023.\mathrm{Re}_D^{0.8}.\mathrm{Pr}^n \tag{3.21}$$

Where: n = 0.4 for heating fluid and n = 0.3 for cooling fluid.

Definitions of the Reynolds number and the Prandtl number complete the equations:

$$\mathrm{Re}_D = \frac{4.\dot{m}}{\pi D\mu} \tag{3.22}$$

Where: μ = dynamic fluid viscosity [N-s/m^2]

$$\mathrm{Pr} = \frac{\mu.C}{k_{fluid}} \tag{3.23}$$

Where: c = specific heat of fluid [kJ/kg-K]

Assuming constant fluid properties, the Prandtl number will be constant for each fluid, and the Reynolds number will vary only with mass flow rate of the fluid. From Equation (3.20), the heat transfer coefficient is proportional to the Nusselt number. Therefore, assuming constant fluid properties, the heat transfer coefficient is proportional to the mass flow rate raised to the 0.8 power:

$$h\ \alpha\ NU \Rightarrow h\ \alpha\ \mathrm{Re}^{0.8} \Rightarrow h\ \alpha\ \dot{m}^{0.8} \tag{3.24}$$

From Equation (3.19), the UA of a heat exchanger must be proportional to the fluid stream mass flow rate as follows:

$$\frac{1}{UA} \alpha \frac{1}{\dot{m}_i^{0.8}} + \frac{1}{\dot{m}_o^{0.8}} \tag{3.25}$$

The same correlation can be written for the reference UA, as a function of its reference inner and outer fluid mass flow rates:

$$\frac{1}{UA_{REF}} \alpha \frac{1}{\dot{m}_{i,REF}^{0.8}} + \frac{1}{\dot{m}_{o,REF}^{0.8}} \tag{3.26}$$

Combining equation (3.25) and (3.26), the partial load UA and mass flow rates relate to the reference UA and mass flow rates through the following relationship:

$$\frac{UA}{UA_{REF}} = \frac{\frac{1}{\dot{m}_{i,REF}^{0.8}} + \frac{1}{\dot{m}_{o,REF}^{0.8}}}{\frac{1}{\dot{m}_i^{0.8}} + \frac{1}{\dot{m}_o^{0.8}}} = \left(\frac{\dot{m}_i^{0.8} . \dot{m}_o^{0.8}}{\dot{m}_{i,REF}^{0.8} . \dot{m}_{o,REF}^{0.8}} \right) \left(\frac{\dot{m}_{i,REF}^{0.8} + \dot{m}_{o,REF}^{0.8}}{\dot{m}_i^{0.8} + \dot{m}_o^{0.8}} \right) \tag{3.27}$$

Finally, it is assumed that the mass flow rates of the inner and outer fluids remain in the same proportion at partial load conditions as at the reference load so that:

$$\frac{\dot{m}_i}{\dot{m}_o} = \frac{\dot{m}_{i,REF}}{\dot{m}_{o,REF}} = K \tag{3.28}$$

Substituting Equation (3.28) into Equation (3.27) and simpe

$$\frac{UA}{UA_{REF}} = \frac{\frac{1}{K . \dot{m}_{o,REF}^{0.8}} + \frac{1}{\dot{m}_{o,REF}^{0.8}}}{\frac{1}{K . \dot{m}_o^{0.8}} + \frac{1}{\dot{m}_o^{0.8}}} = \left(\frac{K . \dot{m}_o^{0.8} . \dot{m}_o^{0.8}}{K . \dot{m}_{o,REF}^{0.8} . \dot{m}_{o,REF}^{0.8}} \right) \left(\frac{\dot{m}_{o,REF}^{0.8} (K+1)}{\dot{m}_o^{0.8} (K+1)} \right) \tag{3.29}$$

Further simplification of Equation (3.29) results in the desired relation.

$$\frac{UA}{UA_{REF}} = \left(\frac{\dot{m}_o}{\dot{m}_{o,REF}} \right)^{0.8} = \left(\frac{\dot{m}_i}{\dot{m}_{i,REF}} \right)^{0.8} \tag{3.30}$$

3.4.2 Steam Generator (Boiler)

The steam generator is a shell-and-tube heat exchanger with liquid feedwater on the shell side and hot HTF through the tube side. Feedwater bs on the surface of the HTF tubes and rises to exit the steam generator as saturated vapor. The flow through the steam generator is controlled such that a constant feedwater level is maintained in the vessel. Figure 3.3 shows the flow diagram for the steam generator.

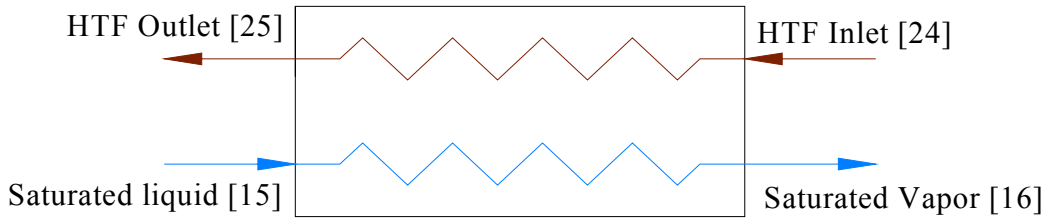

Figure 3-3 Flow diagram for the Steamgenerator with the state points shown

The effectiveness of the steam generator is determined from an effectiveness/NTU relationship, in which the effectiveness and the number of transfer units (NTU) are as defined in Equations (3.2) and (3.11), respectively. In changing phase from saturated liquid to saturated vapor, the heat capacitance of the feedwater/steam is infinite; therefore, the minimum capacitance of the two fluids as defined by Equation (3.8) will always be the capacitance of the hot side fluid (the heat transfer fluid)

$$C_{MIN} = \dot{m}_{HTF}\left(\frac{h_{HTF,in} - h_{HTF,out}}{T_{HTF,in} - T_{HTF,Out}}\right) \tag{3.31}$$

Given that the heat capacitance of the feedwater/steam is effectively infinite, the capacitance ratio as defined in Equation (3.9) for this heat exchanger is zero. Under these conditions, the appropriate effectiveness/NTU relationship for the heat exchanger is [12]:

$$\varepsilon = 1 - \exp(-NTU) \tag{3.32}$$

Where NTU is defined by Equation (3.11)

The exit enthalpy of the steam is assumed to be that of saturated vapor at the inlet pressure to the steam generator (assume no pressure drop over the steam generator):

$$P_{steam,in} = P_{steam,Out} \tag{3.33}$$

$$h_{steam,Out} = h\left(P_{steam,Out}, x = 1\right) \tag{3.34}$$

The mass flow rate of feedwater/steam through the steam generator may be determined from the heat transfer between fluids over the difference in enthalpy from feedwater inlet to steam outlet:

$$\dot{m}_{steam,out} = \frac{\dot{Q}}{\left(h_{steam,out} - h_{steam,in}\right)} \tag{3.35}$$

The exit enthalpy of the HTF is determined from the inlet enthalpy of the HTF minus the heat transfer per unit HTF mass flow rate:

$$h_{HTF,out} = h_{HTF,in} - \frac{\dot{Q}}{\dot{m}_{HTF}} \tag{3.36}$$

Outlet temperature of the heat transfer fluid can be determined as a function of enthalpy by the correlation given in Equation (2.2).

The mass flow rates of the HTF and steam at the outlet will equal the mass flow rates of the streams at the inlet.

$$\dot{m}_{feedwater,in} = \dot{m}_{steam,out} \tag{3.37}$$

$$\dot{m}_{HTF,in} = \dot{m}_{HTF,out} \tag{3.38}$$

3.4.3 Preheater

The preheater raises the temperature of the feedwater from its temperature at the outlet of heater (HP preheater 2) to its saturation temperature at the preheater outlet pressure. Figure 3-4 shows the flow diagram for the HTF – steam preheater.

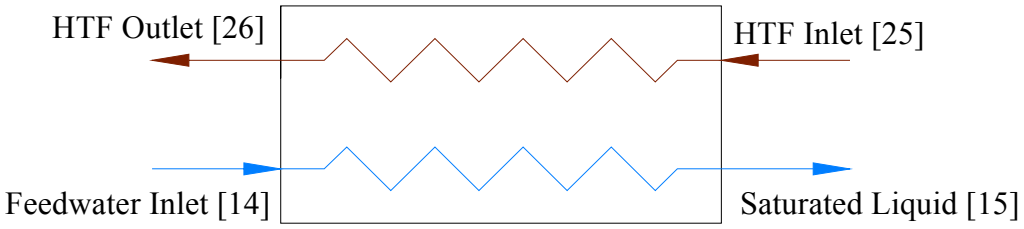

Figure 3-4 Flow diagram of the Preheater with state points shown

The preheater is modeled assuming that the feedwater exit state will be saturated liquid at the outlet pressure of the preheater.

$$h_{feedwater,out} = h\left(P_{feedwater,out}, x = 0\right) \tag{3.39}$$

The heat transfer to the feedwater is calculated, given the feedwater mass flow rate and the known inlet and outlet states of the feedwater:

$$\dot{Q} = \dot{m}_{feedwater}\left(h_{feedwater,out} - h_{feedwater,in}\right) \tag{3.40}$$

For an adiabatic heat exchanger, the heat transfer to the feedwater must equal the heat transfer from the HTF. The exit enthalpy of the HTF (and consequently the HTF exit temperature) is determined from the heat transfer between streams and the HTF mass flow rate:

$$h_{HTF,ou}t = h_{HTF,in} - \frac{\dot{Q}}{\dot{m}_{HTF}} \tag{3.41}$$

Outlet temperature of the heat transfer fluid is determined from outlet enthalpy using the correlation from Equation (2.2).

The overall heat transfer coefficient of the preheater is calculated in a same way as the superheater and the reheater. The outlet temperature of the preheater is the saturation temperature of the steamgenerator pressure (P = 83.43 bar) while the inlet temperature is equal to the outlet temperature of the high pressure preheater 2.

3.4.4 Turbine

The main purpose of the turbines is converting the potential energy of a steam stored as a form pressure and temperature to a rotational mechanical energy. This rotational mechanical energy is then converted to electrical energy by a generator.

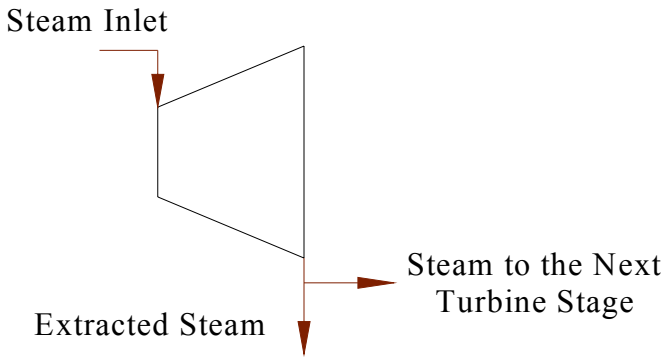

Figure 3-5 Flow diagram for one turbine stage

As explained above in this proposed power plant there are two high and three low pressure turbine stages. At the outlet of each stage mass is extracted to increase the temperature of water in the corresponding feedwater heater. The mass flow of steam demanded by each feedwater heater is determined using the feedwater heater models. The mass flow continuing to the next turbine section is the mass flow into the turbine minus the mass flow of any extractions previous to that section.

The performance of each turbine stage is defined by its isentropic efficiency. The isentropic efficiency of a turbine stage is the ratio of the change in enthalpy of the fluid to the change that would have occurred in an isentropic (reversible) turbine:

$$\eta_{turbine} = \frac{h_{steam,in} - h_{steam,out}}{h_{steam,in} - h_{steam,s}} \tag{3.42}$$

Where $h_{steam,s}$ is the enthalpy that would have occurred at the outlet of the turbine if it were an isentropic process. This ideal enthalpy is evaluated using the outlet pressure and inlet entropy of the fluid:

$$h_{steam,s} = h\left(P_{steam,out}, s_{steam,in}\right) \tag{3.43}$$

The isentropic efficiency of a turbine is determined by measuring the actual work output, and computing the work output from the measured inlet state and the outlet pressure. Isentropic efficiency of turbines usually ranges from 70 % to 90 % [14]. In this modeled power plant the isentropic efficiency of the turbines is taken to be 85 %.

The work per unit mass performed by the turbine stage is equal to the change in fluid enthalpy over the turbine stage:

$$W_{stage} = h_{steam,in} - h_{steam,out} \tag{3.44}$$

As shown in preceding sections the pressures of the feedwater heaters are determined. These pressures are equal to the pressures of the extracted steam to the corresponding heater and to the outlet pressures of the corresponding turbine stage. The outlet pressure of the turbine stage is the inlet pressure to the next turbine stage. The inlet and outlet pressures of each turbine stage are shown in a Table 3-2.

Table 3-3 Inlet and outlet pressures of the Turbines

Name	Inlet pressure (bar)	Outlet Pressure (bar)
Hp Turbine 1	P(1) = 83.434	P(2) = 37.57
Hp Turbine 2	P(2) = 37.57	P(3) = 14.1
Lp Turbine 1	P(4) = 14.1	P(5) = 4.0532
Lp Turbine 2	P(5) = 4.0532	P(5) 0.77983
Lp Turbine 3	P(6) = 0.77983	P(7) = 0.08

3.4.5 Condenser

After exiting the last low pressure turbine stage, the working fluid proceeds to the condenser. The condenser is a closed shell-and-tube heat exchanger, with cooling water flowing on the tube side and condensing steam from the turbine on the shell side. The function of the condenser is to condense the turbine exhaust from vapor to liquid, so the working fluid can be pumped back to the boiler. Figure 3-6 shows the flow diagram for the condenser.

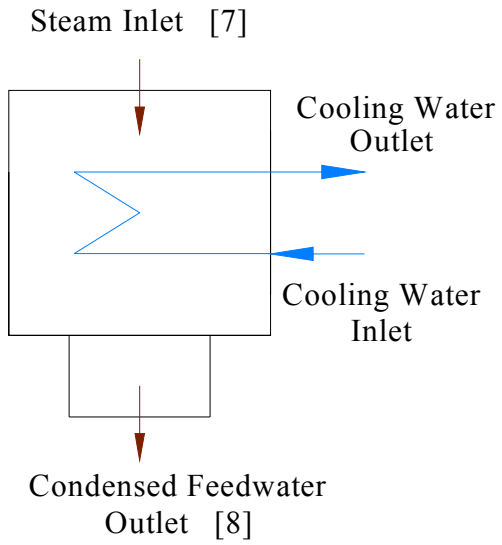

Figure 3-6 Flow diagram of the condenser with state points shown

It is assumed that there is no pressure drop in the steam side of the condenser, and that no subcooling occurs in the condenser. The enthalpy of the condensate at the condenser outlet equals the saturated liquid enthalpy at the condensing pressure:

$$P_{steam,in} = P_{feedwater,out} \tag{3.45}$$

$$h_{feedwater,out} = h\left(P_{feedwater,out}, X = 0\right) \tag{3.46}$$

3.4.6 Pump

The pumps in the cycle serve to increase the pressure of the working fluid. There are two pumping processes on the working fluid side of the power cycle. One set of pumps is located at

the condenser outlet, to pump the fluid from its condensing pressure to flow through the low pressure feedwater heaters and deaerator. Another set of pumps is located at the deaerator outlet, to pump the fluid from the extraction pressure to the high pressures required at the boiler inlet. Figure 3-7 shows the flow diagram for a pump.

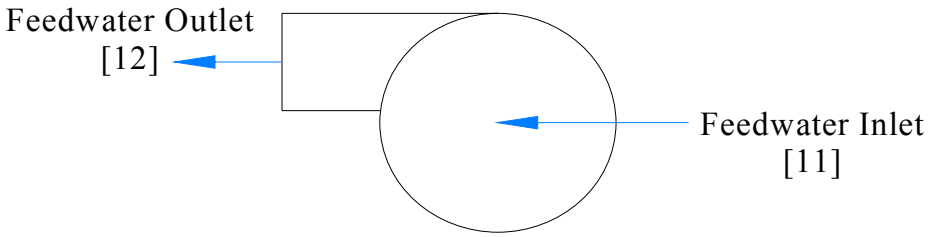

Figure 3-7 Flow diagram of the Feedwater Pump with state points shown

Pump performance is characterized by its isentropic efficiency. The isentropic efficiency of the pump is the ratio of the isentropic (reversible) change in enthalpy of the fluid to the change in enthalpy that actually occurred:

$$\eta_{pump} = \frac{h_{feedwater,in} - h_{feedwater,out,s}}{h_{feedwater,in} - h_{feedwater,out}} \tag{3.47}$$

Where $h_{feedwater,out,s}$ is the enthalpy that would have occurred were the pumping process isentropic. This ideal enthalpy is evaluated using the desired outlet pressure and inlet entropy of the fluid:

$$h_{feedwater,out,s} = h\left(P_{feedwater,out}, S_{feedwater,in}\right) \tag{3.48}$$

Isentropic efficiency of pumps depends on their design and can range from below 70 % to above 85 % [14]. A reference isentropic efficiency of 0.75 (including both pump efficiency and motor efficiency) is assumed for both pumps. The pump efficiency will change with changing load conditions. In the current analysis, the pumps are assumed to operate at maximum efficiency at the corresponding reference states. For constant speed pumps, the change in pump efficiency is expressed as a function of the change in mass flow rate is expressed as [16]:

$$\frac{\eta_{pump}}{\eta_{pump,REF}} = 2\frac{\dot{m}}{\dot{m}_{REF}} - \left(\frac{\dot{m}}{\dot{m}_{REF}}\right) \tag{3.49}$$

The work performed by the pump per unit mass is the change in fluid enthalpy from inlet to outlet:

$$\dot{W}_{pump} = h_{feedwater,in} - h_{feedwater,out} \tag{3.50}$$

Note that the enthalpy of the feedwater at the inlet will always be lower than the enthalpy of the feedwater at the outlet, and thus values for pump work are negative with the sign convention assumed here.

3.4.7 Closed Feedwater Heater

A closed feedwater heater is a shell-and-tube heat exchanger with high pressure feedwater in the tube side and condensing steam extracted from the turbine on the shell side. In essence, a closed feedwater heater is a small condenser that operates at much higher pressure than the main condenser [6]. Closed feedwater heaters are added to the cycle to preheat the steam generator feedwater. While steam extraction for feedwater heating decreases the power output of the turbine, it also increases the temperature of the feedwater to the boiler, reducing the need for heat addition from the solar field and increasing the efficiency of the cycle. Figure 3-8 shows the flow diagram for a closed feedwater heater.

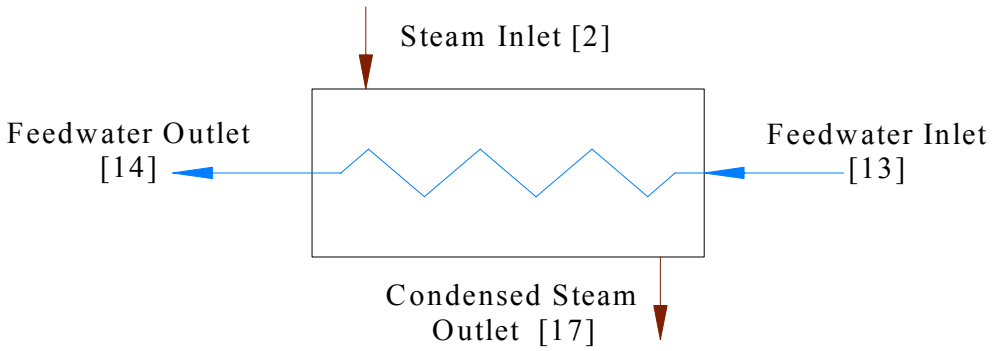

Figure 3-8 Flow diagram of the HP preheater 2 (see Figure 3-1)

Heat transfer in the closed feedwater heater will occur through three zones; the desuperheating zone, in which the steam is reduced to saturated vapor, the condensing zone, in which the steam condenses from saturated vapor to saturated liquid, and a subcooling or drain cooling zone, in which the condensed steam is cooled to a temperature below its saturation temperature. The size and conductance of heat exchangers are characterized by an overall heat transfer coefficient (UA). Each zone in the closed feedwater heater will have an associated UA value. It is assumed here that the condensing zone of each feedwater heater is sufficiently large in comparison to the desuperheating and subcooling zones that the desuperheating and subcooling zones can be neglected. An overall UA for each feedwater heater is defined assuming steam is condensing throughout the length of the feedwater heater.

The exit enthalpy of the condensed steam (condensate) is that of saturated liquid at the inlet pressure to the feedwater heater, assuming that no pressure drop occurs over the condensing steam:

$$P_{steam,in} = P_{steam,out} \tag{3.51}$$

$$h_{steam,out} = h\left(P_{steam,out}, X = 0\right) \tag{3.52}$$

The mass flow rate of the inlet steam is the sum of the mass flow rates of the extracted steam and any drain water from succeeding feedwater heaters in series. Enthalpy of the inlet steam is a mass flow rate – weighted average of the enthalpy of the extracted steam and the enthalpy of any drain water from succeeding feedwater heaters in the series.

$$\dot{m}_{steam} = \dot{m}_{extraction} + \dot{m}_{condensate,in} \tag{3.53}$$

$$\dot{m}_{steam}.h_{steam,in} = \dot{m}_{extraction}.h_{extraction} + \dot{m}_{condensate,in}.h_{condensate,in} \tag{3.54}$$

$$hsteam,in = \frac{\dot{m}_{extraction}.h_{extraction} + \dot{m}_{condensate,in}.h_{condensate,in}}{\dot{m}_{steam}} \tag{3.55}$$

The heat transfer between streams may be calculated either from the change in enthalpy of the steam or from the change in enthalpy of the feed water.

$$\dot{Q}_{water} = \dot{m}_{water}.C_{pwater,in}\left(T_{water,out} - T_{water,in}\right) \tag{3.56}$$

$$\dot{Q}_{steam} = m_{steam}\left(h_{steam,in} - h_{condensate,out}\right) \tag{3.57}$$

But this heat transfer rates are equal for ideal cases. In the above equation the specific heat capacity of the inlet water is calculated at the given water temperature and pressure.

$$C_{p,water,in} = C_p\left(T_{water,in}, P_{water,in}\right) \tag{3.58}$$

The mass of steam can be calculated from equation (3.54):

$$\dot{m}_{steam} = \frac{\dot{Q}_{water}}{\left(h_{steam,in} - h_{condensate,out}\right)} \tag{3.59}$$

For simplification let:

$\dot{m}_e$ = extracted steam

$\dot{m}_{ci}$ = mass of the condensate inlet to the feedwater

$\dot{Q}_w$ = Heat transferred to the water/steam

h_s = the enthalpy of steam into the feedwater heater (Equation (3.54))

h_e = the enthalpy of the extracted steam

h_{co} = the enthalpy of the condensate out of the feedwater

h_{ci} = the enthalpy of the condensate into the feedwater

Equation (3.59) can be thus expressed as shown below.

$$\dot{m}_e + \dot{m}_{ci} = \frac{\dot{Q}_w}{\left(h_s - h_{co}\right)} \tag{3.60}$$

$$\dot{m}_e + \dot{m}_{ci} = \frac{\dot{Q}_w}{\left(\frac{\dot{m}_e.h_e + \dot{m}_{ci}.h_{ci}}{\dot{m}_e + \dot{m}_{ci}} - h_{co} \right)} \tag{3.61}$$

Rearranging the above equation gives,

$$\dot{m}_e + \dot{m}_{ci} = \frac{\dot{Q}_w \left(\dot{m}_e + \dot{m}_{ci} \right)}{\left(\left(\dot{m}_e.h_e + \dot{m}_{ci}.h_{ci} \right) - h_{co} \left(\dot{m}_e + \dot{m}_{ci} \right) \right)} \tag{3.62}$$

The above equation can be further simplified as shown below:

$$\begin{aligned} \dot{Q}_w \left(\dot{m}_e + \dot{m}_{ci} \right) = \dot{m}_e.\left(\left(\dot{m}_e.h_e + \dot{m}_{ci}.h_{ci} \right) - h_{co} \left(\dot{m}_e + \dot{m}_{ci} \right) \right) \\ + \dot{m}_{ci}.\left(\left(\dot{m}_e.h_e + \dot{m}_{ci}.h_{ci} \right) - h_{co} \left(\dot{m}_e + \dot{m}_{ci} \right) \right) \end{aligned} \tag{3.63}$$

Multiplying each term gives,

$$\begin{aligned} \dot{Q}_w.\dot{m}_e + \dot{Q}_w.\dot{m}_{ci} = \dot{m}_e{}^2.h_e + \dot{m}_e.\dot{m}_{ci}.h_{ci} - \dot{m}_e{}^2.h_{co} - \dot{m}_e.\dot{m}_{ci}.h_{co} \\ + \dot{m}_e.\dot{m}_{ci}.h_e + \dot{m}_{ci}{}^2.h_{ci} - \dot{m}_e.\dot{m}_{ci}.h_{co} - \dot{m}_{ci}{}^2.h_{co} \end{aligned} \tag{3.64}$$

Similar terms can be collected to give the following equation,

$$\dot{m}_e{}^2.\left(h_e - h_{co} \right) + \dot{m}_e \left(\dot{m}_{ci}.\left(h_e + h_{ci} - 2h_{co} \right) - \dot{Q}_w \right) + \dot{m}_{ci}.\left(\dot{m}_{ci}.\left(h_{ci} - h_{co} \right) - \dot{Q}_w \right) \tag{3.65}$$

Let:

$$a = \left(h_e - h_{co} \right) \tag{3.66}$$

$$b = \left(\dot{m}_{ci}.\left(h_e + h_{ci} - 2h_{co} \right) - \dot{Q}_w \right) \tag{3.67}$$

$$c = \dot{m}_{ci}.\left(\dot{m}_{ci}.\left(h_{ci} - h_{co} \right) - \dot{Q}_w \right) \tag{3.68}$$

Therefore from the above equations, the extracted steam for the feedwater can be calculated as shown below:

$$\dot{m}_e = \frac{-b + \sqrt{b^2 - 4ac}}{2a} \tag{3.69}$$

The expression under the square root is always positive because expression c is always negative. The exit enthalpy of the feedwater is set to be equal to the enthalpy of the condensate leaving the feedwater heater.

$$h_{feedwater,out} = h_{condensate,out} (3.70) \tag{3.70}$$

The outlet feedwater temperature can be determined as a function of the outlet pressure and outlet enthalpy using a property relation for water:

$$T_{feedwater,out} = T\left(P_{feedwater,out}, h_{feedwater,out}\right) \tag{3.71}$$

The mass flow rates of the feedwater and steam/condensate at the outlet will equal the mass flow rates of the streams at the inlet.

$$\dot{m}_{feedwater,in} = \dot{m}_{feedwater,out} \tag{3.72}$$

$$\dot{m}_{steam,in} = \dot{m}_{steam,out} \tag{3.73}$$

The performance of the closed feedwater heater is characterized by an effectiveness/NTU relationship, where effectiveness is defined as actual heat transfer over maximum heat transfer (Equation (3.2)) and NTU, the number of transfer units, is defined as the UA per unit heat capacitance of the smaller capacity fluid (Equation (3.11)). For the closed feedwater heaters, the smaller heat capacity of the two fluids will always be the heat capacity of the feedwater:

The maximum heat transfer is determined from the capacitance rate of the feedwater multiplied by the difference between inlet temperatures of the two streams:

$$\dot{Q}_{\max} = \dot{m}_{water} . C_{p,water,in} \left(T_{steam,in} - T_{feedwater,in}\right) \tag{3.74}$$

The ratio of actual heat transfer to maximum heat transfer establishes the reference effectiveness of the heat exchanger.

$$\varepsilon = \frac{\dot{Q}_{water}}{\dot{Q}_{\max}} \tag{3.75}$$

For a heat exchanger in which one fluid undergoes a phase change, the ratio of minimum to maximum fluid heat capacities is zero, and the effectiveness/NTU relationship is given in Equation below:

$$\varepsilon = 1 - \exp\left(- NTU_{water}\right) \tag{3.76}$$

Finally, the ratio of the NTU to the heat capacitance of the feed water equals the reference UA of the heat exchanger:

$$NTU_{water} = \frac{UA}{m_{water}.C_{p,water}} \tag{3.78}$$

The heat transfer between streams at the reference state is found from an energy balance using the enthalpies and mass flow rates of the streams provided at the reference states. The reference UAs will have to be adjusted for partial load operation. Equation (3.30) is used to express UA at partial load as a function of UA and mass flow at the reference load. In this application, the UA will vary with the mass flow of the feedwater through the feedwater heater:

$$\frac{UA}{UA_{REF}} = \left(\frac{\dot{m}_{feedwater}}{\dot{m}_{feedwater,REF}} \right)^{0.8} \tag{3.79}$$

3.4.8 Open Feedwater Heater (Deaerator)

The open feedwater heater, like the closed feedwater heaters, uses extracted steam from the turbine to preheat feedwater to the steam generator. Unlike the closed feedwater heaters, however, in the open feedwater heater the extracted steam is directly mixed with the feedwater.

Open feedwater heaters are more effective than closed feedwater heaters, and are beneficial for the removal of non-condensable substances from the feedwater [6]. The disadvantage of open feedwater heaters is that the outlet pressure cannot exceed the pressure of the extracted steam; an

additional pump is required at the feedwater exit to increase fluid pressure to boiling pressure. Figure 3-9 shows the flow diagram for the open feedwater heater.

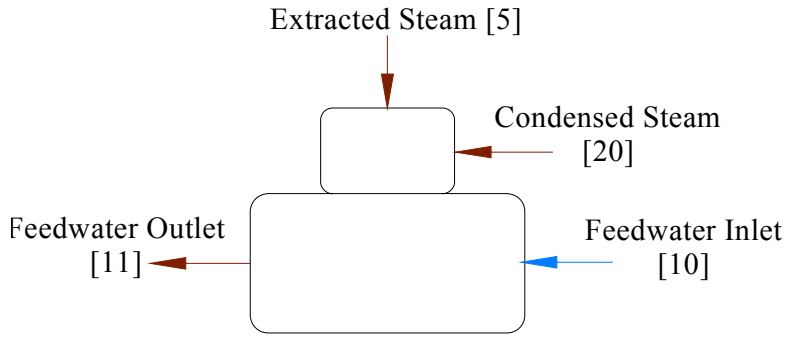

Figure 3-9 Flow diagram of the Open feedwater heater with state points shown

The open feedwater heater is modeled as a fluid mixer with three inlet streams and a single outlet stream (see Figure 3-1). The three inlet streams are the extracted steam from the first stage of the low pressure turbine (state (5)), the drain water from the high pressure feedwater heaters (state (20)), and the feedwater from the low pressure feedwater heaters (state (10)). The mass flow rate of the outlet stream is the sum of the mass flow rates of the three inlet streams:

$$\dot{m}_{steam,extracted} + \dot{m}_{steam,drain} + \dot{m}_{feedwater,in} = \dot{m}_{feedwater,out} \tag{3.80}$$

An energy balance indicates that the enthalpy of the feedwater at the outlet is equal to the weighted average of the enthalpies of the three streams entering the heater:

$$\dot{m}_{extract}.h_{extract} + \dot{m}_{drain} + \dot{m}_{feed,in}.h_{feed,in} = \dot{m}_{feed,out}.h_{feed,out} \tag{3.81}$$

Assuming that the feedwater exits as saturated liquid (x = 0), the enthalpy of the outlet is also equal to the saturated liquid enthalpy at the outlet pressure:

$$h_{feed,out} = h\left(P_{feed,out,X=0}\right) \tag{3.82}$$

Where the pressure at the feedwater outlet is assumed to be the pressure of the extracted steam (the outlet pressure cannot exceed this pressure):

$$P_{feedwater,out} = P_{steam,extracted} \tag{3.83}$$

Since the outlet state is saturated liquid, the temperature at the heater outlet is the saturation temperature at the outlet pressure:

$$T_{feedwater,out} = T\_SAT\left(P_{feedwater,out}\right) \tag{3.84}$$

3.5 Assumptions

The power cycle is modeled assuming all components are adiabatic and operating at steady state. Changes in potential and kinetic energy of fluid streams are assumed negligible. It is assumed that all steam generated provides useful work through the turbine, i.e., gland steam production as well as steam losses through line leaks are neglected. Also changes in fluid state between the outlet of one component and the inlet of the next are assumed negligible.

In this model power plant the collector are chosen to be LS -2. These collectors are chosen because a lot of research has been done on this collectors and enough information is found than other types of collector.

Correlations for the heat transfer fluid properties (Therminol VP-1) as a function of temperature are shown above. It is assumed that the fluid properties (enthalpy, density, and specific heat) do not have any significant dependence on pressure.

In the condenser and feedwater heaters, the condensing steam outlet is located beneath the steam inlet. Flow is held at steady state by maintaining a constant condensate level in the component.

Thus, vapor cannot exit the component. In the steam generator, the opposite situation occurs; the steam generator fluid exit is located above the inlet, and with a constant feedwater level in the steam generator, saturated liquid cannot exit. In addition to the aforementioned assumptions, which apply to all power cycle components, the following assumptions are made for the specific components:

- Preheater: feedwater exits the preheater as saturated liquid (x = 0)
- Steam generator: steam exits the steam generator as saturated vapor (x = 1)

• Closed feedwater heaters: condensed steam exits the heater as saturated liquid (x = 0)

• Open feedwater heater: feedwater exits the deaearator as saturated liquid (x = 0)

• Condenser: feedwater exits the condenser as saturated liquid (x = 0)

3.6 Results of Power Plant Model

The power plant model is done using MATLAB software. This model is used to determine all the state points, overall heat transfer coefficients of shell and tube heat exchangers, and the mass flow rate of the HTF/steam. The MATLAB model developed is also used to determine the area of the solar field needed to meet the needed mass flow rate of the water.

The procedure to find this area is explained below:

- The total energy needed by the steam to raise its temperature from outlet of the last feedwater to the inlet of the first turbine at the given pressure can be determined since all the temperatures are known. This energy is the net energy demanded from the HTF. Next to that the HTF temperature inlet to the superheater is set to $T_{out,\ HTF}$ =390 ^{O}C. The inlet temperature of the HTF coming from the heat exchangers to the parabolic trough collectors is then set to be equal to $T_{in,\ HTF}$ = 300 ^{O}C. The total mass flow rate of the needed from the solar filed thus can be calculated from Equation (2.48):

$$\dot{M} = \frac{\dot{Q}_{net}}{C_p\left(T_{out} - T_{in}\right)} \tag{2.48}$$

- In the above equation the specific heat capacity at constant pressure for the heat transfer fluid (Therminol VP-1) is calculated at average temperature of T_{avg} = 345 ^{O}C.

- For ambient temperature of 16.5 ^{O}C, the difference between collector outlet temperature and ambient temperature becomes, ΔT_{out} = 373.5 ^{O}C. Similarly the difference between collector inlet temperature and ambient temperature becomes, ΔT_{in} = 283.5 ^{O}C.

- Equation (2.51) is used to calculate the maximum efficiency of the collectors at a given DNI and location. Maximum efficiency of the collectors is obtained at midday when the

incident angle is zero. Thus the incident angle modifier is equal to one. Similarly at midday no collector shades other collector this set row shading factor to be equal to one. The end loss factor is also equal to one because theta is set to be equal to zero.

- Clean reflectivity and cleanness of the solar field (CR and CL) factors are set to be equal to the reference value of 0.94. In the model no broken mirrors are considered and the solar field area is also calculated when it is fully operational.

- The reference ambient temperature and reference wind velocity variables are used to calculate the design heat losses, and they do not have a significant effect on the solar field sizing calculations. Reasonable values for those two variables are the average annual measured ambient temperature and wind velocity at the project location. Therefore the reference ambient temperature and wind velocity are found to be 16.1502 $\approx$ 16.5 ^{O}C and 3.9265 $\approx$ 4 m/s respectively for Addis Ababa.

- The reference direct normal radiation value, on the other hand, does have a significant impact on the solar field size calculations. Four factors affect the choice of a reference direct normal radiation value for a given system:

  - Location
  - Thermal energy Storage capacity of the plant
  - Maximum thermal energy storage charge rate (Maximum Power to Storage)
  - Variability of the solar resource over the year, determined by the weather data

  Typically, the reference direct normal radiation value can be set to the actual direct normal radiation value that has a cumulative annual frequency value of about 95%, [19]. For Addis Ababa this value is found to be equal to 806 W/m^2.

- Inserting the above defined values in Equation (2.51) gives reference efficiency of η_{SF} = 58.231%. This efficiency value is a reference maximum value of the solar field. The actual efficiency of the solar field is less than the above value due to several reasons. First of all the DNI is not always found at its maximum value. The incident angle is not

also equal to zero. Although one axis tracking system is governed by the collectors, the incident angle depends on solar time and day of the year. Accordingly the end loss and the row shading factors differ from one. The heat losses in piping and tank vessel are given by Equation (2.53):

$$\dot{Q}_{pipe} = 20\frac{W}{m^2} A_{SF} \frac{T_{avg}}{343^o C} + 2.57 \times 10^6 W \frac{T_{avg}}{275^o C} \quad (2.53)$$

- The net energy can be expressed by Equation (2.50):

$$\dot{Q}_{net} = \dot{Q}_{abs} - \dot{Q}_{pipe} \quad (2.49)$$

- The heat energy absorbed by the solar field is thus given by Equation (2.50)

$$\dot{Q}_{abs} = A_{eff}.DNI.\eta \quad (2.50)$$

- From Equation (2.49) and Equation (2.50) it can be observed that the net energy transferred to the steam is dependent on the effective area of the solar field. From these equations the A_{eff} is found to be, $A_{eff} = 81760\ m^2$. The area on SCA of LS-2 is 235 m^2. This gives the total number of SCA needed for the solar field to be equal to $TN_{coll} = 348$.

The flow chart of the MATLAB code is shown in Figure 3-10. This flow chart begins by stating the necessary initial conditions and assumptions. In this part initial guess for the initial pressure of steam is also made. The flow chart proceeds by making component modeling. Next the STEC model for parabolic trough collector is used to determine the solar field area and the number of the collectors. Finally pinch point temperature difference is checked to ensure if the error in the guessing for initial steam pressure falls in the specified tolerance range. If the error is out of the tolerance range the guess for the initial steam pressure is updated. The MATLAB code is shown in Appendix A.

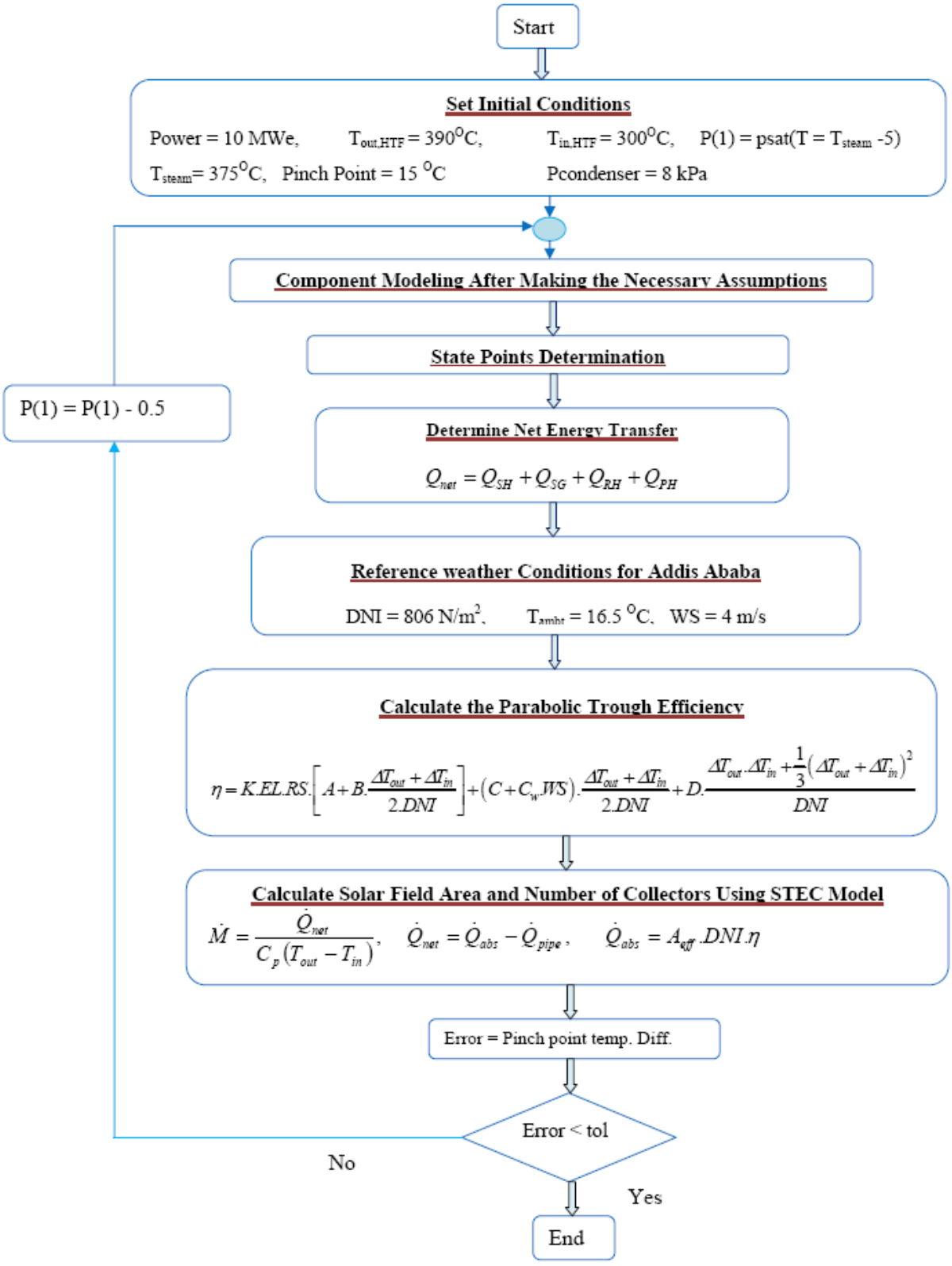

Figure 3-10 Flow Chart for the Developed MATLAB code

Table 3-4 State points of the power plant (See Figure 3-1)

State No.	P[i]	T[i]	h[i]	s[i]
	[bar]	[C]	[kJ/kg]	[kJ/kg·K]
1	83.43	375.00	3058.55	6.2265
2	37.57	275.48	2899.30	6.2782
3	14.10	195.38	2731.23	6.3415
4	14.10	375.00	3203.89	7.2193
5	4.05	235.24	2933.99	7.3152
6	0.78	93.24	2664.96	7.4449
7	0.08	41.51	2380.27	7.6046
8	0.08	41.51	173.85	0.5925
9	4.05	41.57	174.39	0.5931
10	4.05	92.74	388.75	1.2240
11	4.05	144.09	606.77	1.7815
12	83.43	145.60	618.25	1.7885
13	83.43	194.70	831.62	2.2702
14	83.43	246.61	1069.54	2.7518
15	83.43	297.96	1333.38	3.2354
16	83.43	297.96	2753.40	5.7219
17	37.57	246.67	1069.54	2.7629
18	14.10	195.38	1069.54	2.7948
19	14.10	195.38	831.62	2.2870
20	4.05	144.09	831.62	2.3204
21	0.78	92.80	388.75	1.2250
22	0.08	41.51	388.75	1.2755

The overall heat transfer coefficients of the three feedwater heaters and the four heat exchangers are shown below in Table 3-5 and Table 3-6 respectively. This reference values are used in the TRNSYS modeling and simulation of the power plant when the weather conditions deviate from the reference values.

Table 3-5 Overall heat transfer coefficient of the Feedwater Heaters

Heater Type	$\boldsymbol{UA_{REF}\ (kW\ /\ k)}$
Hp preheater 1	253.15
Hp preheater 2	63.69
Lp preheater	263.31

Table 3-6 Overall heat transfer coefficients of the heat exchangers

Heat Exchanger Type	$\boldsymbol{UA_{REF}\ (kW\ /\ k)}$
Preheater	119.53
Steamgenerator	505.09
Superheater	107.42
Reheater	107.39

The T-S diagram for the power plant is shown in Figure 3-11. Condensate and feedwater pumps are used to increase the pressure of the working fluid as it flows through the low and high pressure feedwater heaters. On the T-S diagram State 8 and state 9, condensate before and after pumping, overlap each other. This is because the rise in temperature and enthalpy of the working fluid in condensate pumping process is small due to small increase in pressure. Similarly state 11

and state 12, feedwater before and after pumping, overlap each other on the T-S diagram. This occurs due to assumption made earlier (the feedwater leaves the deaerator as saturated liquid).

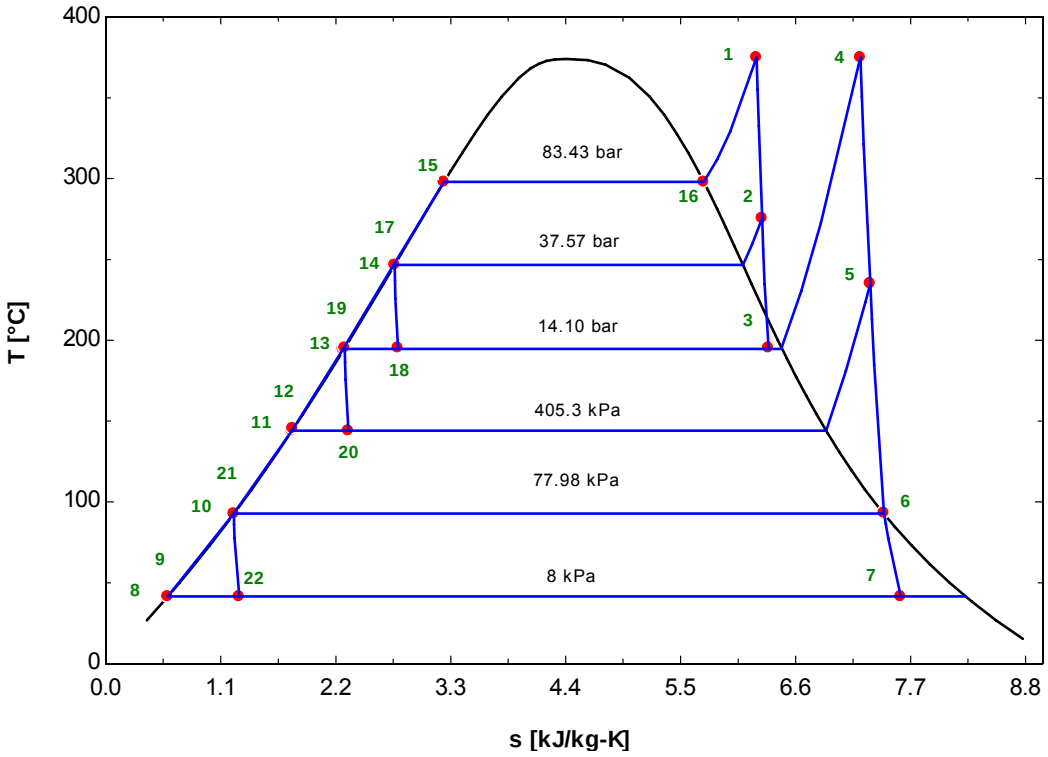

Figure 3-11 T-S diagram of the power plant

CHAPTER 4

SIMULATION OF THE POWER PLANT USING TRNSYS

4.1 Introduction

TRNSYS is a complete and extensible simulation environment for the transient simulation of systems, including multi-zone buildings. It is used by engineers and researchers around the world to validate new energy concepts, from simple domestic hot water systems to the design and simulation of buildings and their equipment, including control strategies, occupant behavior, alternative energy systems (wind, solar, photovoltaic, hydrogen systems), etc.

The DLL-based architecture allows users and third-party developers to easily add custom component models, using all common programming languages (C, C++, PASCAL, FORTRAN, etc.). In addition, TRNSYS can be easily connected to many other applications, for pre- or post-processing or through interactive calls during the simulation (e.g. Microsoft Excel, MATLAB, COMIS, etc.). TRNSYS applications include:

- Solar systems (solar thermal and PV)
- Low energy buildings and HVAC systems with advanced design features (natural ventilation, slab heating/cooling, double façade, etc.)
- Renewable energy systems
- Cogeneration, fuel cells
- Anything that requires dynamic simulation!

A TRNSYS project is typically setup by connecting components graphically in the simulation Studio. Each Type of component is described by a mathematical model in the TRNSYS simulation engine and has a set of matching Proforma's in the Simulation Studio. The proforma has a black-box description of a component: inputs, outputs, parameters, etc.

TRNSYS components are often referred to as Types (e.g. Type 1 is the solar collector). The Multizone building model is known as Type 56. The Simulation Studio generates a text input file for the TRNSYS simulation engine. That input file is referred to as the deck file [23].

The purpose of the TRNSYS modeling and simulation is to study the operation of the power plant at weather condition different from the reference ones. In this weather conditions the power plant operates by producing less power than its rated capacity. Other software's (e.g. MATLAB, EES) can be used to make same analysis of the power plant however TRNSYS is selected for its simplicity and flexibility.

The TRNSYS modeling of the power plant can be divided in two parts, TRNSYS solar field model and TRNSYS power model. The TRNSYS solar field model is used to model the solar field area and TRNSYS power model is used to represent the Rankine power block system.

4.2 TRNSYS Solar Field Model

The TRNSYS solar field model includes weather data processor, HTF splitters, HTF mixers, expansion vessel and the parabolic troughs. The diagram of the model is shown Figure 4-1.

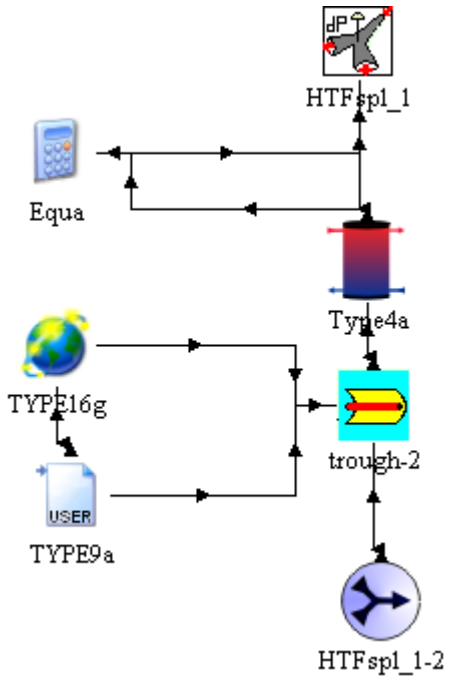

Figure 4-1 TRNSYS solar field model

In this solar field model Type 9a is used to read the weather data in a text format. Type 16 g, a solar radiation processor with total horizontal and normal beam radiation known, is used to find the azimuth and zenith angles which are the inputs to the parabolic trough model (Type 396). An equation in used to set the HTF mass flow rate less or equal to the design point.

The parabolic trough collector (Type 396) which is part of the STEC library (Release 3.0, November 2006), is one of the major components of the solar field model. This component is a model for parabolic trough collector based on the model developed by Lippke. It uses an integrated efficiency equation to account for the different fluid temperature at the field inlet and outlet of the collector field. It calculates the demanded mass flow rate of the heat transfer fluid to achieve a user-defined outlet temperature T_{out} [19].

The HTFspl_1(Type 351), which is part of the STEC library (Release 3.0, November 2006), is used to split the mass flow rate of the HTF from the parabolic trough to the superheater, steamgenerator and preheater train and reheater train at a ratio specified in the MATLAB model of the plant.

The HTFmix_1_2 (Type 11), which is part of the standard TRNSYS library, (Solar Energy laboratory, 2002), is used to mix the mass flow rate of the HTF from the steamgenerator and preheater train and reheater train. This component is used to find the mixture temperature and inputs to the parabolic trough collector.

The expansion vessel is modeled by "Type 4" storage tank component, part of the standard TRNSYS library (Solar Energy Laboratory, 2000). As explained in chapter three the expansion vessel serves to compensate for variation in the volume of the heat transfer fluid throughout the day, since the specific volume of the HTF is dependent on temperature.

4.3 Sizing of the Expansion Vessel

This sizing of expansion vessel should cause positive fluid pressure to the pump's suction side during system startup and should minimize the vapor space in the tank during normal operation. As the term implies, the main function of the expansion vessel in a heat transfer system is to provide for fluid expansion, which can be greater than 25% of its original volume depending on the fluid used and the operating temperature.

Since the tank is usually installed at the highest point in the system, it also can serve as the main venting point of the system for excess levels of low boilers and moisture which may accumulate in the heat transfer fluid. The highest point installation also creates positive head pressure to the pump's inlet, providing flooded pump suction with uninterrupted flow of fluid to the user station [11].

When the power plant operates at its rated capacity the whole volume of the absorber tube in the solar field is filled by the HTF. At this operating condition the mass of the HTF in the solar field can be found as shown below.

$$M_{SF} = \frac{\pi.(D_{HCE})^2}{4}.L_{SCA}.N_{SCA}.\rho(T_{avg}) \tag{4.1}$$

Where: M_{SF} = the mass of the HTF in the solar field [kg]

D_{HCE} = diameter of the steel absorber tube = 70 [mm]

L_{SCA} = length of one solar collector assembly (SCA) loop = 47 [m]

N_{SCA} = number of SCA loops in the solar field = 348

ρ = density of heat transfer fluid (Therminol VP-1) = 767 [kg/m^3]

T_{avg} = Average temperature of the HTF in the solar field = 345 [^{O}C]

This gives the mass of HTF in the solar field to be equal to 48,279 kg. The volume of the HTF in the solar field can thus approximate as;

$$V_{SF} = \frac{M_{SF}}{\rho(T_{avg})} = \frac{48,276}{767} = 63\,m^3/kg \tag{4.2}$$

Fluid expansion between two temperatures can be calculated by dividing the fluid's density at the lower temperature by the density of the fluid at the higher temperature [11]. The lowest and highest operating temperatures are 300 and 390 ^{O}C respectively. This gives the HTF expansion to be:

$$HTF\ Expansion = \frac{\rho_{HTF,300}}{\rho_{HTF,390}} = \frac{817}{709} = 1.152 \tag{4.3}$$

Thus the expansion of the HTF is 115.2 % of the original volume at 300 ^{O}C when heated to 390 ^{O}C. Therefore, an expansion tank for a 63 m^3/kg of a HTF operating between 300 ^{O}C and 390 ^{O}C should be sized for 9.6 m^3/kg of expansion.

The expansion volume can represent between 25% and 75% of the total volume of the expansion vessel [10]. Choosing the expansion volume to take 25 % of the total volume of the expansion vessel sets the volume of the expansion volume to be 39 m^3/kg. Thus the total mass of the HTF in solar field, expansion vessel, the piping systems and the heat exchanger trains becomes:

$$M_{total} = M_{SF} + 0.75 \times V_{EV} \times \rho\left(T_{Out,\mathrm{Re}f}\right) \tag{4.4}$$

This gives the total mass of the HTF in the solar field and in the expansion volume to be equal to 69, 0178 kg.

4.4 TRNSYS Power Model

This part of the TRNSYS modeling is used to estimate the input and output temperature of the steam from the preheater, steamgenerator, superheater, turbine stages, condenser, FWH, and CFWHs. The model also determines their variations with part load operations. Similarly the mass flow rate of the steam, the heat transferred between component stages and the net power output from the plant can be determined.

In the power modeling of the plant using TRNSYS, most of the components are part of STEC model library, Release 3.0,2006. The CFWH used in this model is developed separately based on CFWH model by STEC.

The set-up of the Rankine cycle is shown in Figure 4-2. The boiler section of the system consists of the super heater, the steam generator and the preheater. The links between the components consider two fluid circuits: the heat transfer fluid (HTF), which flows from the HTF splitter in the solar field model, and the water steam circuit which flows from the high pressure closed feed water heater.

The boiler is then linked to a steam turbine with five extraction lines is presented by with two high pressure and three low pressure turbine stages (HP_Turbine1, HP_Turbine2, LP_Turbine1, LP_Turbine2, LP_Turbine3) and four extraction splitters (S-split, S-split-2 S-split-3,S-split-4). Between the high and low pressure turbine stages a reheater (Reheater) exists. The final turbine stage is connected to the condenser component (Condenser).

The extraction splitters are connected to the two high and one low pressure closed feed water heaters (HP_Preheater-1, HP_Preheater-2, LP_Preheater_1) and a deaerator (Deaerator). A standard TRNSYS calculator utility component (power) is used to add up the mechanical power production of all three stages. Additionally a condenser pump (Cond_Pump) and a feedwater pump (FeedWat_PumP) are part of the system.

The relevant links between the TRNSYS components in the modeling of the power plant are discussed as it follows:

- The evaporator demand flow signal is linked to the control input of the feedwater pump which sets the flow rate of the whole system. The condenser pump model uses the input flow rate as flow demand signal.

- Flow rate and enthalpy are connected from turbine stage outlet to splitter and further from the splitter outlet to the turbine stage inlet. The pressure is connected in the opposite direction from condenser to turbine stage outlet to splitter inlet and so on. Pressure and enthalpy are connected from the splitters outlet to the closed feed water heaters (CFWHs)/deaerator inlet is whereas the steam flow rate (demand) is connected in the opposite direction.

- The feedwater flow rate and temperature from the condenser outlet is linked first to the pump, then to the low pressure closed feed water heater, then to the deaerator, then to the feedwater pump, then to the two high pressure CFWH and then to the economizer (preheater) inlet.

- The temperature, quality and flow rate of the condensed extraction steam in the CFWH is linked to the condensate inlet of the CFWH/deaerator.

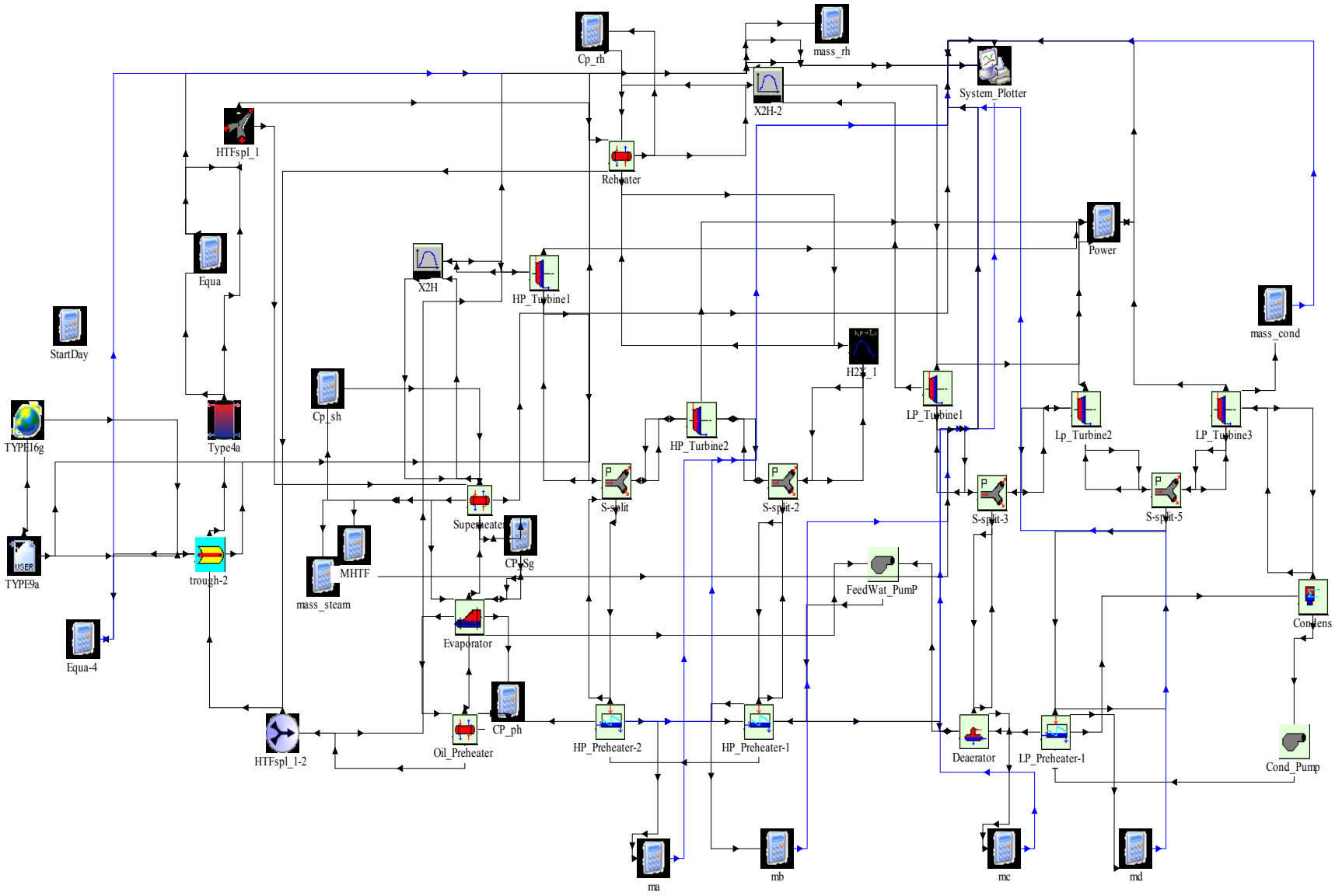

Figure 4-2 TRNSYS representation the power plant model

4.5 TRNSYS Type 860

This is a TRNSYS component used to model the closed feed water preheater. In the model the feed water is designed to pass through the tube side of the heat exchanger and the extracted steam and the condensate inlet to the CFWH are designed to mix in the shell side of the heat exchanger.

The model reads the input values and determines the extracted mass needed. All the calculations are corrected for mass flow rates other than the reference value. The model is based on Type317 STEC model for preheater. The reason to develop this model is that using Type 317 gave an error in the estimation of the power plant outputs. The steps for the calculation of the outputs, the required inputs and the parameters for the model are described below.

4.5.1 Parameters

The parameters needed for this model are shown below. All these values are found from the MATLAB model of the power plant at the reference state point operations.

1. Cold Side Specific Capacity (CPC):

   PAR (1) = CPC

2. Overall Heat Transfer Factor (UAREF):

   PAR (2) = UAREF

3. Cold Side Reference Flow Rate (FLWREF):

   PAR (3) = FLWCREF

4. Power law exponent to UA (EXP_UA)

   PAR (4) = EXP_UA

4.5.2 Inputs

Seven input values are needed for the model. The inputs are shown below. The reference values of these inputs values are found again from the MATLAB model. In the TRNSYS simulation, the inputs are found from outputs of other components.

1. Hot Side Inlet Enthalpy (HHI):

   XIN (1) = HHI

2. Hot Side Inlet Pressure (PHI):

   XIN (2) = PHI

3. Cold Side Inlet Temperature (TCI):

   XIN (3) = TCI

4. Cold Side Inlet Pressure (PFW):

   XIN (4) = PFW

5. Cold Side Inlet Flow Rate (FLCI):

   XIN (5) = FLCI

6. Condensate Inlet Enthalpy (HBI):

   XIN (6) = HBI

7. Condensate Inlet Mass Flow Rate (FLBI):

   XIN (7) = FLBI

The model first reads the parameters and the input values and determines the necessary outputs. Enthalpy of the condensate out of the feedwater heater (HS) can be found from saturated steam enthalpy data at a pressure of PBI.

$$HS = enthalpy\_sat\_p(PBI) \tag{4.5}$$

Enthalpy of feedwater inlet to the CFWH (HI) can be found from compressed steam enthalpy data at a pressure of PFW and temperature of TCI.

$$HI = enthalpy\_PT(PFW, TCI) \tag{4.6}$$

Temperature of the condensate leaving the CFWH (TSAT) can be found from a saturated steam temperature data at a pressure of PBI.

$$TSAT = temperature\_sat\_p(PBI) \tag{4.7}$$

After calculating the above values the next step is to correct the overall heat transfer coefficient by Equation (3.79). The reference mass flow rate and overall heat transfer coefficient values are found from the parameter inputs and the mass flow rate is found from the connected input values.

$$\frac{UA}{UA_{REF}} = \left(\frac{\dot{m}_{feedwater}}{\dot{m}_{feedwater,REF}} \right)^{0.8} \tag{3.79}$$

The effectiveness of the heat transfer can thus be expressed as:

$$EFF = 1 - \exp\left(\frac{-UA}{FLCI.CPC} \right) \tag{4.8}$$

The initial guess for cold side outlet temperature (TCO) can be set by making TCO = TSAT. After making the initial guess of the outlet temperature of the feedwater, the heat transfer between the two fluid streams can be calculated as shown below:

$$Q_{dot} = FLCI.CPC.(TCO - TCI) \tag{4.9}$$

The next step is to determine the extracted steam demanded mass flow rate by using Equations from (3.66) to (3.69).

$$A = (HHI - HS) \tag{3.66}$$

$$B = FLBI\left(HHI + HBI - 2.HS\right) - Qdot \tag{3.67}$$

$$C = FLBI\left(FLBI\left(HBI - HS\right) - Qdot\right) \tag{3.68}$$

$$help = B^2 - 4AC \tag{4.10}$$

IF (help > 0)

$$FLHDM = MAX\left(0, \frac{\left(-B + \sqrt{help}\right)}{2.A}\right) \tag{3.69}$$

ELSE

FLHDM = 0

END

Total mass flow rate of the condensate out of the CFWH becomes:

$$FLHO = FLHDM + FLBI \tag{4.11}$$

The steam inlet to CFWH is composed of the extracted steam and also the incoming condensate. The linearly averaged steam enthalpy can thus be given by Equation (3.55).

$$h_{steam} = \frac{FLHDM.HHI + FLBI.HS}{FLHO} \tag{3.55}$$

The corresponding steam temperature at h_{steam} and hot side inlet pressure (PHI) can be calculated from steam data:

$$Tsteam = temperature_{ph}\left(PHI, hsteam\right) \tag{4.12}$$

The maximum possible heat transfer is thus calculated using Equation (3.74)

$$Q_{\max} = FLCI.CPC.\left(T_{steam} - TCI\right) \tag{3.74}$$

The effectiveness from the guessed cold side outlet temperature is found by using Equation (3.75)

$$EFF2 = \frac{Q_{dot}}{Q_{\max}} \tag{3.75}$$

The difference between the actual and the guessed effectiveness becomes,

$$err = \left(EFF2 - EFF\right) \tag{4.13}$$

If the difference between the guessed and the actual effectiveness is large another guess for TCO is made until err falls into the allowable tolerance. The steps applied for correcting the TCO are shown below.

If EFF2 is greater than EFF, Qdot is higher than expected. Therefore, guessed TCO must be minimized and vice versa.

DO While (err> tole.)

If (EFF2 > EFF)

TCO = TCO – 0.05

Else

TCO = TCO + 0.05

End

End

Again similar calculations are made for Q_{dot}, FLHDM, hsteam, Tsteam, Qmax, and EFF2. The difference between EFF2 and EFF is again checked. If err is less or equal to the tolerance the program terminates out of the loop.

4.5.3 Outputs

The outputs from the program are listed below.

1. Demanded hot inlet flow rate (FLHDM):

   OUT (1) = FLHDM

2. Cold side outlet temperature (TCO):

   OUT (2) = TCO

3. Cold side outlet flow rate (FLCO):

   OUT (3) = FLCO = FLCI

4. Hot side outlet enthalpy (HBO):

   OUT (4) = HBO = HS

5. Hot side outlet flow rate (FLBO):

   OUT (5) = FLBO

6. Hot side outlet temperature (TSAT):

   OUT (6) = TSAT

7. Transferred Power (Qdot):

   OUT (7) = Qdot

8. Effectiveness (EFF):

   OUT (8) = EFF

The actual simulation of Type 860 in the power plant model developed in TRNSYS is very slow. This drawback sets the simulation time to be very large. To avoid this drawback another model

for the preheater is developed by modifying Type 860. The name of this new model of the preheater is Type 850.

The modification made for Type 860 is to leave out the correction procedure for the effectiveness and set the outlet temperature of the feedwater from the CFWH to be equal to the saturation temperature of steam at the pressure of the extracted steam. The approximation made shows that, for the HP preheater2 CFWH only a 0.1 ^{O}C difference exists between the actual and the approximated value. For the HP preheater1 and the LP preheater CFWH the difference between the actual and the approximated feed water outlet temperature are 0.7 ^{O}C and 0.069 ^{O}C respectively. All the temperature differences are taken at a full load operation of the power plant. At full load operation the errors in the approximations made are less than 0.5%. In the estimation of steam properties Steam IAPWS 97 data are used.

4.6 Result of TRNSYS Modeling and Simulation

The result of TRNSYS modeling and simulation of the power plant is briefly outlined in this section of the chapter. The reference values for this simulation are found from the full load operation of the power plant which is modeled using MATLAB. The reference values include area of the solar field, overall heat transfer coefficients of the heat exchangers, design mass flow rate of water/steam, design inlet and outlet pressure of each turbine stage and, mass flow rate of the steam/water and HTF in the steam generator, superheater, reheater, and preheater.

The simulation is done for year 2001 G.C under Addis Ababa weather condition. The selection of the year is random. The weather data for the Addis Ababa considered is found from SEWERA website [25] in a text and TMY formats. The analysis is made for the representative days of the year.

The result of the simulation for two days of operation, one clear day (March 16), and one cloudy day (May 15) are given in the next pages. The results for other representative days of the year are shown in Appendix B.

4.6.1 Simulation Result for Clear Day March 16, 2001

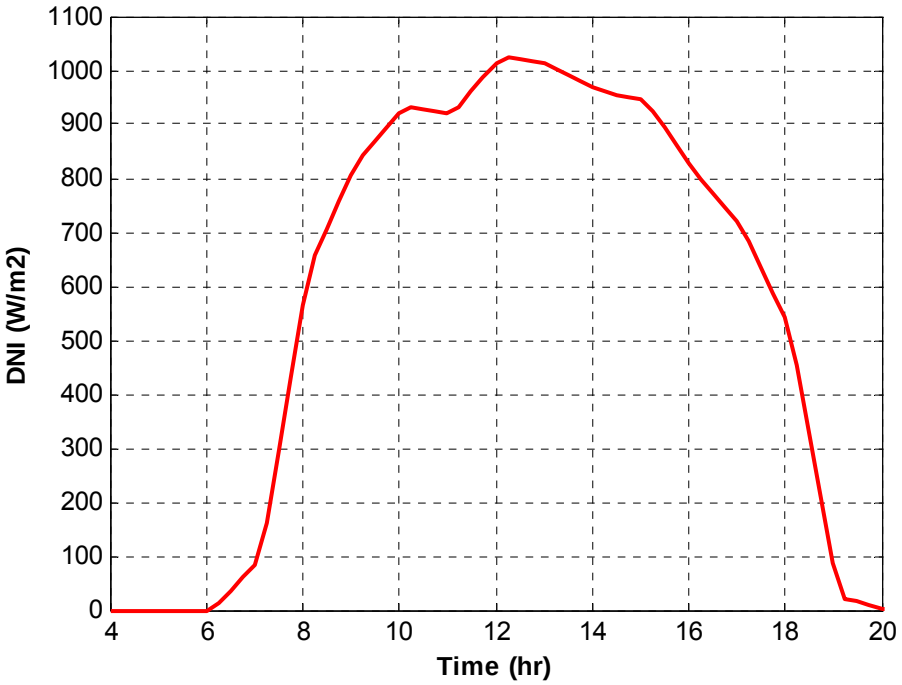

Figure 4-3 Direct Normal Insolation (DNI)

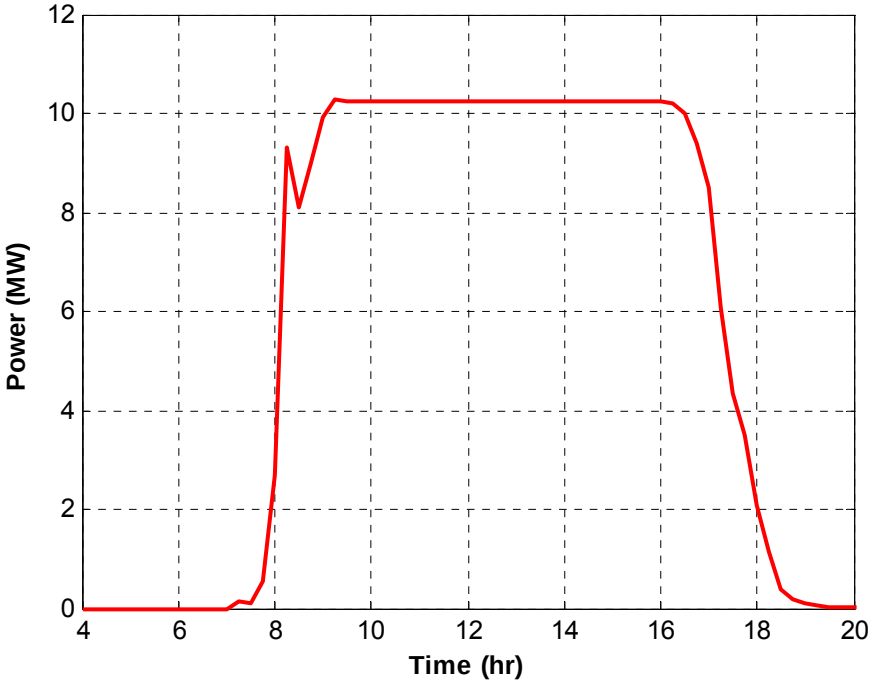

Figure 4-4 Net power

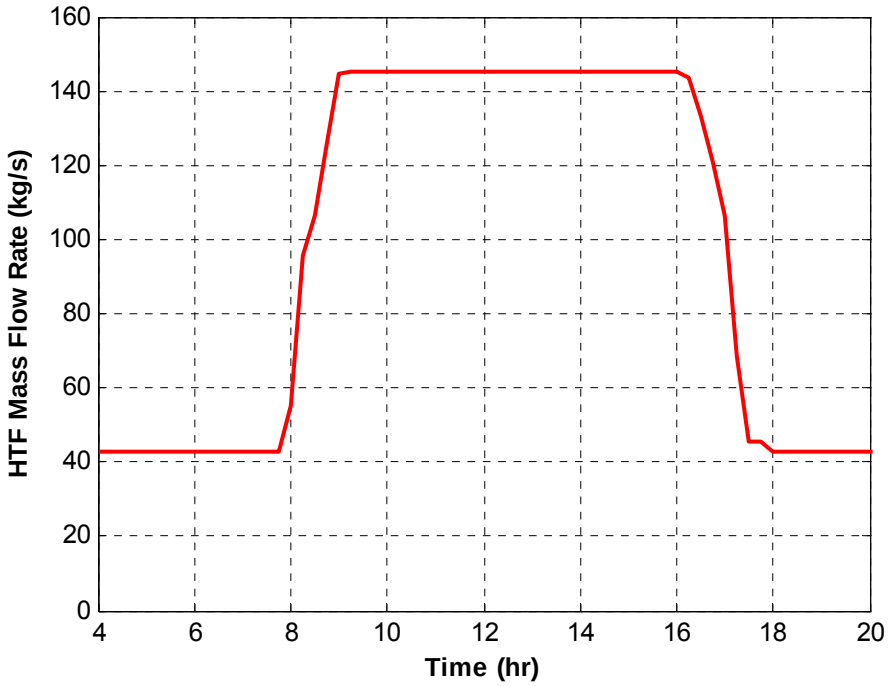

Figure 4-5 Solar field HTF mass flow rate

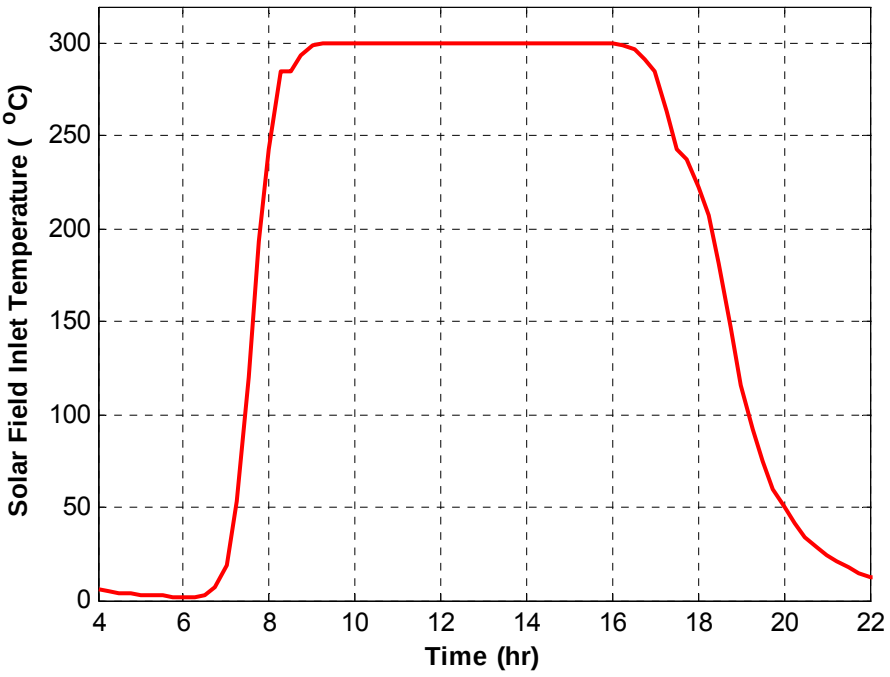

Figure 4-6 Solar field inlet temperature

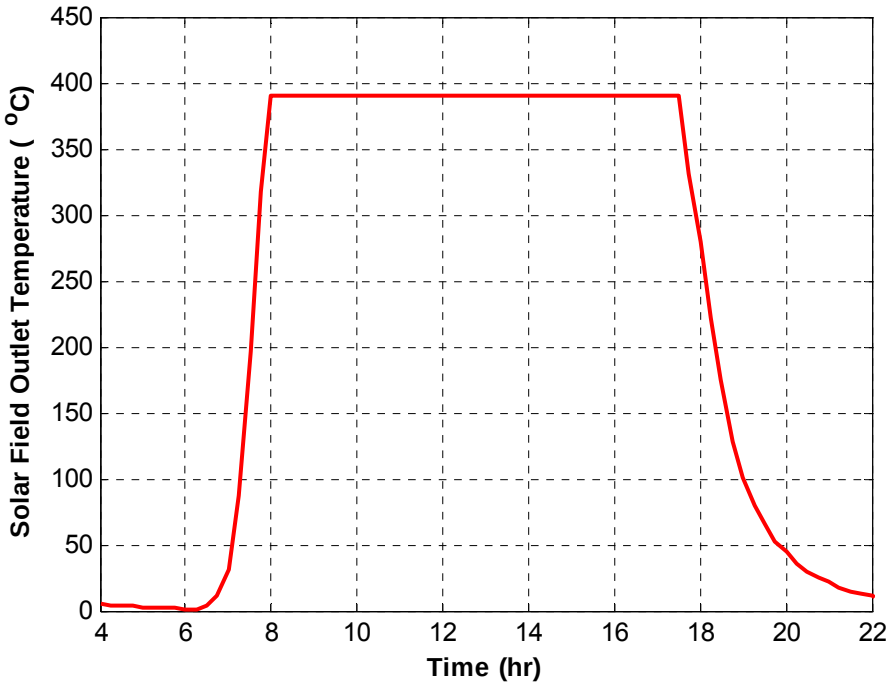

Figure 4-7 Solar field outlet temperature

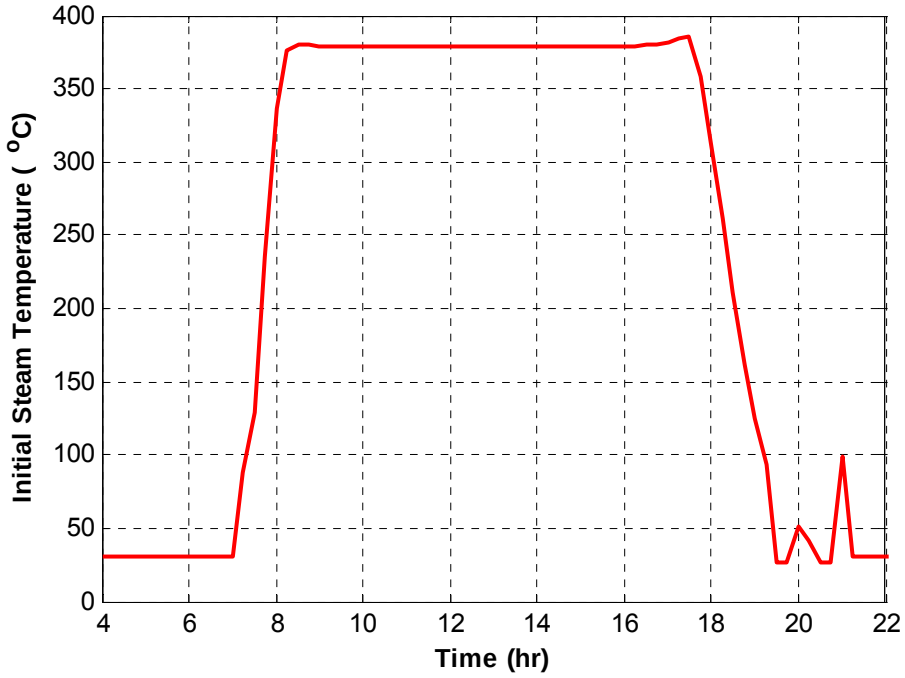

Figure 4-8 Initial steam temperature

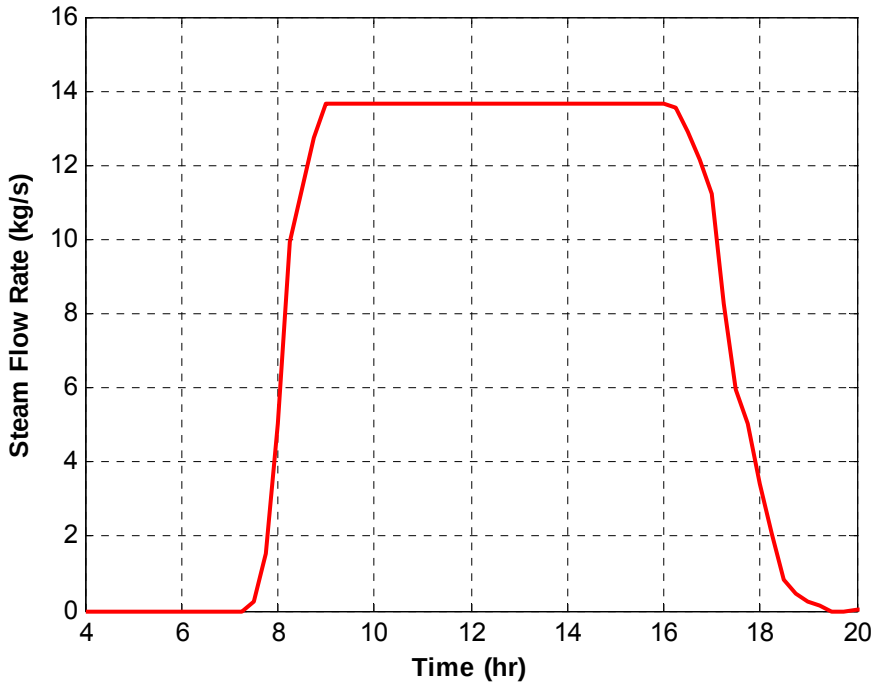

Figure 4-9 Steam mass flow rate

4.6.2 Simulation Result for cloudy day May 15, 2001

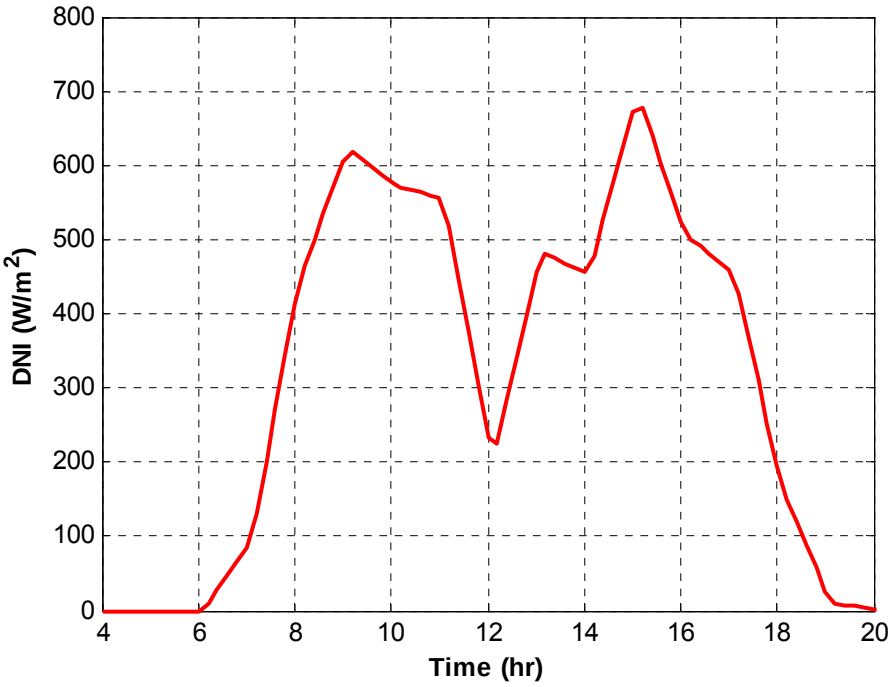

Figure 4-10 Direct Normal Insolation (DNI)

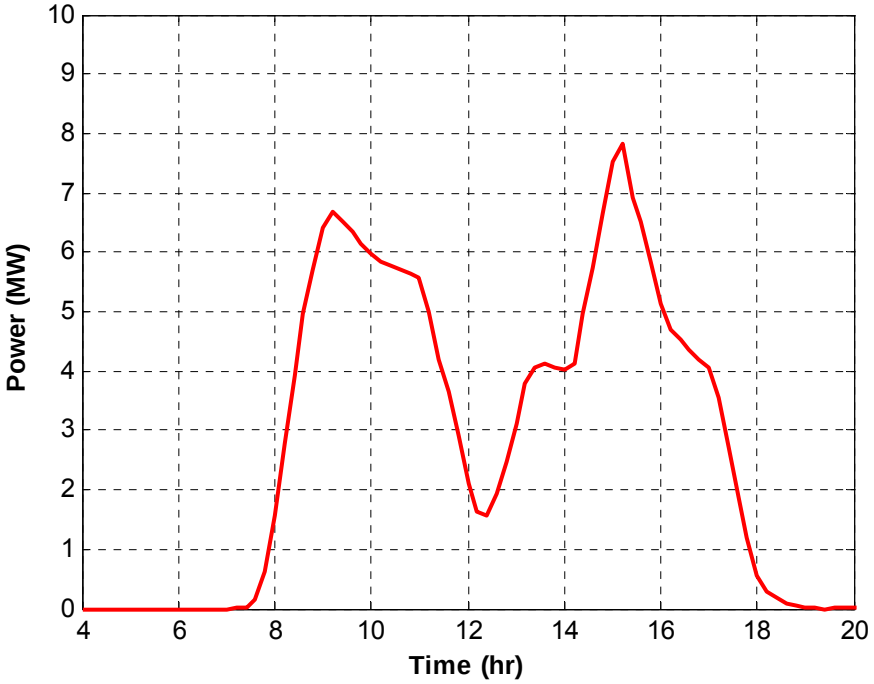

Figure 4-11 Net power

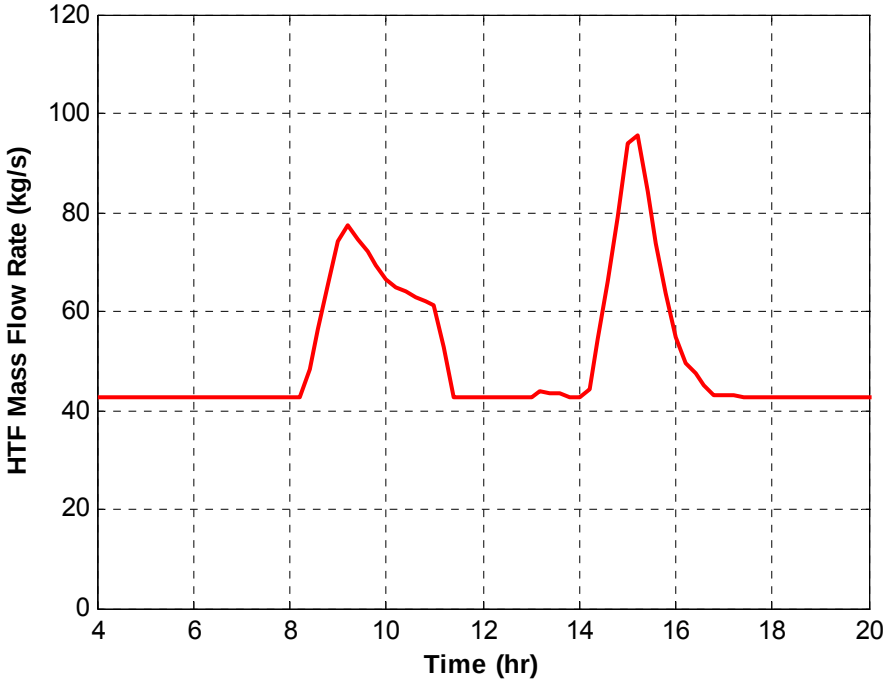

Figure 4-12 Solar field HTF mass flow

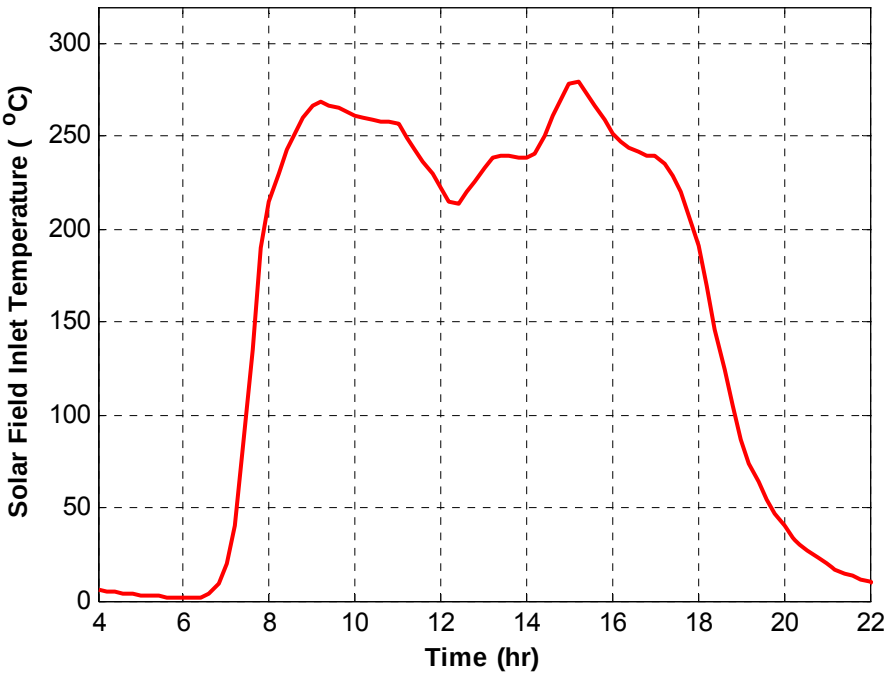

Figure 4-13 Solar field inlet temperature

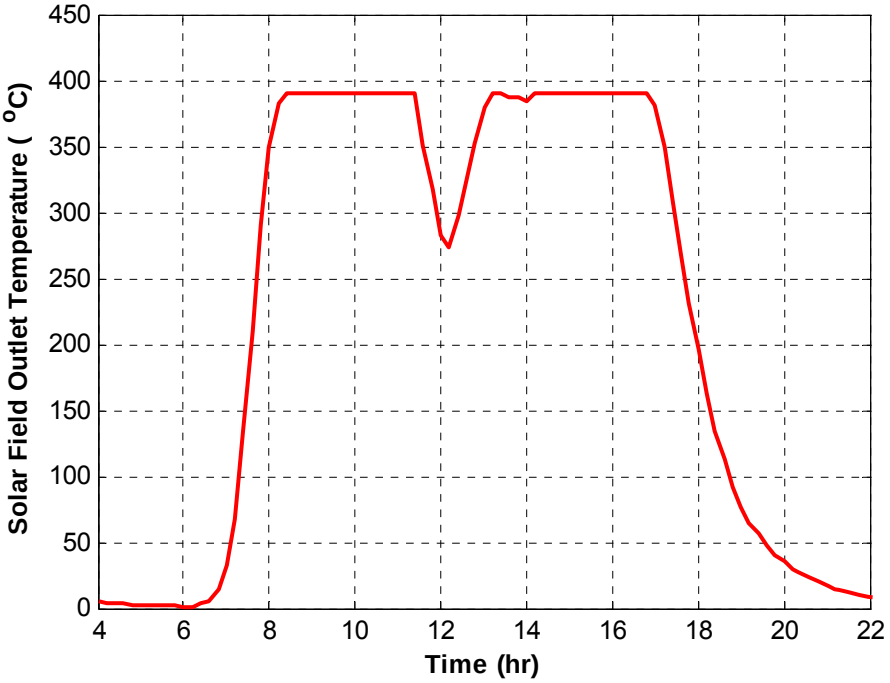

Figure 4-14 Solar field outlet temperature

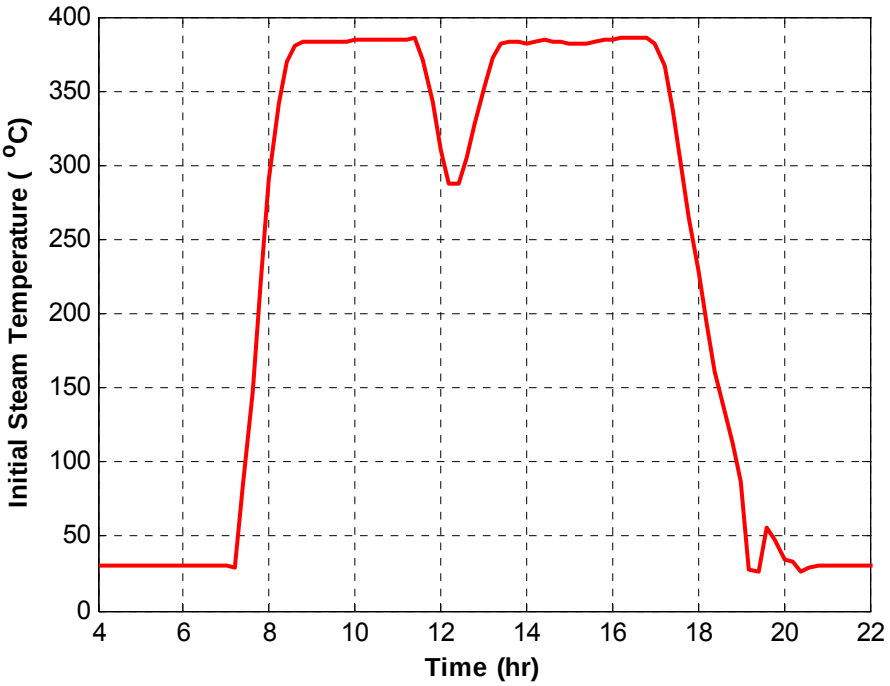

Figure 4-15 Initial steam temperature

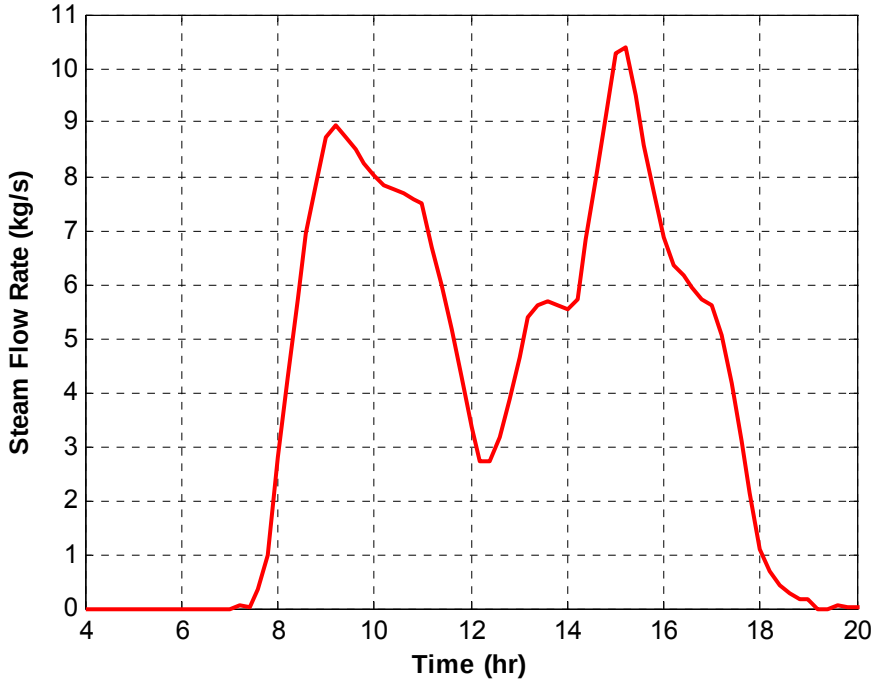

Figure 4-16 Steam mass flow rate

CHAPTER 5

COST AND FINANCIAL ANALYSIS OF THE POWER PLANT

5.1 Solar Advisor Model

Solar Advisor Model (SAM) is used to make cost and financial analysis of the power plant. Solar Advisor is based on an hourly simulation engine that interacts with performance, cost, and finance models to calculate energy output, energy costs, and cash flows. Its application ranges from photovoltaic systems for residential and commercial markets to concentrating solar power and large photovoltaic systems for utility markets. (SAM Users Guide).

5.1.1 User Interface Overview

The main window consists of a navigation menu and data page. Navigation buttons in the navigation menu select the data page to display. Data pages display results and input data. Tabs along the top of the window provide access to each case in the file. The menu bar provides access to command menus.

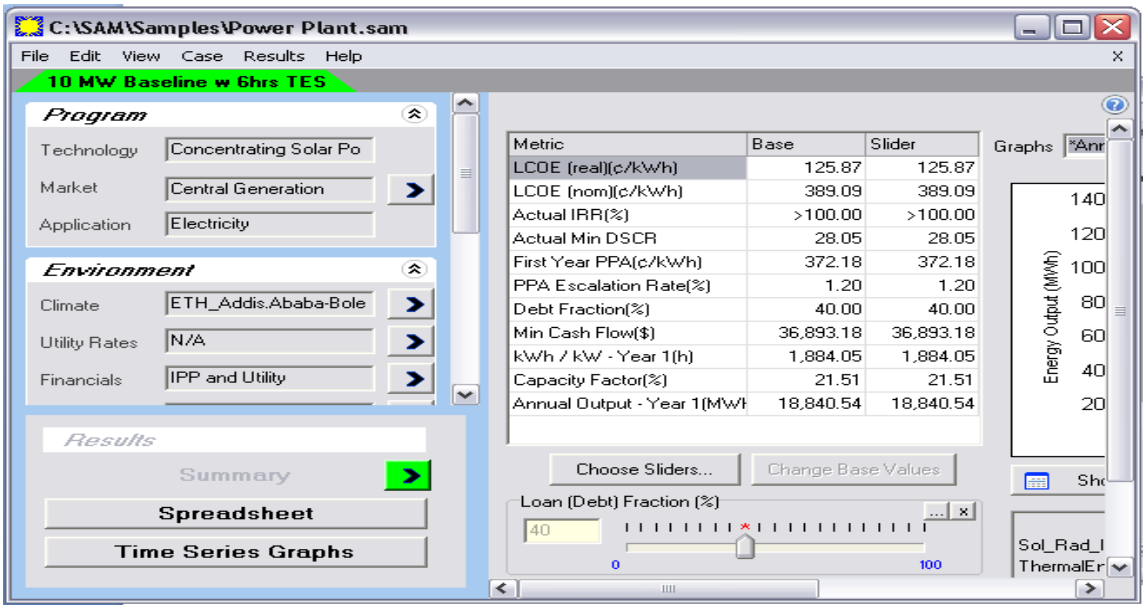

Figure 5-1 SAM user interface

5.1.2 Input Pages

Here there are thirteen input pages. The navigation menu provides access to the input pages, which are categorized in to three groups: Program, Environment, and System.

5.1.2.1 Program

The program page displays options that determine the set of input variables that Solar Advisor makes available for the case. The Technology options determine the set of options that appear on the system pages, for a Photovoltaic System, Concentrating Solar Power System, or Generic System. For each Technology option, a different set of Market options is available. The market options determine what set of financing variables appears on the Financial Page.

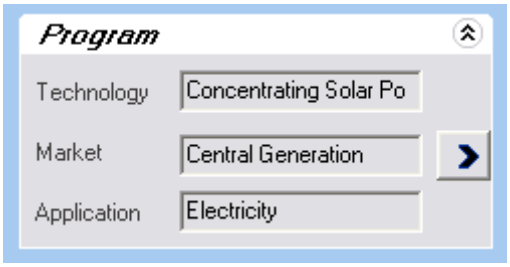

Figure 5-2 Program input options

5.1.2.2 Environment

The five environment options include variables and options that describe the characteristics of the system that can be considered to be outside of the technical description or specification of the system itself. The environment options include climate, Utility Rates, Loads, Incentives, and Financial parameters.

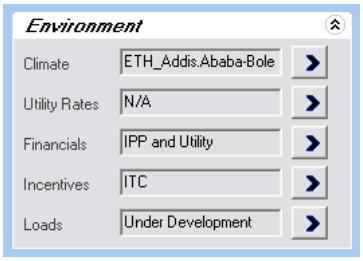

Figure 5-3 Environment input options

5.1.2.3 System

This option describes the system input pages that are available when the program technology on the Program Page is Concentrating Solar Power. Table 1-1 summarizes the purpose of each system input option pages.

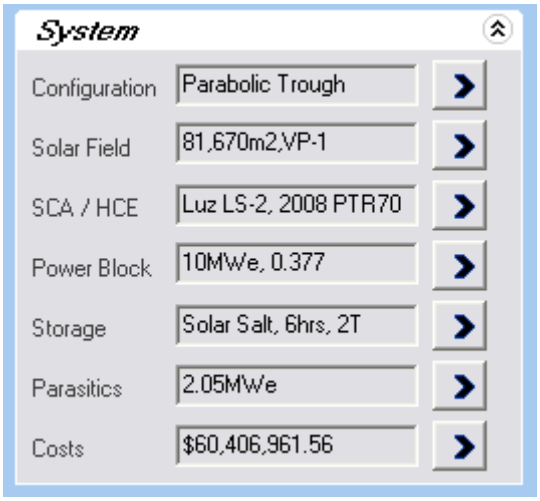

Figure 5-4 System input options

Table 5-1 System input options pages

No.	Option Name	Function Description
1	Configuration	Parabolic Trough, Central Receiver, and Dish Sterling
2	Solar Field	The Solar Field page displays variables and options that describe the size and properties of the solar field, properties of the heat transfer fluid, reference design specifications of the solar field, and collector orientation.
3	SCA/HCE (Solar Collector Assembly/Heat Collection Element)	The SCA/HCE parameters describe the solar collector assembly (SCA) and heat collection element (HCE).
4	Power Block	The turbine parameters determine the size of the steam turbine. Here plant capacity, the solar field area and plant downtime are described.

5	Storage	The parameters on the Storage page describe the properties thermal energy storage system and the storage dispatch controls
6	Parasitics	The parasitics page displays parameters describing losses due to parasitic electrical loads, such as drive motors, electronic circuits and pump motors.
7	Costs	The costs page provides access to all system costs. Project cost input data in Solar Advisor are divided into two main categories: Capital Costs and Operation and Maintenance (O&M) costs.

5.2 Costs Associated with Parabolic Trough Solar Electric Generating Systems (PTSEGs)

Project cost input data in Solar Advisor are divided into two main categories:

- Capital costs: include services and equipment purchases associated with the installation of the system and applied in year zero of the project cash flow.
- Operation and maintenance (O&M) costs: include equipment and labor expenses that occur after the system is installed.

5.2.1 Capital Costs

The capital costs represent expenses associated with the purchase of equipment and services for the project. These costs are classified as direct and indirect costs.

5.2.1.1 Direct Capital Cost

A direct capital cost represents an expense for a specific piece of equipment or installation service. For concentrating solar power systems, direct capital costs are expressed as dollar per area of solar field ($/m^2), dollars per power block rated capacity ($/MWe), or dollars per maximum thermal energy storage capacity ($/MWht).

For central generation systems, the contingency cost is a percentage of the sum of direct costs to account for expected uncertainties in the direct cost estimates. The direct cost also includes site improvement costs ($/m^2), solar field cost ($/m^2), and HTF system cost ($/kWe).

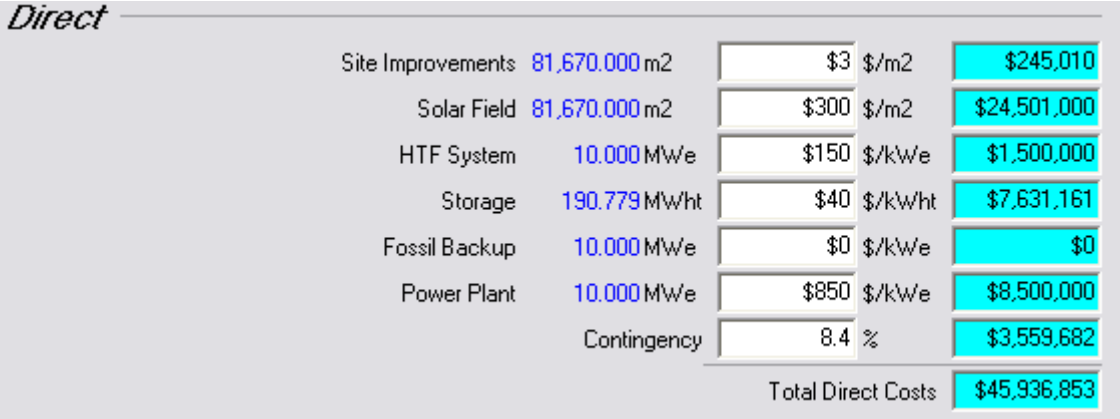

Figure 5-5 Direct cost estimate

The estimates of these costs are taken from sample Solar Advisor Model for 100MW Baseline with 6 hrs TES.

5.2.1.2 Indirect Capital Cost

An indirect cost is typically one that cannot be identified with a specific piece of equipment or installation service, and may include all other costs that are built into the price of the system, such as profit, overhead, and shipping costs. For central generation systems, indirect costs include three categories.

- Engineer, Procure, Construct costs may include costs associated with design and construction of the project.
- Project, Land, Miscellaneous costs may include real estate and other costs.
- Sales taxes are calculated by applying the sales tax rate to the percentage of the total direct costs.

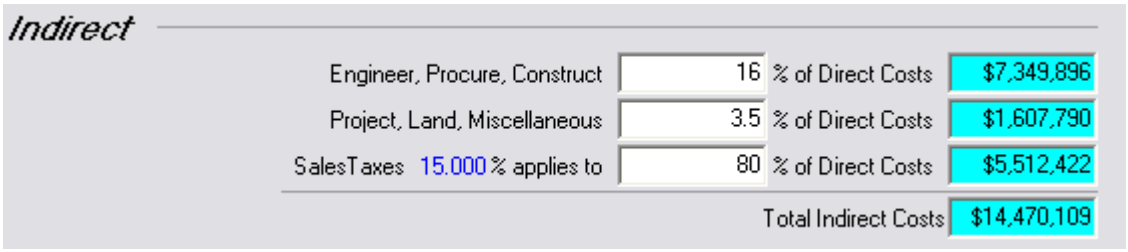

Figure 5-6 Indirect cost estimate

The indirect cost panel of the cost page uses the calculated direct cost estimates to calculate the indirect costs. The estimates of these costs are taken from sample Solar Advisor Model for 100MW Baseline with 6 hrs TES.

5.2.1.3 Total Installed

Total installed cost is the sum of direct and indirect costs. This installed cost is used to calculate the cash flow, levelized cost of energy, and other output metrics.

Figure 5-7 Total installed cost estimate

5.2.2 Operation and Maintenance Costs

Operation and Maintenance (O&M) costs represent expenditures on equipment and services that recur each year throughout the project's life after the system is installed. O&M Cost categories are specified in Table 5.2.

Table 5-2 Operation and maintenance costs

O&M Cost Category	Units	Description
Cost of Fuel	$/MMBTU	The cost of fuel for the fossil-fired backup system. The efficiency and operating level of the backup system is defined by the Fossil Fill Fraction and Fossil Fill LHV Efficiency on the Storage page.
Fixed (per year)	$	Annual fixed first year cost.
Fixed (per capacity)	$/kW-yr	Annual first year cost proportional to the system size in kW, where the system size for concentrating solar power systems is Rated Turbine Net Capacity on the Power Block page. For parabolic trough systems, fixed costs typically include all recurring costs except for water-related costs.
Variable (per production)	$/MW-h	Annual first year cost proportional to the calculated system production for that year in MWh. For parabolic trough systems, variable costs typically include cost of chemicals, water purchases, and chemical treatment of water.

Solar Advisor uses the first year O&M cost input variables to calculate O&M costs in year one of the project cash flow. The first year O&M cost, annual inflation rate on the Financials page, and Escalation Rates for each O&M cost category determine the O&M cost in subsequent years. The escalation rate can be used to represent an expected annual increase in O&M cost above the annual inflation rate.

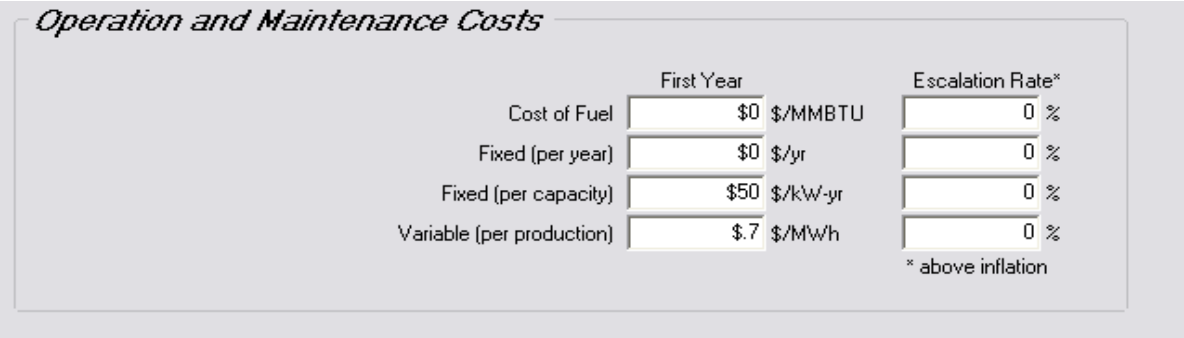

Figure 5-8 Operation and maintenance cost estimate

5.3 Financial Analysis of PTSEGs

The financial analysis is used to calculate project cash flows and other related financial metrics. Type of financing determines which groups of variables appear on the analysis of finance for the project.

Table 5-3 Type of financing for concentrating solar power

Concentrating Solar Power	Central Generation	Independent Power Producer (IPP) Investor-owned Utility (IOU)
	Distributed Generation	Cash Loan Third-Party Ownership

For utility projects two types of financing methods are employed: Independent Power Producer (IPP) and Investor-Owned Utility (IOU). All utility projects are funded through a combination of debt and equity that earn revenues from electricity sales.

5.3.1 Utility Independent Power Producer (IPP)

The project earns revenues through electricity sales to cover project costs. The owner pays cash for the equity portion of the total installed cost in year zero of the cash flow, and makes an interest and principal payment in subsequent years. Depreciation, interest payments and sales tax (in year one) are tax deductible. A first year power purchase price that meets internal rate of return, minimum debt service coverage ratio and positive cash flow requirements are calculated.

The variables that appear in calculating finance for CSP depend on the type of financing defined for the project. Table 5.4 shows the variables involved in utility IPP, commercial third party system ownership.

5.3.2 Investor-Owned Utility (IOU)

The project earns revenues through electricity sales to cover project costs. The owner pays cash for the equity portion of the total installed cost in year zero of the cash flow, and makes an

interest and principal payment in subsequent years. A first power purchase price that meets an internal rate of return requirement is calculated. The different financial terms used in SAM are listed in Table 5-4.

Table 5-4 Financial terms

Analysis Type	Variable Name	Description
General	Analysis Period	Number of years covered by the analysis. Typically equivalent to the project or investment life.
	Inflation rate	Annual rate of change of prices, typically based on a price index.
	Real Discount Rate	A measure of the time value of money expressed as an annual rate.
Taxes and Insurance	Federal and State Tax	Federal and state income tax rate. Applies to annual income from incentives and to revenues from electricity sales.
	Property Tax	Annual tax paid on project property, expressed as a percentage of total installed costs.
	Sales Tax	A one-time tax paid in year one on equipment purchases during installation, expressed as a percentage of the taxable portion of installed costs.
	Insurance	An annual operating expense expressed as a percentage of total installed costs.
Power Purchase Agreement	PPA Escalation Rate	Electricity sales price for each year in the project life is modified using the PPA (Power Purchase Agreement), Escalation Rate, and First year IPP projects with a goal or minimizing LCOE, the loan fraction and PPA escalation rate should be adjusted so that the minimum constraining assumptions are met
Constructing Assumptions	Minimum Required IRR	The lowest value of the internal rate of returned required for the project to be financially feasible. The internal rate of return is the discount rate that results in a project net present value of zero.
	Minimum	The lowest value of the debt-service coverage ratio required for the

	Required DSCR:	project to be financially feasible. The debt-service coverage ratio is the ratio of operating income to expenses in a given year.
Loan	Amount	The amount of money borrowed to cover installation expenses
	Term	Number of years required to repay a loan. Can be more or less than the analysis period.
	Rate	Loan interest rate.
	Loan (Debt) Fraction	Percentage of the total installed cost that can be borrowed. For analysis of Utility IPP projects with a goal of minimizing LCOE, the loan fraction and PPA escalation rate should be adjusted so that the minimum constructing assumptions are met.
Weighted Average Cost of Capital		The weighted average cost of capital (WACC) is defined as the minimum return that the project must earn to cover financing costs.
Federal and State Depreciation	MACRS Mid Quarter Convention	Modified Accelerated Cost Recovery System depreciation schedule offered by the Federal government and some states in USA. This tax deduction, expressed as a percentage of the total installed cost applies to the first years of the project life.

5.3.3 Financial Values

5.3.3.1 The Levelized Cost of Energy (LCOE)

The levelized cost of energy is defined as the present value of the total cost of installing and operating a power project over its economic life expressed in dollars per total kWh of energy produced over the project life.

For projects financed by cash, mortgage, or loan, the levelized cost of energy LCOE is calculated using the annual project cost, where C_n is the cost in Year n, and $C_n = 0$ is the cost in year 0, equivalent to the capital cost. Q_n is the electric energy produced by the system in year n. N is the project life time and d is the discount rate, both of which can be found on the financials page:

$$LCOE = \frac{\sum_{n=0}^{N} \frac{C_n}{(1+d)^n}}{\sum_{n=0}^{N} \frac{Q_n}{(1+d)^n}} \quad (5.1)$$

For utility projects with independent power producer financing or commercial projects with third party ownership financing, the LCOE is calculated as above, except that the annual required revenue $R_{Required,n}$ replaces the annual cost:

$$LCOE = \frac{\sum_{n=0}^{N} \frac{R_{Required,n}}{(1+d)^n}}{\sum_{n=0}^{N} \frac{Q_n}{(1+d)^n}} \quad (5.2)$$

5.3.3.2 Real and nominal LCOE

For real LCOE, the real discount rate appears in the total energy output term:

$$real\ LCOE = \frac{\sum_{n=0}^{N} \frac{C_n}{(1+d)^n}\ or \sum_{n=0}^{N} \frac{R_{Required,n}}{(1+d)^n}}{\sum_{n=0}^{N} \frac{Q_n}{(1+d)^n}} \quad (5.3)$$

Similarly, for the nominal LCOE, the nominal discount rate appears in the total energy output term:

$$nominal\ LCOE = \frac{\sum_{n=0}^{N} \frac{C_n}{(1+d)^n}\ or \sum_{n=0}^{N} \frac{R_{Required,n}}{(1+d)^n}}{\sum_{n=0}^{N} \frac{Q_n}{(1+d_{nominal})^n}} \quad (5.4)$$

The real discount rate and nominal discount rate are related by Equation below.

$$d_{nominal} = (1+d_{real})(1+e) - 1 \quad (5.5)$$

Where: $d_{nominal}$ is the nominal discount rate,

d_{real} is the real discount rate and,

e is the inflation rate.

5.3.4 Actual IRR, Actual Min DSCR, and First Year PPA

For utility projects with IPP financing and commercial projects with third party ownership financing, Solar Advisor Model calculates the Internal Rate of Return (Actual IRR), minimum Debt Service Coverage Ratio (Actual Min DSCR), and first year electricity sales price (First Year PPA) to meet a set constraints, which are inputs on the Financials page.

The actual internal rate of return is the discount rate, IRR, which corresponds to a project net present value, NPV, of zero:

$$NPV = \sum_{n=1}^{N} \frac{\mathrm{Re}\,quired\,\mathrm{Re}\,venue_n - AfterTaxCashFlow_n}{(1+IRR)^n} + AfterTaxCashFlow_o = 0 \qquad (5.6)$$

The debt service coverage ratio in each analysis year ($DSCR_n$) is the ratio of operating income to expenses in that year:

$$DSCRn = \frac{\mathrm{Re}\,quired\,\mathrm{Re}\,venue_n - OperatingCost_n}{InterestPayment_n + \mathrm{Pr}\,incipalPayment_n} \qquad (5.7)$$

The project's debt service coverage ratio is the lowest value of the DSCR that occurs in the life of the project:

$$DSCR = \min_{n=[1..N]} DSCR_n \qquad (5.8)$$

The first year sales price, *FirstYearPPA*, is calculated by using an iterative method to find the first year sales price that, when inflated using the escalation rate meets the minimum required IRR and the minimum required DSCR constraint, and results in a positive cash flow for each year if that is a requirement.

Find *FirstYearPPA* such that

Actual IRR = Minimum Required IRR, and

Actual Min DSCR = minimum Required DSCR, and

Cash Flow in Year n>0 (When the cash flow requirement is positive)

The minimum required IRR and DSCR are selected by the designer or concerned personal of the project.

5.3.4.1 kWh / kW - Year 1

The kilowatt-hour per kilowatt-year metric is the annual electric output in year one $E_{outputYear1}$ divided by the system capacity $P_{systemCapacity}$. For concentrating solar power systems, the system capacity is the rated turbine net capacity on the power block page.

$$\frac{kWh}{kW}\ Year1 = \frac{E_{outputYear1}}{P_{systemCapacity}} \tag{5.9}$$

5.3.4.2 Capacity Factor

The capacity factor CF is the first year annual electric output $E_{outputYear1}$ divided by the system capacity $P_{systemCapacity}$ divided by 8,760 hours per year.

$$CF = \frac{E_{OutputYear1}}{P_{SystemCapcity,8760}} \tag{5.10}$$

5.3.4.3 Annual Output-Year 1

The annual output in year one is the number of kilowatt-hours or megawatt-hours produced by the system in its first year of operation

Payback Cash Flow = After Tax Cash Flow + Debt Interest Payment × (1 – Effective Tax Rate)

+ Debt Repayment

The cumulative cash flow for each year is:

Cumulative Cash Flow = Payback Cash Flow + Cumulative Cash Flow (of previous year)

The two calculated values on the financial analysis are the loan amount and the weighted average cost of capital.

5.3.4.4 Loan

The amount in dollars borrowed by the project is calculated as a percentage of the total installed costs from the Costs page:

$$A_{LoanAmount} = C_{TotalInstalled} \cdot F_{DebtFraction} \quad (5.11)$$

Where: $A_{LoanAmount}$ = Amount

$C_{TotalInstalled}$ = Total Installed Costs (on the Costs page)

$F_{DebtFraction}$ = Loan (Debt) Fraction

5.3.4.5 Weighted Average Cost of Capital (WACC)

Weighted Average Cost of Capital (WACC) is defined as the minimum return that the project must earn to cover financing costs.

$$WACC = F_{ReturnOnEquity}.(1 - F_{DebtFraction}) + (1-F_{EffectiveTaxRate}).F_{LoanRate}.F_{DebtFraction} \quad (5.12)$$

The effective tax rate is a single number that includes both the federal income tax rate and state income tax rate. Solar Advisor uses the effective tax rate for several calculations requiring a total income tax value. The effective tax rate is calculated as:

$$F_{EffectiveTaxRate} = F_{FederalTaxRate}.(1 - F_{StateTaxRate}e)+F_{StateTaxRate} \quad (5.13)$$

The federal tax rate and state tax rate are input variables on the Financials page.

For utility projects, the return on equity is the required internal rate of return, also an input on the Financials page:

$$F_{ReturnOnEquity} = F_{RequiredIRR} \quad (5.14)$$

Where: $F_{FederalTAXRate}$ = Federal Tax

$F_{StateTaxRate}$ = State Tax

$F_{DebtFraction}$ = Loan (Debt) Fraction

$F_{LoanRate}$ = Rate

$F_{RequiredIRR}$ = Required Internal Rate of Return (IRR)

5.4 Results of SAM Analysis

Solar Advisor Model software can use weather data files in two formats: Typical Meteorological Year format and Energy Plus Weather format (EPW).

5.4.1 Costs

In the costs page, SAM calculates the different estimates for direct, indirect, and operation and maintenance cost components for the project. This page is used to determine the total installed cost that can be used as input for the financial page.

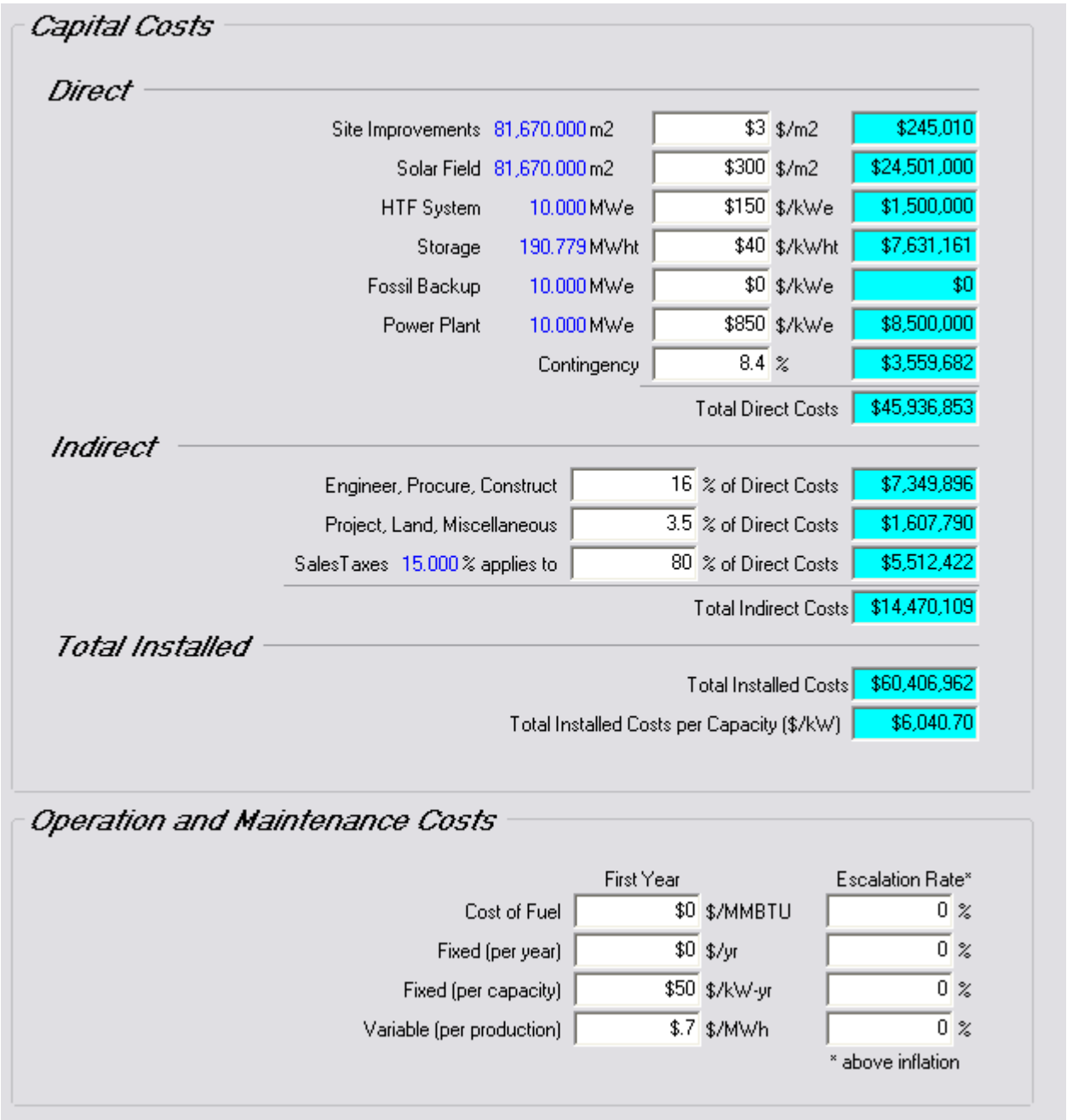

Figure 5-9 The costs page

5.4.2 Solar Field Input

The plant layout, The Heat Transfer Fluid, Solar Filed Areas are found in the Solar Field input of SAM. The data from the Solar Field Model are used to determine the Capital and Operation and Maintenance costs in the Costs Page.

Figure 5-10 The solar field page

5.4.3 Financial Page

The Financial page displays the variables that Solar Advisor uses to calculate project cash flows and other related financial metrics. Type of Financing determines which groups of variables appear on the Financials page. In the financials page the loan amount, the project life, taxes and insurance, power purchase agreements and other inputs are found.

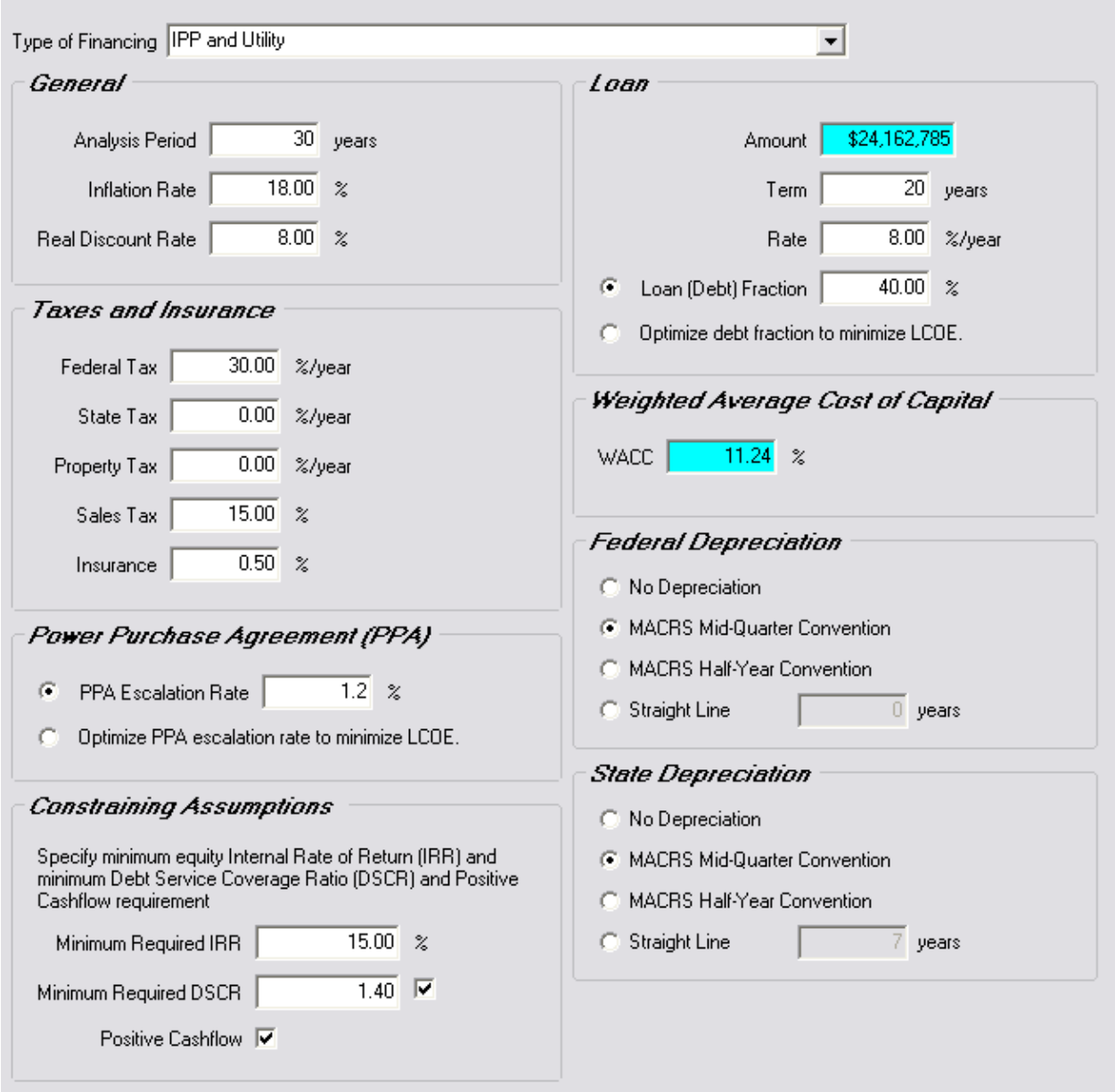

Figure 5-11 Financial input page

5.4.4 Power Block

The Power block parameters describe the equipment in the system that converts thermal energy from the solar filed or thermal energy storage system into electricity. The power block is based on a steam turbine that runs on a conventional Rankine power cycle and may or may not include fossil fuel backup. Power block components include a turbine, heat exchangers or transfer heat

from the solar field or thermal energy storage to the turbine, and a cooling system to dissipate waste heat.

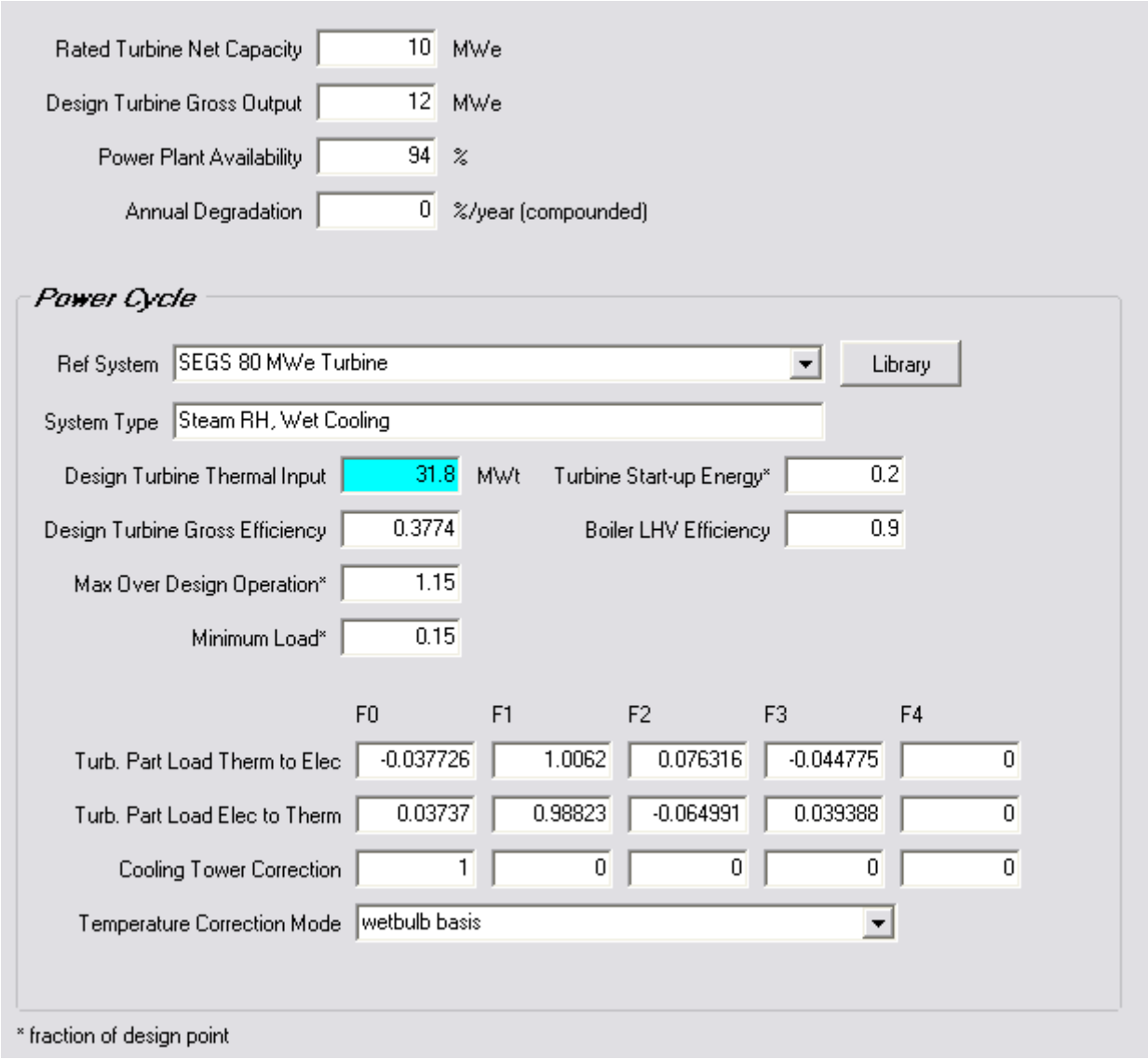

Figure 5-12 Power block page

5.4.5 SCA/HCE

The SCA/HCE parameters describe the solar collector assembly (SCA) and heat collection element (HCE). Solar Collector Assembly (SCA) parameters are for an individually tracking component of the solar field that includes mirrors, supporting structure, and heat collection elements or receivers.

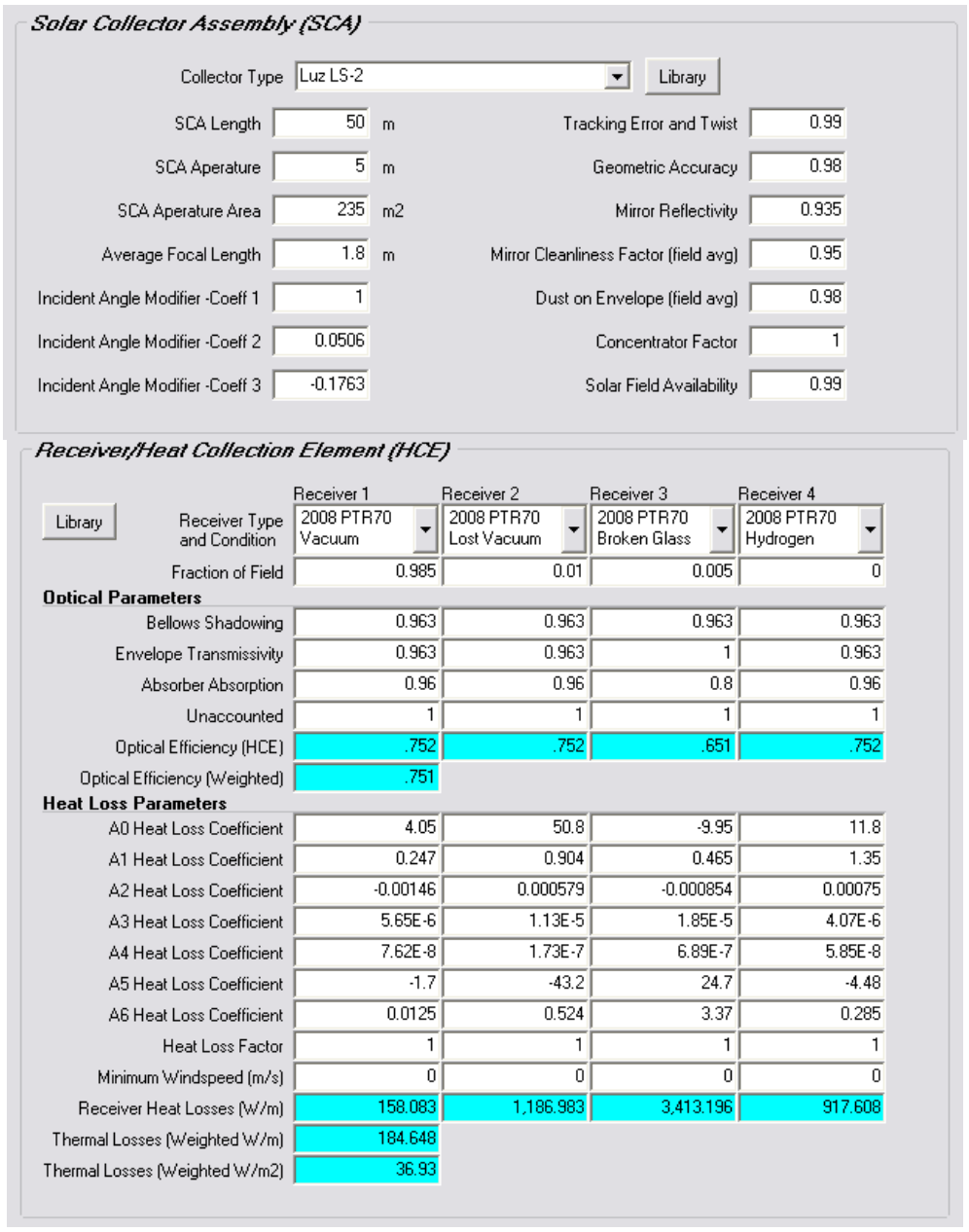

Solar Collector Assembly (SCA)

Collector Type	Luz LS-2	Library		
SCA Length	50	m	Tracking Error and Twist	0.99
SCA Aperature	5	m	Geometric Accuracy	0.98
SCA Aperature Area	235	m2	Mirror Reflectivity	0.935
Average Focal Length	1.8	m	Mirror Cleanliness Factor (field avg)	0.95
Incident Angle Modifier -Coeff 1	1		Dust on Envelope (field avg)	0.98
Incident Angle Modifier -Coeff 2	0.0506		Concentrator Factor	1
Incident Angle Modifier -Coeff 3	-0.1763		Solar Field Availability	0.99

Receiver/Heat Collection Element (HCE)

Library		Receiver 1	Receiver 2	Receiver 3	Receiver 4
	Receiver Type and Condition	2008 PTR70 Vacuum	2008 PTR70 Lost Vacuum	2008 PTR70 Broken Glass	2008 PTR70 Hydrogen
	Fraction of Field	0.985	0.01	0.005	0
Optical Parameters					
	Bellows Shadowing	0.963	0.963	0.963	0.963
	Envelope Transmissivity	0.963	0.963	1	0.963
	Absorber Absorption	0.96	0.96	0.8	0.96
	Unaccounted	1	1	1	1
	Optical Efficiency (HCE)	.752	.752	.651	.752
	Optical Efficiency (Weighted)	.751			
Heat Loss Parameters					
	A0 Heat Loss Coefficient	4.05	50.8	-9.95	11.8
	A1 Heat Loss Coefficient	0.247	0.904	0.465	1.35
	A2 Heat Loss Coefficient	-0.00146	0.000579	-0.000854	0.00075
	A3 Heat Loss Coefficient	5.65E-6	1.13E-5	1.85E-5	4.07E-6
	A4 Heat Loss Coefficient	7.62E-8	1.73E-7	6.89E-7	5.85E-8
	A5 Heat Loss Coefficient	-1.7	-43.2	24.7	-4.48
	A6 Heat Loss Coefficient	0.0125	0.524	3.37	0.285
	Heat Loss Factor	1	1	1	1
	Minimum Windspeed (m/s)	0	0	0	0
	Receiver Heat Losses (W/m)	158.083	1,186.983	3,413.196	917.608
	Thermal Losses (Weighted W/m)	184.648			
	Thermal Losses (Weighted W/m2)	36.93			

Figure 5-13 SCA/HCE input pages

5.4.6 Annual Energy Flow

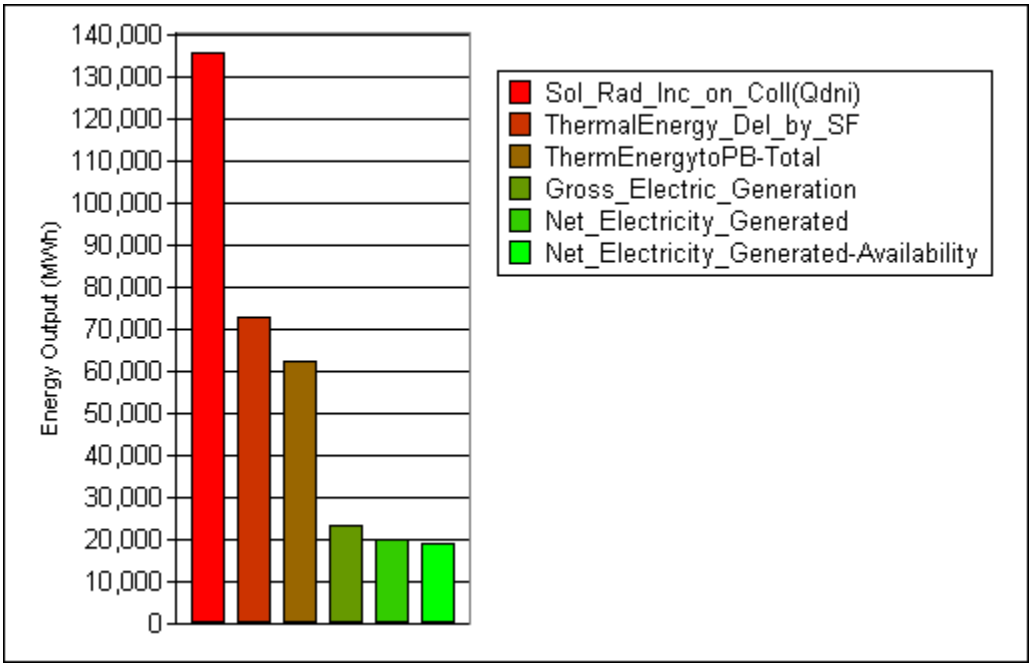

Figure 5-14 Annual energy flow

Table 5-5 Annual energy flow

Energy	Energy Flow (MWH)
Solar Radiation Incident on the Collector (Q_{dni})	135,770.82
Thermal Energy Delivered by the Solar Field	73,010.78
Total Thermal Energy to Power Block	62,314.23
Gross Electric Generation	23,318.05
Net Electricity Generated	20,046.16
Net Electricity Generated-Availability	18,843.39

5.4.7 Cash Flow

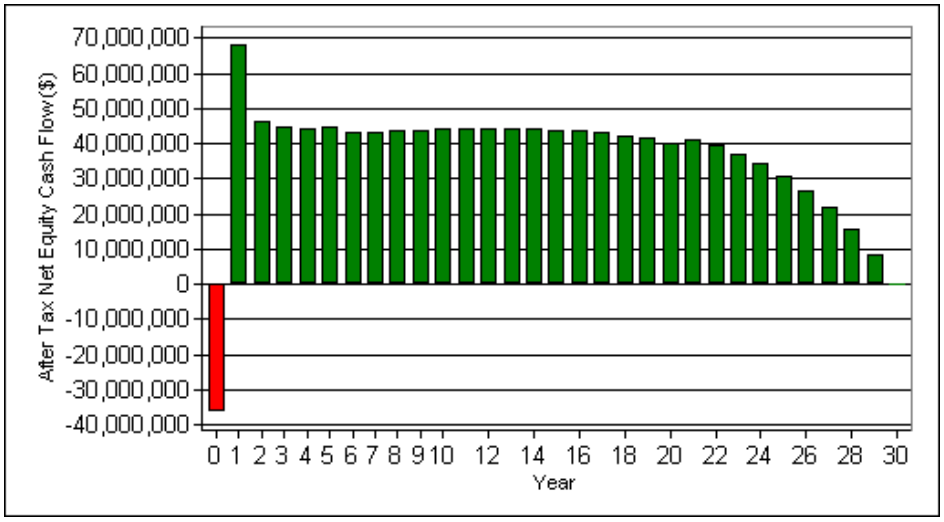

Figure 5-15 Cash flow

Table 5-6 After tax net equity cash flow ($)

Year	Cash Flow ($)		Year	Cash Flow ($)
0	-36,244,176.94		16	43,596,054.64
1	68,179,469.16		17	43,081,243.56
2	46,594,126.73		18	42,374,495.25
3	44,953,049.39		19	41,440,418.29
4	44,438,713.25		20	40,237,268.56
5	44,808,012.35		21	41,176,841.18
6	43,264,033.40		22	39,354,300.00
7	43,313,498.66		23	37,092,888.94
8	43,601,398.80		24	34,312,281.66
9	43,849,915.44		25	30,917,677.15
10	44,051,039.41		26	26,797,194.05
11	44,195,322.82		27	21,818,796.00
12	44,271,621.22		28	15,826,663.59
13	44,266,789.46		29	8,636,913.16
14	44,165,322.94		30	32,545.06
15	43,948,934.40			

5.4.8 Cost Stacked Bar

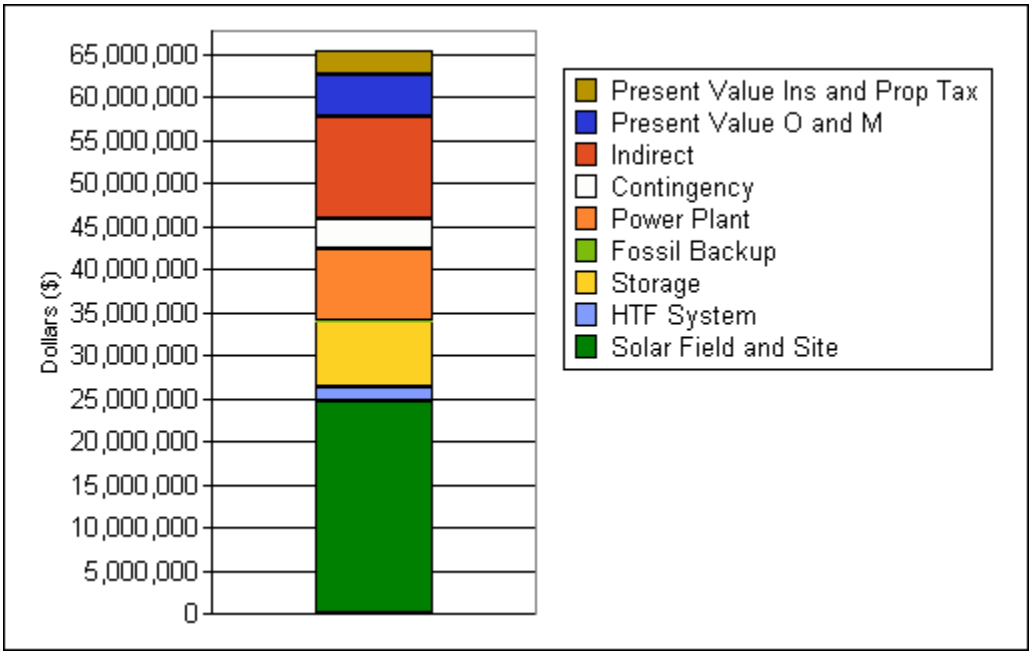

Figure 5-16 Cost stacked bar

Table 5-7 Cost stacked bar values

Cost Type	Single Value
Solar Field and Site	24,746,010.00
HTF System	1,500,000.00
Storage	7,631,160.57
Fossil Backup	0.00
Power Plant	8,500,000.00
Contingency	3,559,682.33
Indirect	11,805,771.20
Present Value O and M	4,896,070.84
Present Value Ins and Prop Tax	2,754,465.90

5.4.9 LCOE

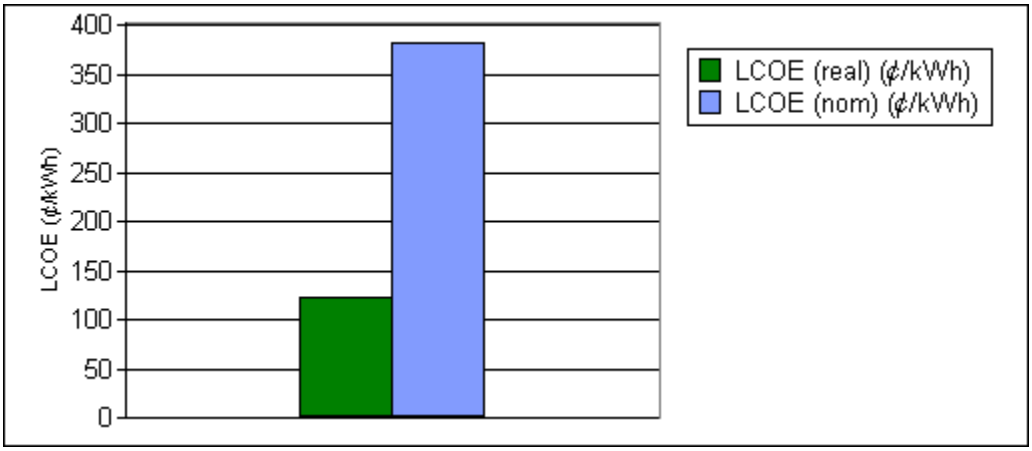

LCOE (real) (¢/kWh)	LCOE (nom) (¢/kWh)
123.754	382.557

Figure 5-17 LCOE

5.4.10 Monthly energy flow

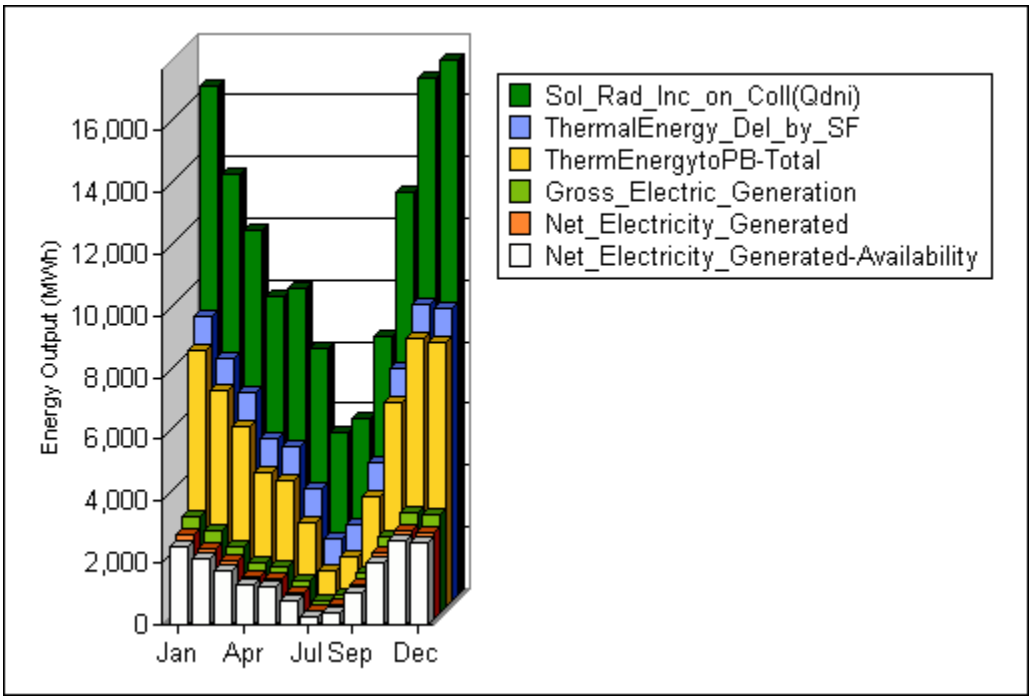

Figure 5-18 Monthly energy flow

Table 5-8 Monthly energy flow

Month	Solar Radiation Incident on Collector (Qdni)	Thermal Energy Delivered by Solar Field	Total Thermal Energy to Power Block	Gross Electric Generation	Net Electricity Generated	Net Electricity Generated-Availability
Jan	16,433.96	9,187.82	8,263.61	3,099.37	2,709.21	2,546.66
Feb	13,594.62	7,839.89	7,016.35	2,633.59	2,292.60	2,155.04
Mar	11,784.33	6,725.66	5,806.84	2,167.20	1,871.52	1,759.22
Apr	9,660.17	5,218.70	4,310.44	1,608.99	1,374.29	1,291.84
May	9,943.98	5,001.88	4,076.70	1,517.90	1,292.15	1,214.62
Jun	7,990.43	3,602.16	2,738.42	1,032.04	849.00	798.06
Jul	5,239.95	1,985.09	1,155.30	413.98	274.46	257.99
Aug	5,671.16	2,457.98	1,602.75	600.11	443.78	417.15
Sep	8,366.11	4,460.96	3,546.34	1,320.67	1,111.45	1,044.77
Oct	13,038.70	7,511.45	6,592.63	2,457.64	2,139.71	2,011.33
Nov	16,747.90	9,565.19	8,669.65	3,265.05	2,875.13	2,702.63
Dec	17,299.50	9,454.01	8,535.20	3,199.38	2,809.81	2,641.23

Table 5-9 Summary of the results

Metric	Base
LCOE (real)(¢/kWh)	125.87
LCOE (nom)(¢/kWh)	389.09
Actual IRR (%)	>100.00
Actual Min DSCR	28.05
First Year PPA(¢/kWh)	372.18
PPA Escalation Rate (%)	1.2
Debt Fraction (%)	40
Min Cash Flow($)	32,545.06
kWh / kW - Year 1(h)	1,884.05
Capacity Factor (%)	21.51
Annual Output - Year 1(MWh)	18,840.54

CHAPTER 6

CONCLUSION AND RECOMMENDATIONS

6.1 Conclusion

In this paper a power plant is designed using appropriate considerations and assumptions. The designed power plant is modeled in two simulation programs, MATLAB and TRNSYS. The MATLAB program is used only to model full load operation of the power plant. The output of the model developed by this program is used as a reference state operation in the TRNSYS model. The TRNSYS model of the power plant is used to model both the solar field and the power field. This model is developed by using component from STEC library, the TRNSYS built in library and a developed component, Type 850. The main purpose of the model developed by the TRNSYS is to investigate the operation of the power plant at weather conditions different from the reference values. Both models are used only for solar only operation.

The performance of the model developed in the TRNSYS is evaluated for year 2001. Representative days for the selected year are used for the simulation. The results of the simulation have shown that the mass flow rate of the HTF from the solar field and gross power produced are heavily dependent on DNI. This can be seen from graphs above the mass flow rate graph and gross power graph retained the shape of the DNI graph.

Cost and financial analysis is made for this power plant using Solar Advisor Model (SAM). The analysis is made by modeling the power plant with a specified capacity under Addis Ababa weather condition. The results of this model give for rated net turbine capacity of 10 MWe the total installed cost is $60,409,962. From the figures it can also be seen that the solar field is the major source of direct costs ($24,501,000).

6.2 Recommendations

Although the model developed a detailed prediction of the operation of the designed power plant, the model cannot be validated with actual operation of power plants. This is because there are no power plants that operate using PTSEGs in Addis Ababa or Ethiopia.

The thermal losses and efficiency of the HCEs are evaluated for LS-2 parabolic trough collectors. Currently there are parabolic trough collectors that have a better performance than LS-2. Therefore it is recommended to have experimentation made for this improved collectors and be applied in the model.

The performance of HCEs degrades due to several years of operations. The HCEs are manufactured with the annulus space being vacuum. Through operation of the HCEs this vacuum is replaced by ambient air and Hydrogen coming from the HTF. This gases increase thermal losses and consequently decrease the heat energy collected by the HTF. The effect of the annulus gas in the power output is not studied in this paper.

Addis Ababa is not the best place in Ethiopia to install PTSEGs. Afar and Somali regions obtain the best locations for SEGs plants in Ethiopia with higher DNI values and more clear days than Addis Ababa. Lack of detailed weather data in TMY2 and EPW formats impeded the use of the sites in this thesis paper.

In the MATLAB modeling of the power plant the isentropic efficiency of steam turbines are assumed to equal to 85% and also the isentropic efficiency of the pumps is taken to be 70%. But these assumptions can be further improved by making experimentation of steam turbines (pumps) with the same rated design.

The both TRNSYS and MATLAB mode of the power plant pressure loss in the heat exchangers and feedwater heater is neglected. This is due to a fact that pressure loss depends on the physical data of the components.

Finally in both models thermal storage is not modeled. Hence the models can be further improved by including this component.

APPENDIXES

Appendix A

MATLAB Code for the Power Plant Model at Reference Weather Condition

```
clear
clc
format short g

%************************************************************************
% Water and steam properties according to IAPWS IF-97
% By Magnus Holmgren, www.x-eng.com
% XSteam provides accurate steam and water properties from 0 - 1000 bar
% and from 0 - 2000 deg C according to the standard IAPWS IF-97.
%************************************************************************

%*** Nomenclature *****************************************************
% T   Temperature (deg C)
% Ts  Temperature at Constant Specific Entropy of Previous State (deg C)
% p   Pressure    (bar)
% h   Enthalpy    (kJ/kg)
% v   Specific volume (m3/kg)
% s   Specific entropy
% Cp  Specific isobaric heat capacity
% CFWH      Closed Feed Water Heater
% OFWH      Open Feed Water Heater
% HP2       High Pressure CFWH 2
% HP1       High Pressure CFWH 1
% LP        Low Pressure CFWH
% SH        Superheater
% SG        Steam Generator
% PH        Preheater
```

```
% RH        Reheater


W_dot_net=12000;  % [kW]      Power needed to be Produced from the Plant
T(1) = 375;       % [C]       Initial Temperature of Steam
T1_SH = 390;      % [C]       Inlet Temperature of the HTF in to the SH
T2_PH = 300;      % [C]       Outlet Temperature of the HTF from the PH
T_1 = T(1) - 5;
P(1)= XSteam('psat_T',T_1);   % [bar]     Guess for P(1)
P(7) = 0.08;                  % [bar]     Condenser Pressure
err = 10;

while(err>0.5)
P(1)= P(1) - 0.5;             % [bar]  Guess for P(1)
n_fwh = 5;                    %        Number of FWHs (4) Plus one
T_satp1=XSteam('Tsat_p',P(1)); % [C] Saturation Temperature of Steam at P(1)
T_7 = XSteam('Tsat_p',P(7));  % [C]   Saturation Temperature of Steam at P(7)
Delta_t = (T_satp1 - T_7)/n_fwh;    % [C]    Temperature Rise between FWHs
T_6 = T_7 + Delta_t ;               % [C]    Temperature of FW in the Lp FWH
P(6) = XSteam('psat_T',T_6);        %   [bar]     Pressure   of   FW   in   the
LP(Pressure of Steam inlet to LP Turbine 3)

T_5= T_6 + Delta_t;           % [C]    Temperature of FW in the Deaerator
P(5) = XSteam('psat_T',T_5);  %    [bar]       Pressure    of    FW    in    the
Deaerator(Pressure of Steam  inlet to LP Turbine 2)
T_3 = T_5 + Delta_t;           % [C]    Temperature of FW in the HP1 FWH
P(3) = XSteam('psat_T',T_3);  % [bar]  Pressure of FW in the HP1(Pressure of
Steam inlet to LP Turbine 1)

P(4) = P(3);
T_2 = T_3 + Delta_t;                % [C]    Temperature of FW in the HP2 FWH
P(2) = XSteam('psat_T',T_2);        %   [bar]     Pressure   of   FW   in   the
HP2(Pressure of Steam inlet to HP Turbine 2)
```

```
P(8) = P(7) ;     % [bar]  Pressure of FW from the Condenser
P(9) = P(5) ;     % [bar]  Pressure of FW into the LP FWH
P(10) = P(5) ;    % [bar]  Pressure of FW from the LP FWH
P(11) = P(5) ;    % [bar]  Pressure of FW from the Deaerator
P(12) = P(1) ;    % [bar]  Pressure of FW into the HP1 FWH
P(13) = P(1);     % [bar]  Pressure of FW from the HP1 FWH
P(14) = P(1);     % [bar]  Pressure of FW from the HP2 FWH
P(15) = P(1);     % [bar]  Pressure of FW into SG
P(16) = P(1);     % [bar]  Pressure of FW from SG
T(4) = T(1);      % [C]       Reheater Temperature equal to T(1)

    %HP Turbine 1
Eta_t1 = 0.85;                      %           Turbine isentropic efficiency
h(1)= XSteam('h_pT',P(1),T(1));     % [kJ/kg]   Steam Enthalpy at State (1)
s(1) = XSteam('s_pT',P(1),T(1));    % [kJ/kg.K] Steam Entropy at State (1)
v(1) = XSteam('v_pT',P(1),T(1));    % [m^3/kg]  Specific Volume at State (1)
s_s(2)=s(1);
hs(2)=XSteam('h_ps',P(2),s_s(2));
Ts(2)=XSteam('T_ps',P(2),s_s(2));

h(2) =(h(1)-Eta_t1*(h(1)-hs(2))); % [kJ/kg] Steam Enthalpy at State (2)
T(2)=XSteam('T_ph',P(2),h(2));    % [C]     Temperature of Steam at State (2)
s(2)=XSteam('s_ph',P(2),h(2));    % [kJ/kg.K] Steam Entropy at State (2)


    %HP Turbine 2
Eta_t2 = 0.85;                     %           Turbine isentropic efficiency
s_s(3)= s(2);
hs(3)=XSteam('h_ps',P(3),s_s(3));
Ts(3)=XSteam('T_ps',P(3),s_s(3));
```

```
h(3) = (h(2)-Eta_t2*(h(2)-hs(3)));  % [kJ/kg]   Steam Enthalpy at State (3)
T(3)  = XSteam('T_ph',P(3),h(3));   % [C]   Temperature of Steam at State (3)
s(3)=XSteam('s_ph',P(3),h(3));      % [kJ/kg.K] Steam Entropy at State (3)
 v(3)=XSteam('v_ph',P(3),h(3));     % [m^3/kg]  Specific Volume at State (3)

      % LP Turbine 1
Eta_t3 = 0.85;                      %           Turbine isentropic efficiency
h(4)=XSteam('h_pT',P(4),T(4));      % [kJ/kg]   Steam Enthalpy at State (4)
s(4)=XSteam('s_pT',P(4),T(4));      % [kJ/kg.K] Steam Entropy at State (4)
v(4)=XSteam('v_ph',P(4),h(4));      % [m^3/kg]  Specific Volume at State (4)

s_s(5)=s(4);
hs(5)= XSteam('h_ps',P(5),s_s(5));
Ts(5)= XSteam('T_ps',P(5),s_s(5));
h(5) =(h(4)- Eta_t3*(h(4)-hs(5)));  % [kJ/kg]   Steam Enthalpy at State (5)
T(5)=XSteam('T_ph',P(5),h(5));      % [C] Temperature of Steam at State (5)
s(5)=XSteam('s_ph',P(5),h(5));      % [kJ/kg.K] Steam Entropy at State (5)
v(5)=XSteam('v_ph',P(5),h(5));      % [m^3/kg]  Specific Volume at State (5)


    % LP Turbine 2
Eta_t4 = 0.85;                      %           Turbine isentropic efficiency
s_s(6) = s(5);
hs(6)= XSteam('h_ps',P(6),s_s(6));
Ts(6)= XSteam('T_ps',P(6),s_s(6));

h(6) = (h(5)- Eta_t4*(h(5)-hs(6))); % [kJ/kg]   Steam Enthalpy at State (6)
T(6) = XSteam('T_ph',P(6),h(6));    % [C]   Temperature of Steam at State (6)
s(6) = XSteam('s_ph',P(6),h(6));    % [kJ/kg.K] Steam Entropy at State (6)
v(6) = XSteam('v_ph',P(6),h(6));    % [m^3/kg]  Specific Volume at State (6)
```

```
    % LP Turbine 3
Eta_t4 = 0.85;                        % Turbine isentropic efficiency
s_s(7) = s(6);
hs(7)= XSteam('h_ps',P(7),s_s(7));
Ts(7)= XSteam('T_ps',P(7),s_s(7));

h(7) =(h(6)- Eta_t4*(h(6)-hs(7)));  % [kJ/kg]   Steam Enthalpy at State (7)
T(7) = XSteam('T_ph',P(7),h(7));    % [C]    Temperature of Steam at State (7)
s(7) = XSteam('s_ph',P(7),h(7));    % [kJ/kg.K] Steam Entropy at State (7)
v(7) = XSteam('v_ph',P(7),h(7));    % [m^3/kg]  Specific Volume at State (7)

h(8) = XSteam('hL_p',P(8));         % [kJ/kg]   Steam Enthalpy at State (8)
T(8) = XSteam('Tsat_p',P(8));       % [C]   Temperature of Steam at State (8)
s(8) = XSteam('sL_p',P(8));         % [kJ/kg.K] Steam Entropy at State (8)
v(8) = XSteam('vL_p',P(8));         % [m^3/kg]  Specific Volume at State (8)

    % Condensate Pump analysis
Eta_pump1 = 0.75;                   %     Pump isentropic efficiency
w_pump1_s = v(8)*(P(9)-P(8))*100;   %     SSSF isentropic pump work assuming
constant specific volume
w_pump1 = w_pump1_s/Eta_pump1;      % Definition of pump efficiency
h(9) = h(8)+w_pump1;                %     Steady-flow conservation of energy
T(9)= XSteam('T_ph',P(9),h(9));     % [C]   Temperature of Steam at State (9)
s(9)= XSteam('s_ph',P(9),h(9));     % [kJ/kg.K] Steam Entropy at State (9)


    % HP Preheater 2 CFH analysis
P(17)=P(2);
h(17)=XSteam('hL_p',P(17)); % Condensate leaves heater as sat. Liquid at (17)
T(17)=XSteam('Tsat_p',P(17));       % [C]   Temperature of Steam at State (8)
s(17)=XSteam('sL_p',P(17));         % [kJ/kg.K] Steam Entropy at State (8)

h(14) = h(17);    % Enthalpy FW Out of FWH HP1 is taken to be Equal to h(17)
```

```
T(14) = XSteam('T_ph',P(14),h(14)); % [C]  Temperature of Steam at State (14)
s(14)=XSteam('s_ph',P(14),h(14));   % [kJ/kg.K] Steam Entropy at State (14)

h(13) = XSteam('hL_p',P(3));        % Enthalpy FW Out of FWH HP1 is taken to
be Equal to h(19)

T(13)=XSteam('T_ph',P(13),h(13)); % [C] Temperature of Steam at State (13)
s(13)=XSteam('s_ph',P(13),h(13));  % [kJ/kg.K] Steam Entropy at State (13)

    % Fraction of Steam Extracted at FWH HP2
a   = (h(14)-h(13))/(h(2)-h(17));   % Steady-flow conservation of energy



    % HP Preheater 2CFWH Overall heat transfer analysis
T_in_steam_HP2 = T(2);        % [C]       Temperature of Steam inlet to HP2
TAVG_HP2 = (T(14) + T(13))/2; % [C]       Average  Temperature  of  the  FW  in
the FWH HP2

C_water_HP2  =  XSteam('Cp_pT',P(13),TAVG_HP2); % [kJ/kg.K]  FW  Specific  Heat
Capacity

q_water_HP2 = C_water_HP2*(T(14) - T(13));      %  [kJ/kg]      Change  of  FW
enthalpy in the FWh HP2

q_max_HP2 = C_water_HP2*(T(2)-T(13));           %  [kJ/kg]      Max.  Possible
Change of enthalpy in the FWH HP2

epsilon_water_HP2 = q_water_HP2/q_max_HP2;      %     Effectiveness   of   the
Heat Transfer in the FWH HP2

NTU_water_HP2 = -log(1 - epsilon_water_HP2) ;   %     Number of Heat Transfer
Units in the FWH HP2
```

```
    % Trap Analysis between FWHs HP2 and HP1
P(18) = P(3);
h(18) = h(17);                      %     Steady-flow conservation of energy
for the trap operating as a throttle

T(18) = XSteam('T_ph',P(18),h(18));  % [C] Temperature of Steam at State (18)
s(18) = XSteam('s_ph',P(18),h(18));  % [kJ/kg.K] Steam Entropy at State (18)
h(11)=XSteam('hL_p',P(11));% Condensate leaves heater as sat. Liquid at P(11)
T(11)=XSteam('Tsat_p',P(11)); % [C]        Temperature of Steam at State (11)
s(11)=XSteam('sL_p',P(11));   %  [kJ/kg.K]  Steam  Entropy  at  State  (11)
v(11)=XSteam('vL_p',P(11));   % [m^3/kg]  Specific Volume at State (11)

    % Boiler condensate pump or Pump 2 analysis
Eta_pump2 = 0.75;                   %     Pump isentropic efficiency
w_pump2_s=v(11)*(P(12)-P(11))*100;  %     SSSF  isentropic  pump  work  assuming
constant specific volume

w_pump2=w_pump2_s/Eta_pump2;        %     Definition of pump efficiency
h(12) = h(11)+w_pump2;              %     Steady-flow conservation of energy



    % HP Preheater 1 CFWH analysis
s(12)=XSteam('s_ph',P(12),h(12));   % [kJ/kg.K] Steam Entropy at State (12)
T(12)=XSteam('T_ph',P(12),h(12));   % [C]  Temperature of Steam at State (12)
P(19)=P(3);
h(19) = XSteam('hL_p',P(19));       % Condensate leaves heater as sat. liquid
at P(19)
T(19) = XSteam('Tsat_p',P(19)); % [C]      Temperature of Steam at State (19)
s(19) = XSteam('sL_p',P(19));   % [kJ/kg.K] Steam Entropy at State (19)

    % Fraction of Steam Extracted at FWH HP1
 b = ((h(13) - h(12)) - a*(h(18)- h(19)))/(h(3) - h(19));   % Steady-flow
conservation of energy
```

```
    % Trap analysis Between FWHs HP1 and Deaerator
P(20) = P(5);
h(20) = h(19);                      % Steady-flow conservation of energy for
the trap operating as a throttle

T(20)= XSteam('T_ph',P(20),h(20));  % [C]  Temperature of Steam at State (20)
s(20) = XSteam('s_ph',P(20),h(20)); % [kJ/kg.K] Steam Entropy at State (20)

    % HP Preheater 1 CFWH Overall heat transfer analysis
Cp_AVG_HP1 = (h(13) - h(12))/(T(13) - T(12)); % [kJ/kg.K] FW Specific Heat
Capacity in HP1

h_in_steam_HP1= (b*h(3) + a*h(18))/(a+b);       % [kJ/kg] Enthalpy of Steam
inlet to the FWH HP1

T_in_steam_HP1 = XSteam('T_ph',P(3),h_in_steam_HP1);    % [C]      Temperature
of Steam inlet to FWH HP1

q_water_HP1 = Cp_AVG_HP1*(T(13) - T(12));             % [kJ/kg] Change of FW
enthalpy in the FWH HP1

q_max_HP1 = Cp_AVG_HP1*(T_in_steam_HP1-T(12));  %   [kJ/kg]   Max.   Possible
Change of enthalpy in the FWH HP1

epsilon_water_HP1 = q_water_HP1/q_max_HP1;      %     Effectiveness   of   the
Heat Transfer in the FWH HP1

NTU_water_HP1 = -log(1 - epsilon_water_HP1);    %     Number of Heat Transfer
Units in the FWH HP1

h(10)=XSteam('hL_p',P(6));                      %     Condensate        leaves
heater as sat. liquid at P(6)
```

```
T(10)=XSteam('T_ph',P(10),h(10));   % [C] Temperature of Steam at State (10)
s(10)=XSteam('s_ph',P(10),h(10));   % [kJ/kg.K] Steam Entropy at State (10)



    % Fraction of Steam Extracted at OFWH
c = (h(11)- (1-a-b)*h(10)-(a+b)*h(20))/(h(5) - h(10)); %    Steady-flow
conservation of energy

    % LP Preheater CFWH analysis
P(21)= P(6);
h(21) = XSteam('hL_p',P(21));       %     Condensate  leaves  heater  as  sat.
liquid at P(21)

T(21) = XSteam('Tsat_p',P(21));     % [C]  Temperature of Steam at State (21)
s(21) = XSteam('sL_p',P(21));       % [kJ/kg.K] Steam Entropy at State (21)

    % Fraction of Steam Extracted at LP CFWH
d  =((1-a-b-c)*h(10)  -  (1-a-b-c)*h(9))/(h(6)  -  h(21));  %  Steady-flow
conservation of energy

    % LP Preheater CFWH Overall heat transfer analysis
TAVG_LP = (T(9) + T(10))/2;                     % [C] Average  Temperature  of
the FW in the CFWH LP

Cp_AVG_LP = XSteam('Cp_pT',P(10),TAVG_LP);      % [kJ/kg.K] FW Specific Heat
Capacity in CFWH LP

q_water_LP1 = Cp_AVG_LP *(T(10)-T(9));          %  [kJ/kg]      Change  of  FW
enthalpy in the CFWH LP

T_in_steam_LP1 = XSteam('T_ph',P(6),h(6));      % [C]          Temperature of
Steam inlet to CFWH LP
```

```
q_max_LP1 = Cp_AVG_LP *(T_in_steam_LP1-T(9));   %  [kJ/kg]      Max.  Possible
Change of enthalpy in the CFWH LP

epsilon_water_LP1 = q_water_LP1/q_max_LP1;      %     Effectiveness   of   the
Heat Transfer in the CFWH LP

NTU_water_LP1 = -log(1 - epsilon_water_LP1);    %     Number of Heat Transfer
Units in the CFWH LP



    % Trap analysis Between CFWH LP and the Condenser
P(22) = P(7) ;
h(22) = h(21);                      %     Steady-flow conservation of energy
for the trap operating as a throttle

T(22) = XSteam('T_ph',P(22),h(22)); % [C]  Temperature of Steam at State (22)
s(22)=XSteam('s_ph',P(22),h(22));   % [kJ/kg.K] Steam Entropy at State (22)

    % Heat Transfer Analysis of the Boiler
q_in = h(1)+(1-a-b)*h(4)-h(14)- (1-a-b)*h(3);   %  SSSF  First  Law  for  the
Boiler

    % Specific Work done in the Turbine [kJ/kg]
w_turb = (h(1) - h(2)) + (1-a)*(h(2) - h(3)) + (1-a-b)*(h(4) -h(5)) + (1-a-b-
c)*(h(5) - h(6)) + (1-a-b-c-d)*(h(6)-h(7));

    % Condenser analysis
q_out = (1-a-b-c-d)*h(7)+(d)*h(22)-(1-a-b-c)*h(8);    %     SSSF   First   Law
for the Condenser

    % Cycle Statistics
w_net=w_turb - ((1-a-b-c)*w_pump1+ w_pump2); % [kJ/kg] Net Specific Work done
```

```
Eta_th=w_net/q_in;            %     Thermal Efficiency of the Power Plant
mwater =  W_dot_net/w_net;    % [kg/s]    Mass Flow Rate of Water

UA_HP2  =  NTU_water_HP2*mwater*C_water_HP2;  % [kW/K]  Overall  Heat  Transfer
Coeff. in CFWH HP2

UA_HP1 = NTU_water_HP1*mwater*Cp_AVG_HP1;       %  [kW/K]        Overall  Heat
Transfer Coeff. in CFWH HP1

UA_LP1 = NTU_water_LP1*mwater*Cp_AVG_LP;        % [kW/K]    Overall       Heat
Transfer Coeff. in CFWH LP



    %Heat Transfer in the Super Heater
t2_SH = T(1);                         %     Outlet temperature of the steam
t1_SH = XSteam('Tsat_p',P(1));      % [C] Inlet temperature of the steam
h(16) =XSteam('hV_p',P(1));         % [kJ/kg]   Steam Enthalpy at State (16)
T(16) = t1_SH;                        % [C]  Temperature of Steam at State (16)
s(16) = XSteam('sV_p',P(1));        % [kJ/kg.K] Steam Entropy at State (16)

Tavg = (t2_SH +t1_SH)/2;    % [C] Average Temperature of Steam in the SH
Cp_water_SH =(h(1)-h(16)) /(T(1) -T(16));          % [kJ/kg.K] Specific heat
Capacity of Steam in the SH

C_cold = Cp_water_SH *(mwater);     % [kW/K]    Steam Capacitance in the SH
Q_SH=C_cold*(t2_SH-t1_SH);          % [kW]      Heat Transfer in the SH



    % Heat Transfer in the Steam Generator
t1_SG = XSteam('Tsat_p',P(1));      % [C] Saturation  Temperature  of  Steam  in
the SG

h(15)  =XSteam('hL_p',P(1));        % [kJ/kg]   Steam Enthalpy at State (15)
```

```
T(15) = t1_SG;                      % [C]  Temperature of Steam at State (15)
s(15) = XSteam('sL_p',P(1));        % [kJ/kg.K] Steam Entropy at State (15)
hfg = h(16) -     h(15);            % Latent heat of vaporization at t1_SG
Q_SG=mwater*hfg;                    % [kW]      Heat Transfer in the SG

    % Heat Transfer in Preheater
tph2 = t1_SG;                       % [C] Outlet  Temperature  of  Steam  from
Preheater (State (15))

tph1=T(14);                         % [C] Inlet Temperature of Steam into the
Preheater(State (14))

Cp_water_PH = (h(15) -h(14))/(T(15) -T(14));      % [kJ/kg.K] Specific heat
Capacity of the HTF in the PH
C_cold_PH = mwater*Cp_water_PH;     % [kW/K]    Steam Capacitance in the PH
Q_PH=C_cold_PH*(tph2-tph1);         % [kW]      Heat Transfer in the PH

    %Heat Transfer in Reheater
t2_RH = T(4);     % [C] Outlet Temperature of Steam from Reheater(State (4))
t1_RH = T(3); % [C] Inlet Temperature of Steam into the Preheater(State (3))
mwater_RH =(1- a -b)*mwater;  % [kg/s]    Flow Rate of Steam in the Reheater
Cp_water_RH  =  (h(4)  -h(3))/(t2_RH  -  t1_RH);     %  [kJ/kg.K]  Specific  heat
Capacity of the HTF in the RH

C_cold_RH = Cp_water_RH*(mwater_RH); % [kW/K] Steam Capacitance in the RH
Q_RH=C_cold_RH*(t2_RH-t1_RH);       % [kW]     Heat Transfer in the PH

     % Total heat received by the steam from the HTF
Q_total = Q_SH + Q_PH + Q_SG + Q_RH;      % [kW]      Total  Heat  Transfer  in
the Plant

[mHTF_T,Aeff,TN_coll] = fsolarfield(Q_total,T1_SH, T2_PH);  % [kg/s]     Total
HTF Mass Flow Rate
```

```
Qmain = Q_SH+Q_PH+Q_SG; % [Kw] Total Heat Transfer in the SH, SG, and PH
T_avg_HTF = (T1_SH + T2_PH)/2;
Cp_HTF =    (0.0007755*T_avg_HTF^2 + 2.484*T_avg_HTF + 1511)/1000;      %
[kJ/kg.K] Specfic heat Capacity of the HTF

mHTF = Qmain/(Cp_HTF*(T1_SH - T2_PH)); % [kg/s]    HTF Mass Flow Rate in the
SH, SG, and PH

mHTF_RH = Q_RH/(Cp_HTF*(T1_SH - T2_PH));  % [kg/s]    HTF Mass Flow Rate in
the PH

   % superheater UA Calculation
   % Heat Capacitance Calculation
Cp_HTF_SH=2.588;  % [kJ/kg.K] Specific heat Capacity of the HTF in the SG
 err1 = 10;
    while(err1>eps)
        C_hot_SH = Cp_HTF_SH*mHTF;
        T2_SH= T1_SH - Q_SH/C_hot_SH;
        T_avg_SH = (T1_SH+T2_SH)/2;
        Cp_HTFn_SH =   (0.0007755*T_avg_SH^2 + 2.484*T_avg_SH + 1511)/1000;
        err1 = abs(Cp_HTFn_SH -Cp_HTF_SH);
        Cp_HTF_SH = Cp_HTFn_SH;
    End
T2_SH= T1_SH - Q_SH/C_hot_SH;       % [C] HTF Outlet Temperature from the SH
C_min_SH = min(C_cold,C_hot_SH);    % [kW/K]   Minimum Capacitance in the SH
C_max_SH = max(C_cold,C_hot_SH);    % [kW/K]   Maximum Capacitance in the SH
Cr_SH = C_min_SH/C_max_SH;          %           Ratio  of  Minimum  to  Maximum
Capacitance in the SH

Qmax_SH = C_min_SH*(T1_SH -t1_SH);  % [kW]      Maximum Possible Heat Transfer
in the SH
```

```
epsilon_SH =Q_SH/Qmax_SH ;          %           Effectiveness   of   the   Heat
Transfer in the SH

%     NTU_SH= (-1/(1-Cr_SH)*log((1-epsilon_SH)/(1-Cr_SH*epsilon)));         %
Number of Transfer Units in the SH



E_SH = (2/(epsilon_SH) - (1+Cr_SH))/sqrt(1+Cr_SH^2);
NTU_SH = -log((E_SH -1)/(E_SH +1))/sqrt(1+Cr_SH^2);
UA_SH = NTU_SH*C_min_SH;                                %  [kW/K]  Overall  Heat
Transfer Coefficient in the SH

    % Steam Generator UA Calculation
    % Heat Capacitance Calculation
Cp_HTF_SG = 2.588;                                  %   [kJ/kg.K]   Specific   heat
Capacity of the HTF in the SG

T1_SG =T2_SH;                                       % [C]       Inlet  Temperature
of the HTF into the SG
    err2 = 10;
    while(err2>0)
        C_hot_SG = Cp_HTF_SG*(mHTF);
        T2_SG = T1_SG - Q_SG/C_hot_SG;
        T_avg_SG = (T1_SG+T2_SG)/2;
        Cp_HTFn_SG =    (0.0007755*T_avg_SG^2 + 2.484*T_avg_SG + 1511)/1000;
        err2 = abs(Cp_HTFn_SG-Cp_HTF_SG);
        Cp_HTF_SG = Cp_HTFn_SG;
    end

T2_SG= T1_SG -Q_SG/C_hot_SG ;       % [C] HTF Outlet Temperature from the SG
C_min_SG = C_hot_SG;                % [kW/K]   Minimum Capacitance in the SG
Qmax_SG = C_min_SG*(T1_SG -t1_SG); % [kW]      Maximum Possible Heat Transfer
in the SG
```

```
epsilon_SG =Q_SG/Qmax_SG ;          %     Effectiveness of the Heat Transfer
in the SG

NTU_SG = -log(1 - epsilon_SG) ;     %     Number of Transfer Units in the SG
UA_SG = NTU_SG*C_min_SG ;           %     kW/K]    Overall    Heat    Transfer
Coefficient in the SG

    % Preheater UA Calculation
T1_PH = T2_SG;                      % [C] Inlet Temperature of the HTF in to
the PH

C_hot_PH = Q_PH/(T1_PH - T2_PH);    % [kW/K]    HTF Capacitance in the SH
Cp_HTF_PH = C_hot_PH /mHTF;         % [kJ/kg.K] Specific heat Capacity of the
HTF in the PH

C_min_PH = min(C_cold_PH,C_hot_PH); % [kW/K]    Minimum Capacitance in the PH
C_max_PH = max(C_cold_PH,C_hot_PH); % [kW/K]    Maximum Capacitance in the PH
Cr_PH = C_min_PH/C_max_PH;          %           Ratio  of  Minimum  to  Maximum
Capacitance in the PH

Qmax_PH = C_min_PH*(T1_PH -tph1);   % [kW]      Maximum     Possible     Heat
Transfer in the PH
    epsilon_PH =Q_PH/Qmax_PH;       %           Effectiveness   of   the   Heat
Transfer in the PH

E_PH = (2/(epsilon_PH) - (1+Cr_PH))/sqrt(1+Cr_PH^2);
NTU_PH = -log((E_PH-1)/(E_PH+1))/sqrt(1+Cr_PH^2);
UA_PH = NTU_PH*C_min_PH; %[kW/K] Overall Heat Transfer Coefficient in the PH
T1_RH = T1_SH;          % [C]       Inlet Temperature of the HTF in to the RH
T2_RH = T2_PH;          % [C]       Outlet Temperature of the HTF from the RH

C_hot_RH = mHTF_RH*Cp_HTF;          % [kW/K]    HTF Capacitance in the RH
```

```
C_min_RH = min(C_cold_RH,C_hot_RH); % [kW/K]    Minimum Capacitance in the RH
C_max_RH = max(C_cold_RH,C_hot_RH); % [kW/K]    Maximum Capacitance in the RH
Cr_RH = C_min_RH/C_max_RH;          %           Ratio of Minimum to Maximum
Capacitance in the RH

Qmax_RH = C_min_RH*(T1_RH -t1_RH); % [kW]      Maximum Possible Heat Transfer
in the RH

epsilon_RH =Q_RH/Qmax_RH;           %           Effectiveness of the Heat
Transfer in the RH

NTU_RH=    (-1/(1-Cr_RH)*log((1-epsilon_RH)/(1-Cr_RH*epsilon_RH)));          %
Number of Transfer Units in the RH

UA_RH= NTU_RH*C_min_RH; % [kW/K] Overall Heat Transfer Coefficient in the RH
T2SG= XSteam('Tsat_p',P(1)) + 15;
err = abs(T2_SG -T2SG);
end

%************************************************************************
%                     SUMMARY of the Results
%************************************************************************

% State Points
i = 1:22;
fprintf('\n')
fprintf('       STATE POINTS    \n')
fprintf('\n')
fprintf('     ST NO.     T [C]    P [bar]     h [kJ/kg]     s [KJ/kg.K] \n')
sp = ( [i' T(i)' P(i)' h(i)' s(i)']);
disp(sp)

fprintf('\n')
```

```
fprintf('\n')


% Mass flow Rates
fprintf('       MASS FLOW RATES\n')
fprintf('\n')
fprintf('Mass of Steam = %f [kg/s] \n',mwater)
fprintf('\n')
fprintf('Mass of HTF Total = %f [kg/s] \n',mHTF_T)
fprintf('\n')
fprintf('Mass of HTF in the  H.E. = %f [kg/s] \n',mHTF)
fprintf('\n')
fprintf('Mass of HTF in the RH = %f [kg/s] \n',mHTF_RH)
fprintf('\n')
fprintf('\n')

% STEAM MASS EXTRACTED
fprintf('       STEAM MASS EXTRACTED\n')
fprintf('\n')
fprintf('At HP2 = %f [kg/s] \n',a*mwater)
fprintf('\n')
fprintf('At HP1 = %f [kg/s] \n',b*mwater)
fprintf('\n')
fprintf('At the Deareator = %f [kg/s] \n',c*mwater)
fprintf('\n')
fprintf('At LP = %f [kg/s] \n',d*mwater)
fprintf('\n')
fprintf('\n')

% OVERALL HEAT TRANSFER COEFFICIENTS
fprintf('       OVERALL HEAT TRANSFER COEFFICIENTS\n')
fprintf('\n')
```

```
fprintf('UA_SH = %f [kW/K] \n',UA_SH)
fprintf('\n')
fprintf('UA_SG = %f [kW/K] \n',UA_SG)
fprintf('\n')
fprintf('UA_PH = %f [kW/K] \n',UA_PH)
fprintf('\n')
fprintf('UA_RH = %f [kW/K] \n',UA_RH)
fprintf('\n')
fprintf('UA_HP2 = %f [kW/K] \n',UA_HP2)
fprintf('\n')
fprintf('UA_HP1 = %f [kW/K] \n',UA_HP1)
fprintf('\n')
fprintf('UA_LP = %f [kW/K] \n',UA_LP1)
fprintf('\n')
fprintf('\n')

% AVERAGE SPECFIC HEAT OF WATER
fprintf('       AVERAGE SPECFIC HEAT OF WATER\n')
fprintf('\n')
fprintf('Cp_HP2 = %f [kJ/kg.K] \n',C_water_HP2)
fprintf('\n')
fprintf('Cp_HP1 = %f [kJ/kg.K] \n',Cp_AVG_HP1)
fprintf('\n')
fprintf('Cp_LP = %f [kJ/kg.K] \n',Cp_AVG_LP)
fprintf('\n')
fprintf('\n')

fprintf('SOLAR FIELD AREA = %f [m^2] \n',Aeff)
fprintf('\n')
fprintf('TOTAL NUMBER OF COLLECTORS = %f  \n',TN_coll)
fprintf('\n')
fprintf('\n')
```

```
fprintf('THERMAL EFFICIENCY = %f  \n', Eta_th)
fprintf('\n')

% PLOT OF TEMPERATURE VS. HEAT TRANSFER IN THE HEAT EXCHANGERS
SP = [T(1) T(16) T(15) T(14)];
HTFP = [T1_SH T2_SH T2_SG T2_PH];
HT = [0 Q_SH Q_SG+Q_SH Q_SH+Q_PH+Q_SG];
plot(HT,HTFP,'-rs',HT,SP,'-
bs','LineWidth',1.5,'MarkerEdgeColor','k','MarkerFaceColor','g','MarkerSize',
7)
legend('HTF','STEAM',1);
hold on
xlabel('\bfHEAT TRANSFER [kW]')
ylabel('\bfTEMPERATURE [ ^oC]')
grid on
axis([0,Q_SH+Q_PH+Q_SG,240,400])
%**************************************************************************

function [mHTF_T,Aeff,TN_coll] = fsolarfield(Q_total,T_out, T_in)
%**************************************************************************
% This Function is used to Calculate the Solar Field According to STEC
% Model for Parabolic Trough.
% **************************************************************************

% The HTF is Thermionol-VP1

% A, B, C, Cw and D are empirical factors describing the performance of the %
collector. They can ve found for the SEGS LS -2 collector in Dudely.
% For Black Chrome coating with vacuum, the coefficients are given below.

Aref= 73.6;            %          Thermal Efficiency of a LS-2 SCA
CR =0.94;              %          Clean Reflectivity
Cl =0.94;              %          Cleanliness Solar Field
```

```
A = Aref*(CR/0.94)*Cl*(1+Cl)/2;
B=-0.004206;
C = 7.44;
Cw = 0;
D = -0.0958;

f = 1.8;              % [m]      Focal Length of the SCA
Lsca = 47;            % [m^2]    Length of one SCA
theta = 0;

% Shading of Parallel Rows
% This factor can be taken to be equal to 1 because at solar non, no SCA shades other SCA.
% sh = min (max(0,(12.5/5)*cos(zenith(h))/cos(teta(h))),1.0);
sh =1;  %
Ws = 3;                % [m/s]    Wind Speed
T_amb = 16.5;           % [oC]    Ambient Temperature
DNI = 0.806;            % [W/m^2] Direct normal Insolation
A_sca = 235;            % [W/m^2] Aperture area of one SCA

% Incident Angle Modifier
K= cos(theta) - 0.0003512*theta -0.00003137*(theta)^2;

% End Losses
M = 1 - (f*tan(theta)/Lsca);

DeltaT_in = T_in -T_amb;      % [oC]      Diff. between collector inlet temp. and ambient temp.

DeltaT_out = T_out-T_amb;       %[oC]         Diff. between collector outlet temp. and ambient temp.

%Efficiency
```

```
eta_SF = K*M*sh*(A + B*((DeltaT_in+DeltaT_out)/2)) + (C+ Cw*Ws)* ...
    (((DeltaT_in+DeltaT_out)/(2000*DNI)))+D*(DeltaT_in*DeltaT_out + ...
    ((DeltaT_out-DeltaT_in)^2)/3)/(1000*DNI);

Qnet = Q_total;
%Average Temperature of the Solar Field Inlet and Outlet Temperatures
Tavg_sf = (T_out + T_in)/2;

xx=(0.02*Tavg_sf/343);
yy = (2.57*10^3)*Tavg_sf/275;
zz=DNI*eta_SF/100;

% Effective Area of the Solar Field
Aeff= (Qnet +yy)/(zz-xx);

% Piping Heat Loss
Qpipe =(xx *Aeff + yy);

% Total Number of Collector in the Solar Field
TN_coll = Aeff/A_sca;

% Absorbed Energy
Qabs = Aeff*zz;

% Specific Heat of HTF at Average Temperature
Cp_HTF =   (0.0007755*Tavg_sf^2 + 2.484*Tavg_sf+ 1511)/1000;

% Reference Maximum Flow Rate of the HTF to Achieve Tout
mHTF_T= (Qnet/(Cp_HTF*(T_out -T_in))) ;
```

Appendix B

Simulation Result for Representative Days of Year 2001

B.1 January 17

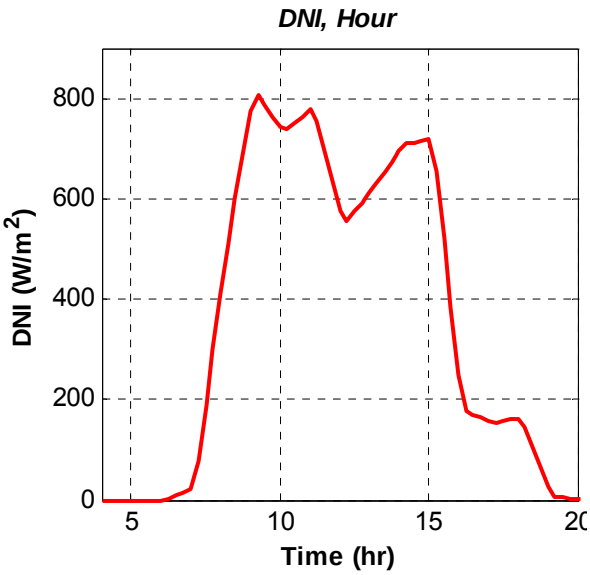

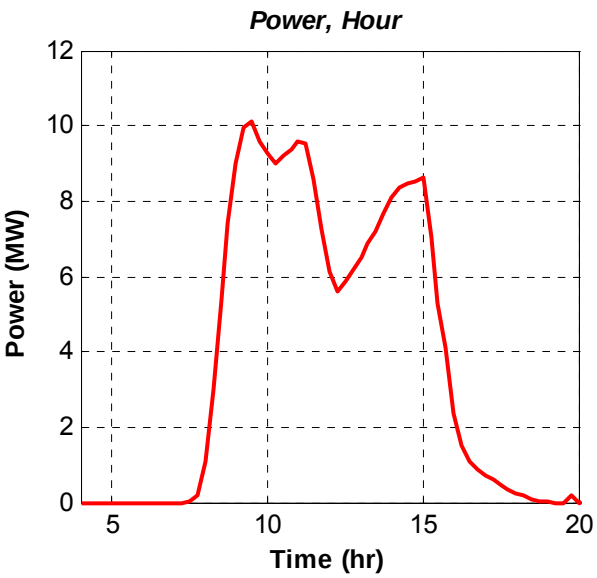

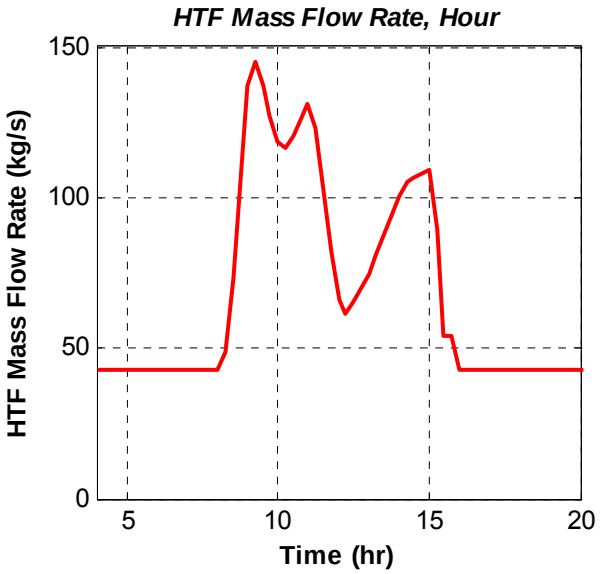

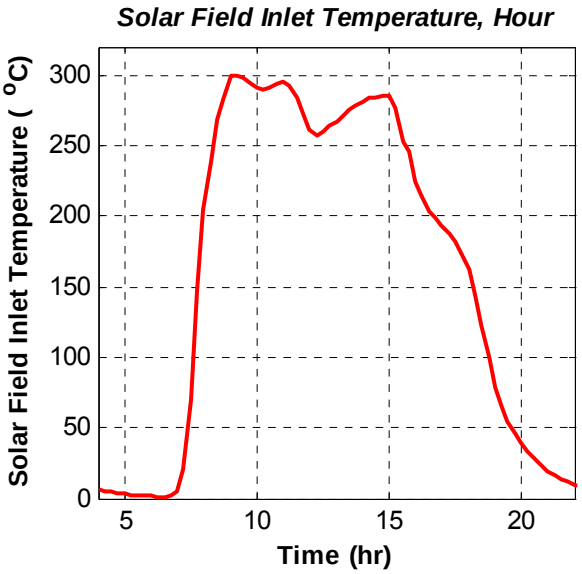

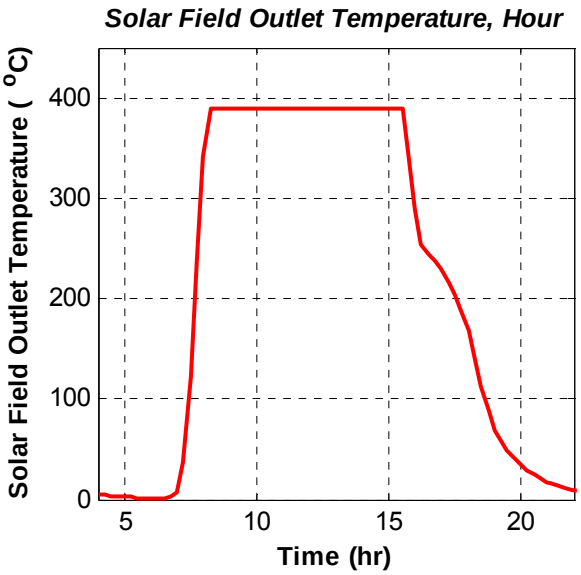
Solar Field Outlet Temperature, Hour
Solar Field Outlet Temperature (°C)
400
300
200
100
0
5
10
15
20
Time (hr)

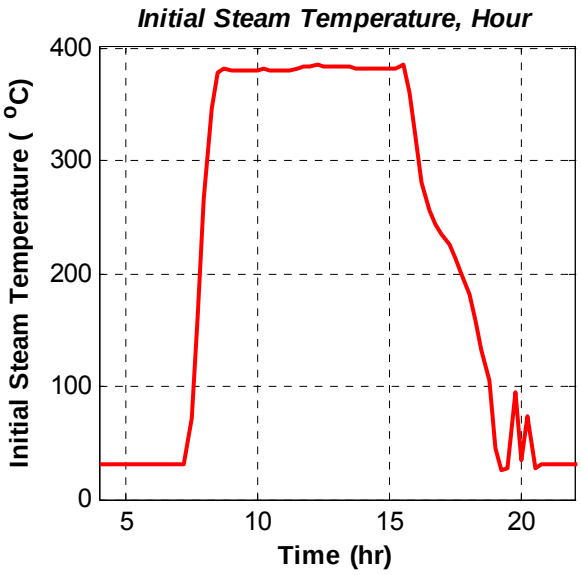
Initial Steam Temperature, Hour
Initial Steam Temperature (°C)
400
300
200
100
0
5
10
15
20
Time (hr)

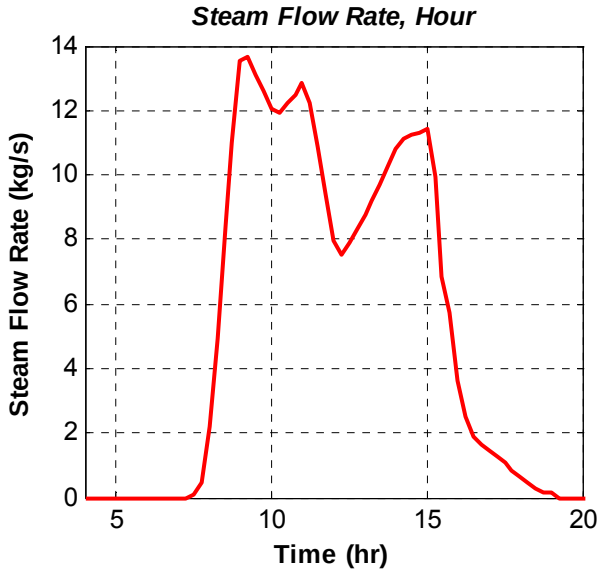
Steam Flow Rate, Hour
Steam Flow Rate (kg/s)
14
12
10
8
6
4
2
0
5
10
15
20
Time (hr)

B.2 February 16

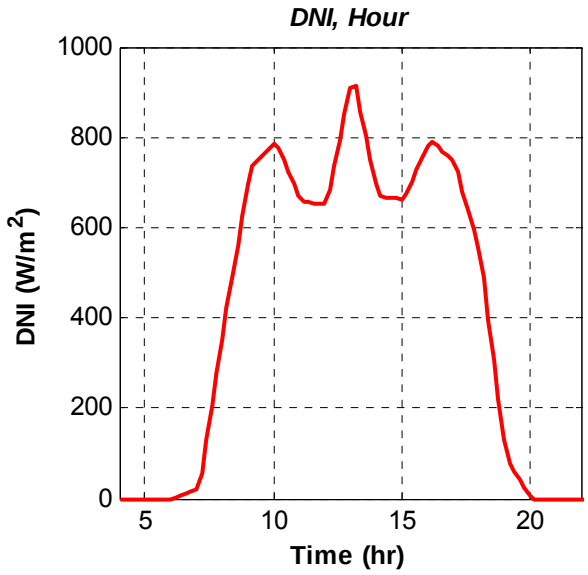

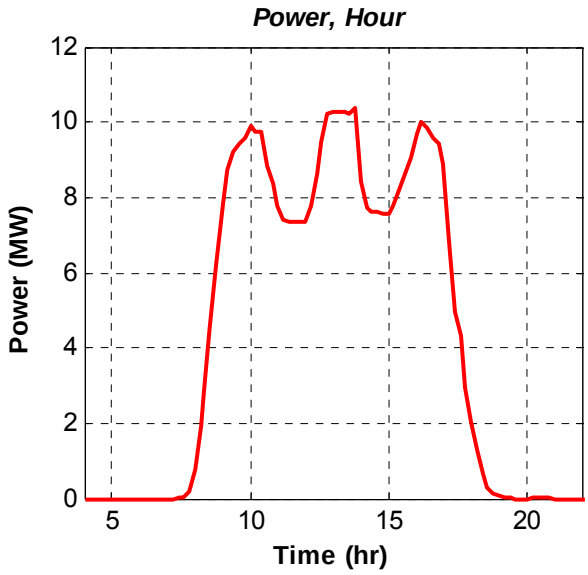

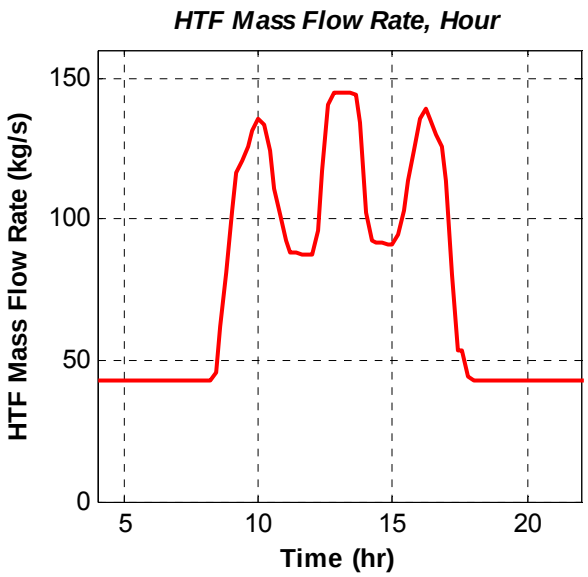

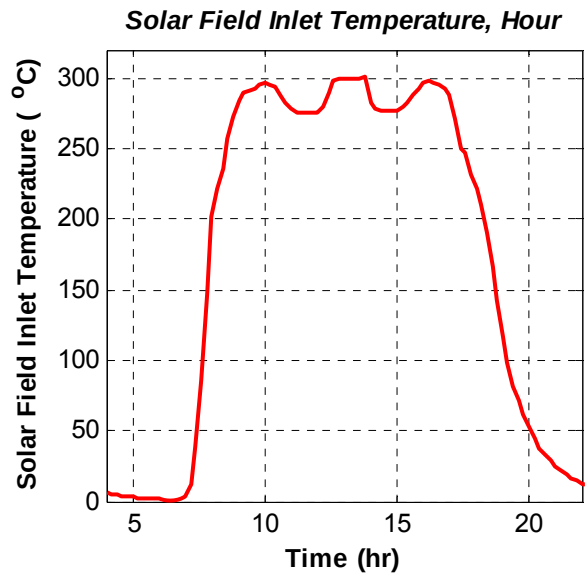

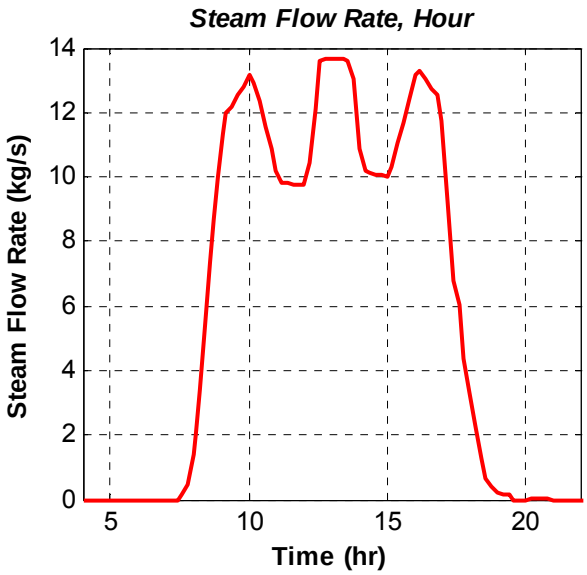
Steam Flow Rate, Hour
Steam Flow Rate (kg/s)
Time (hr)
0
2
4
6
8
10
12
14
5
10
15
20

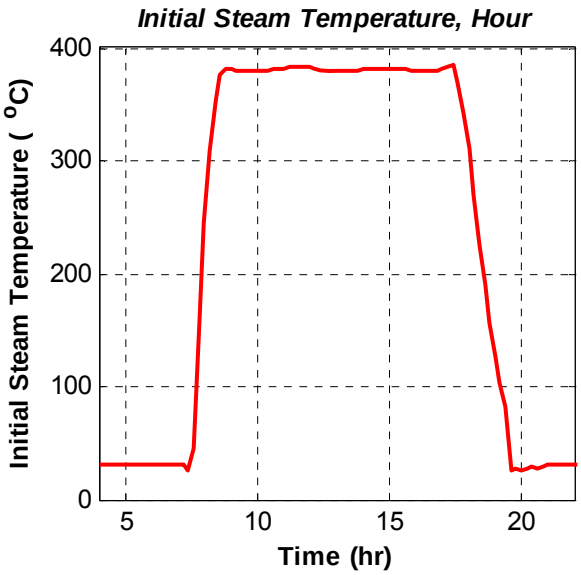
Initial Steam Temperature, Hour
Initial Steam Temperature (°C)
Time (hr)
0
100
200
300
400
5
10
15
20

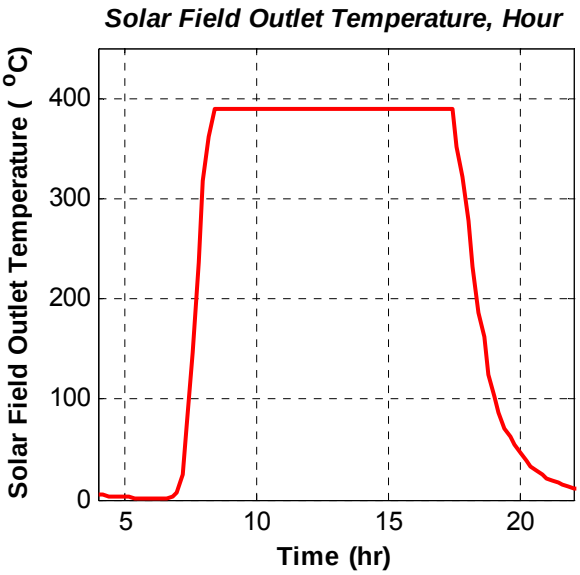
Solar Field Outlet Temperature, Hour
Solar Field Outlet Temperature (°C)
Time (hr)
0
100
200
300
400
5
10
15
20

B.3 April 15

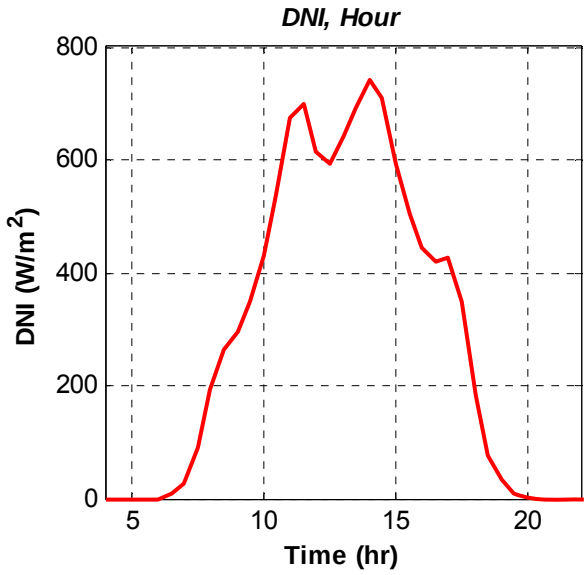
DNI, Hour
DNI (W/m2)
800
600
400
200
0
5
10
15
20
Time (hr)

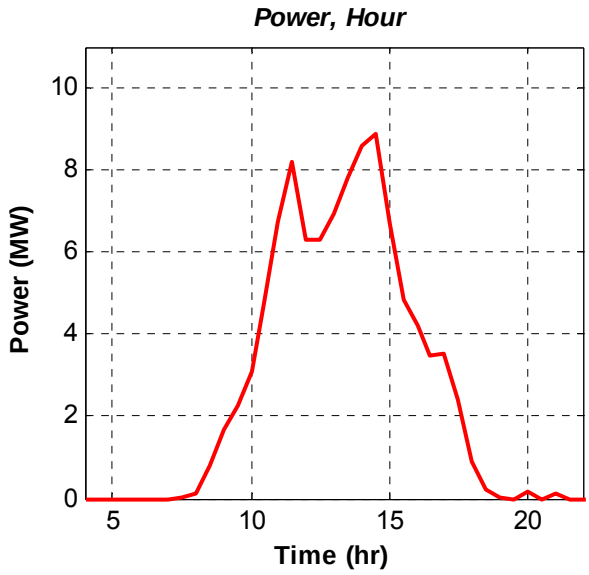
Power, Hour
Power (MW)
10
8
6
4
2
0
5
10
15
20
Time (hr)

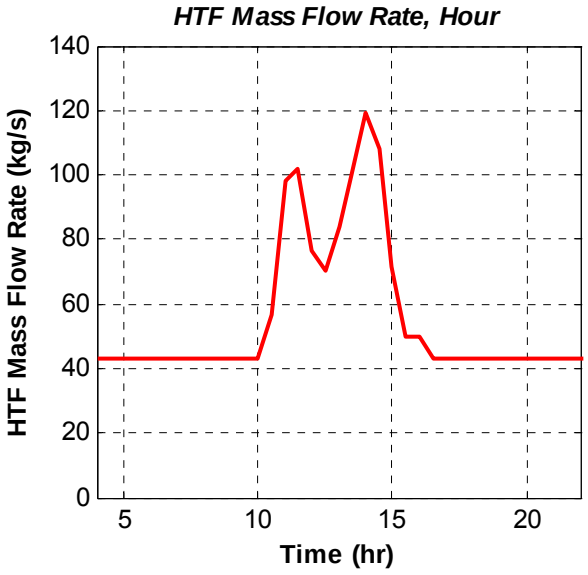
HTF Mass Flow Rate, Hour
HTF Mass Flow Rate (kg/s)
140
120
100
80
60
40
20
0
5
10
15
20
Time (hr)

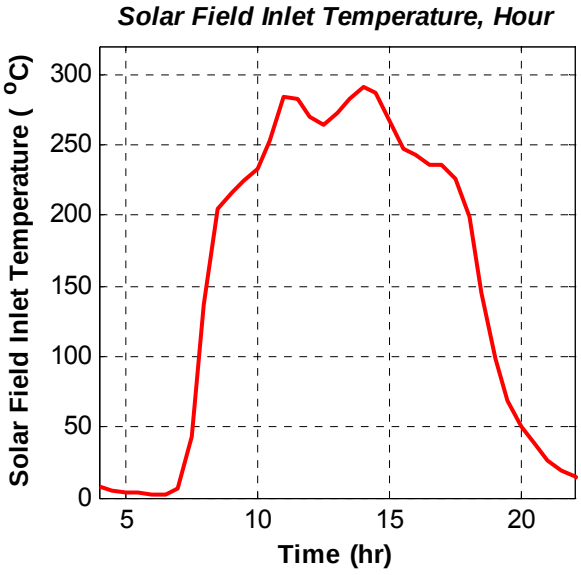
Solar Field Inlet Temperature, Hour
Solar Field Inlet Temperature (oC)
300
250
200
150
100
50
0
5
10
15
20
Time (hr)

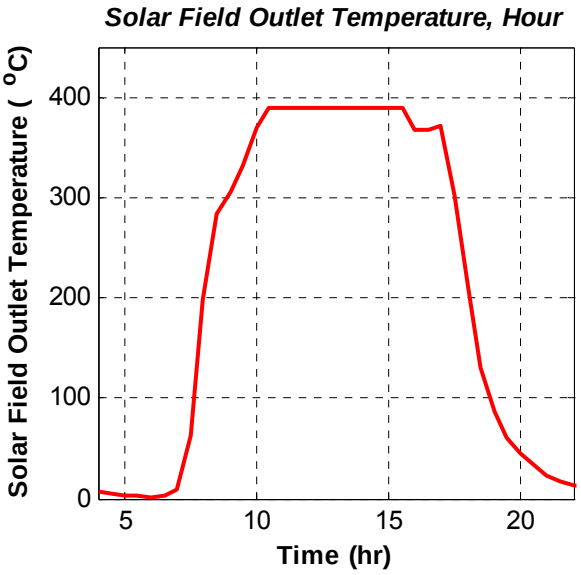
Solar Field Outlet Temperature, Hour
Solar Field Outlet Temperature (°C)
0
100
200
300
400
5
10
15
20
Time (hr)

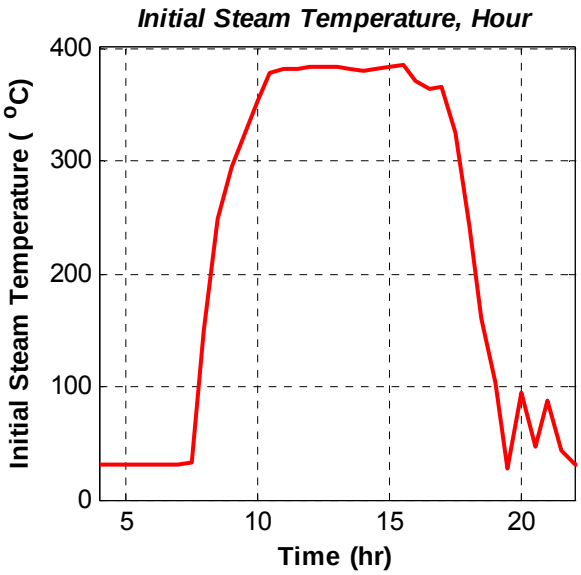
Initial Steam Temperature, Hour
Initial Steam Temperature (°C)
0
100
200
300
400
5
10
15
20
Time (hr)

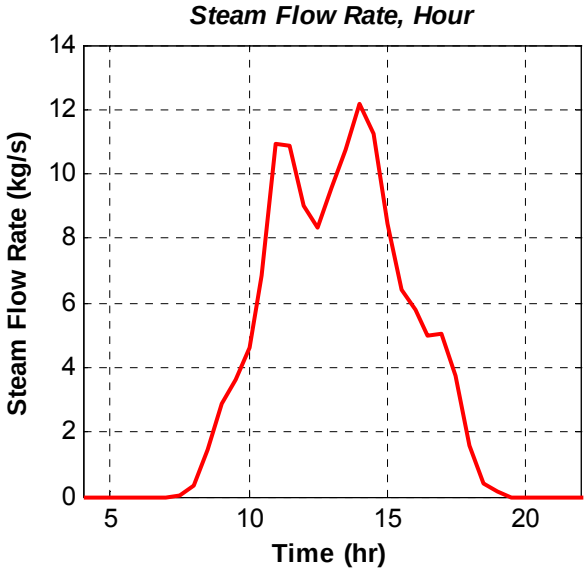
Steam Flow Rate, Hour
Steam Flow Rate (kg/s)
0
2
4
6
8
10
12
14
5
10
15
20
Time (hr)

B.4 June 11

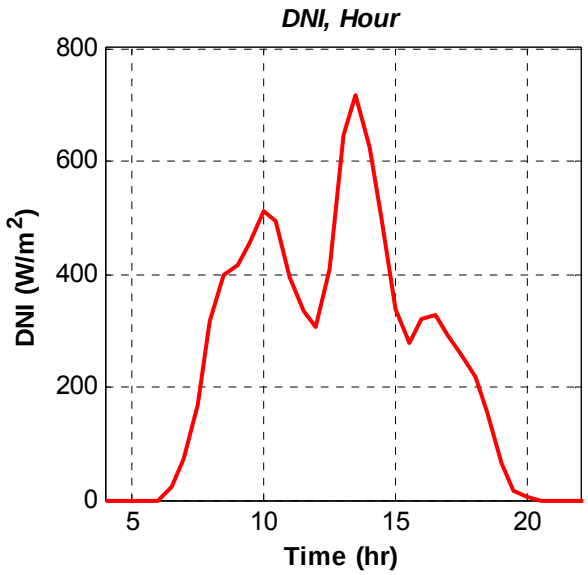
DNI, Hour
DNI (W/m2)
Time (hr)
800
600
400
200
0
5
10
15
20

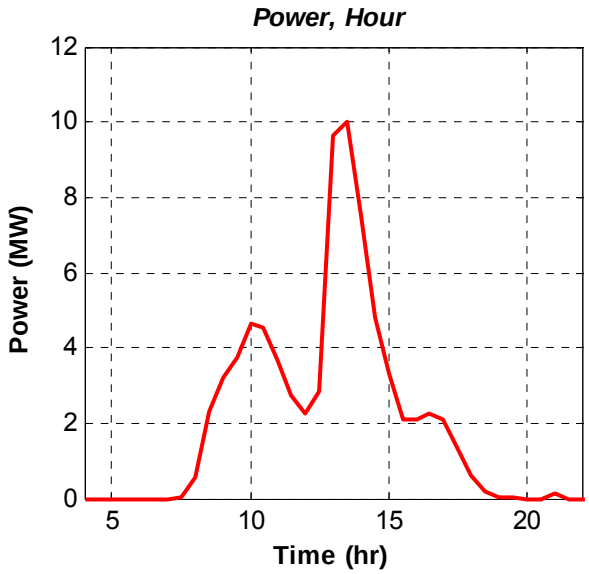
Power, Hour
Power (MW)
Time (hr)
12
10
8
6
4
2
0
5
10
15
20

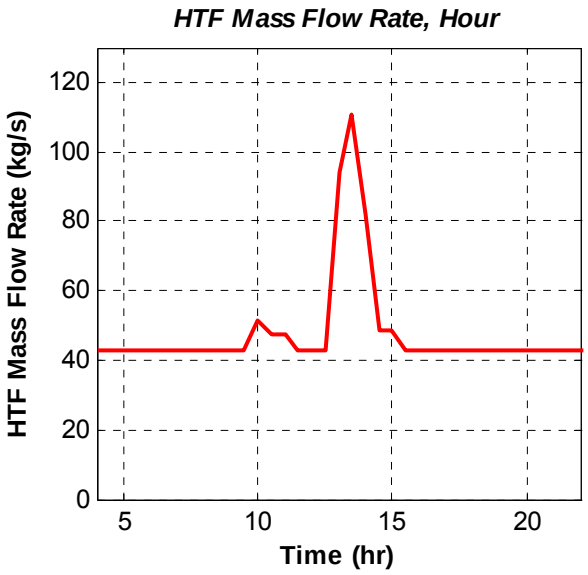
HTF Mass Flow Rate, Hour
HTF Mass Flow Rate (kg/s)
Time (hr)
120
100
80
60
40
20
0
5
10
15
20

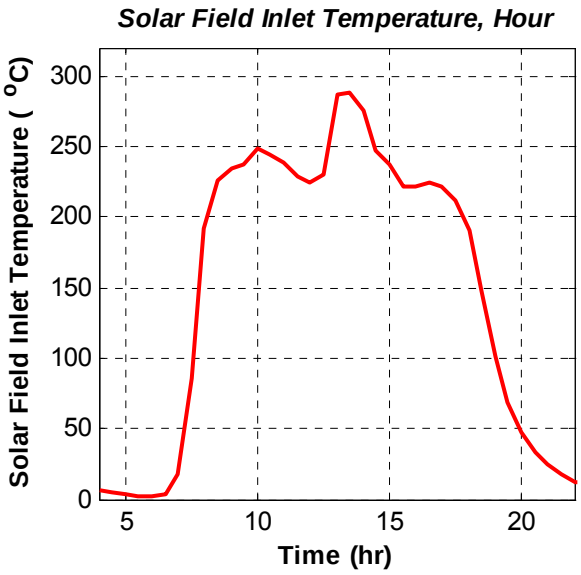
Solar Field Inlet Temperature, Hour
Solar Field Inlet Temperature (oC)
Time (hr)
300
250
200
150
100
50
0
5
10
15
20

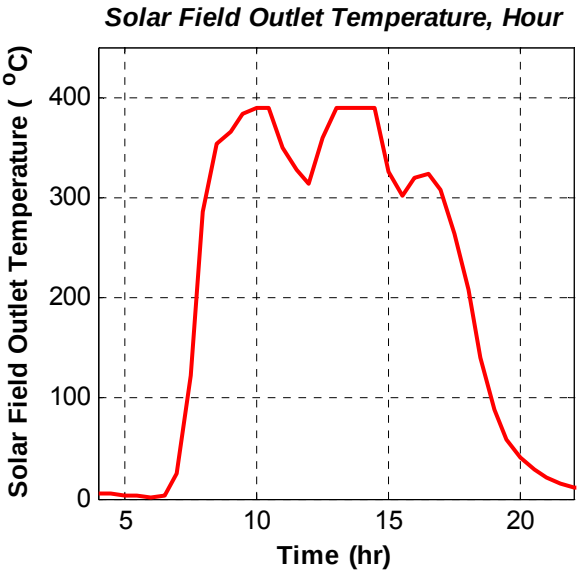
Solar Field Outlet Temperature, Hour
Solar Field Outlet Temperature (°C)
400
300
200
100
0
5
10
15
20
Time (hr)

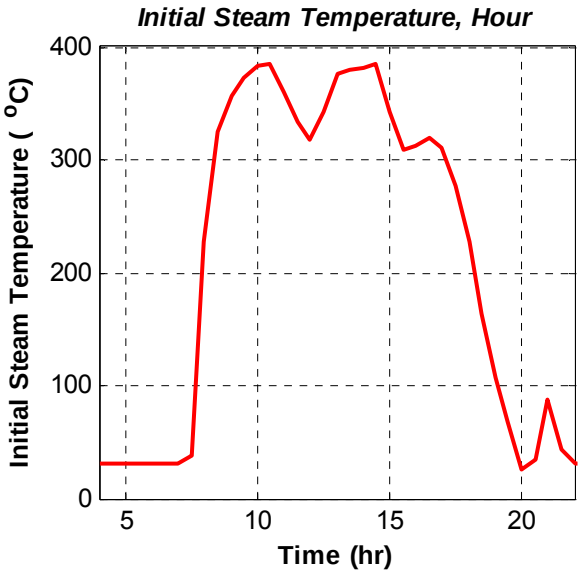
Initial Steam Temperature, Hour
Initial Steam Temperature (°C)
400
300
200
100
0
5
10
15
20
Time (hr)

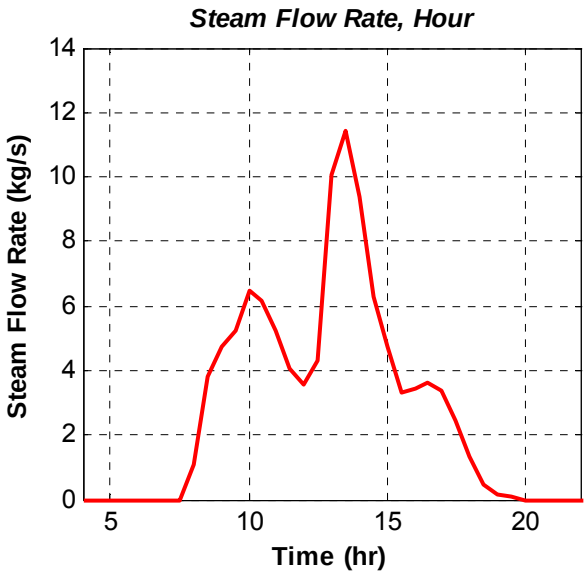
Steam Flow Rate, Hour
Steam Flow Rate (kg/s)
14
12
10
8
6
4
2
0
5
10
15
20
Time (hr)

B.5 July 17

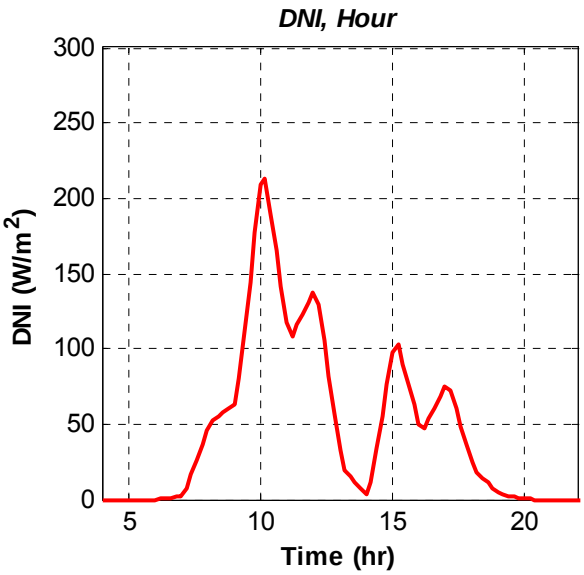
DNI, Hour
DNI (W/m2)
Time (hr)
300
250
200
150
100
50
0
5
10
15
20

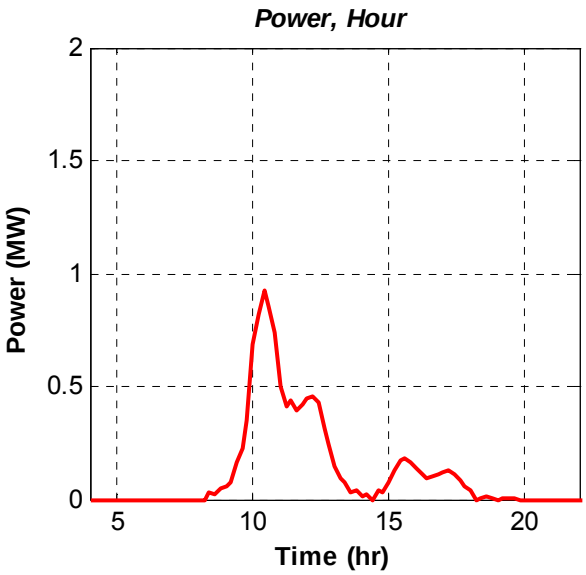
Power, Hour
Power (MW)
Time (hr)
2
1.5
1
0.5
0
5
10
15
20

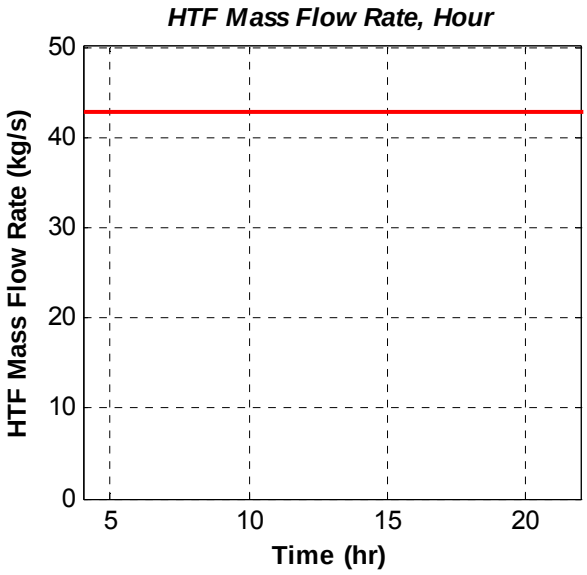
HTF Mass Flow Rate, Hour
HTF Mass Flow Rate (kg/s)
Time (hr)
50
40
30
20
10
0
5
10
15
20

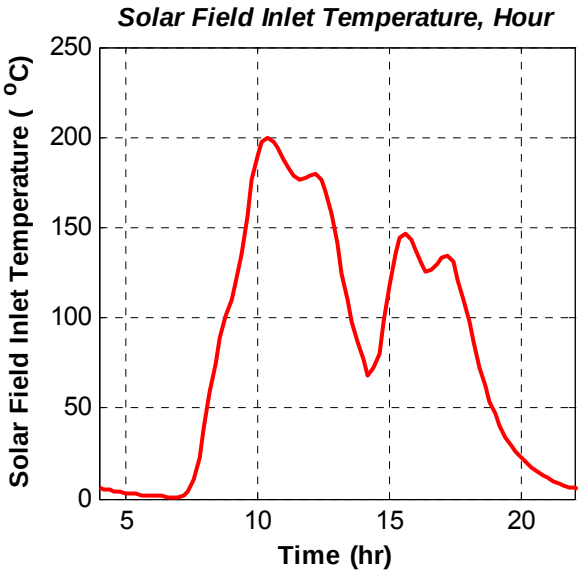
Solar Field Inlet Temperature, Hour
Solar Field Inlet Temperature (oC)
Time (hr)
250
200
150
100
50
0
5
10
15
20

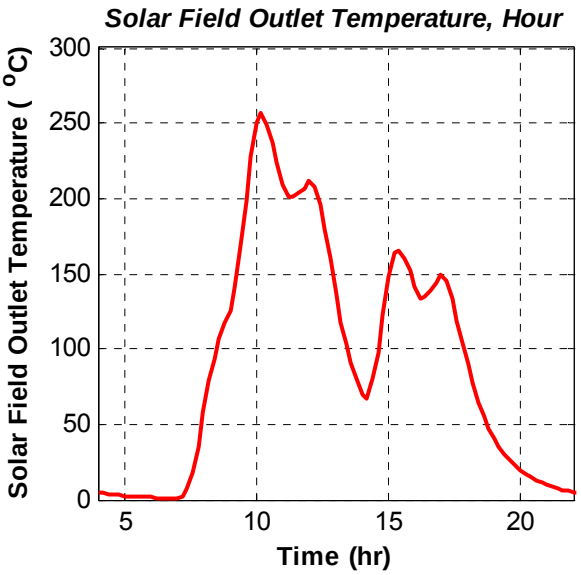
Solar Field Outlet Temperature, Hour
Solar Field Outlet Temperature (°C)
300
250
200
150
100
50
0
5
10
15
20
Time (hr)

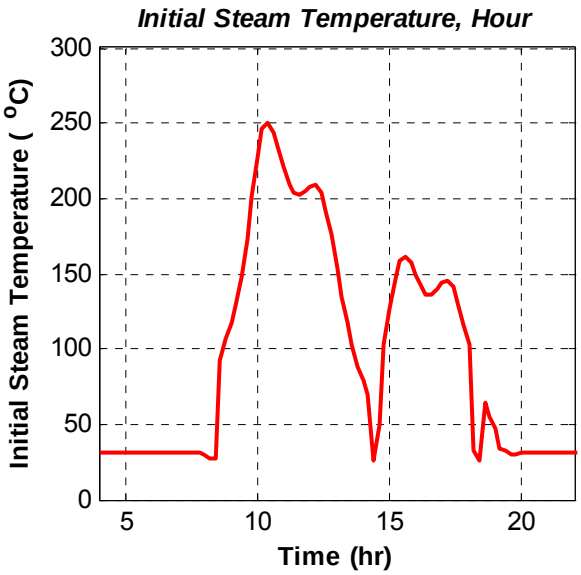
Initial Steam Temperature, Hour
Initial Steam Temperature (°C)
300
250
200
150
100
50
0
5
10
15
20
Time (hr)

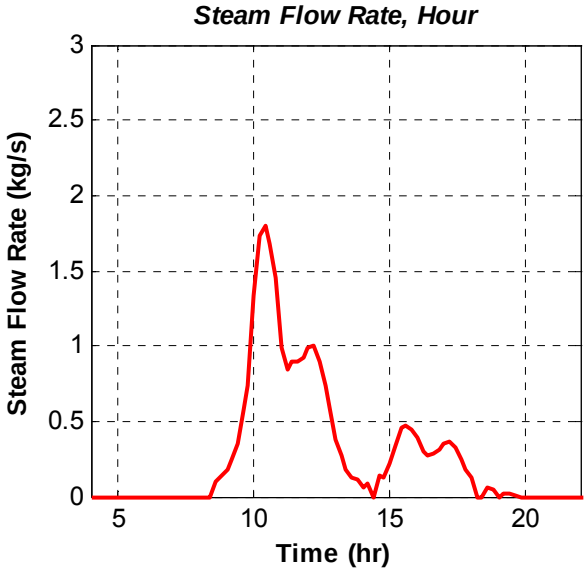
Steam Flow Rate, Hour
Steam Flow Rate (kg/s)
3
2.5
2
1.5
1
0.5
0
5
10
15
20
Time (hr)

B.6 August 16

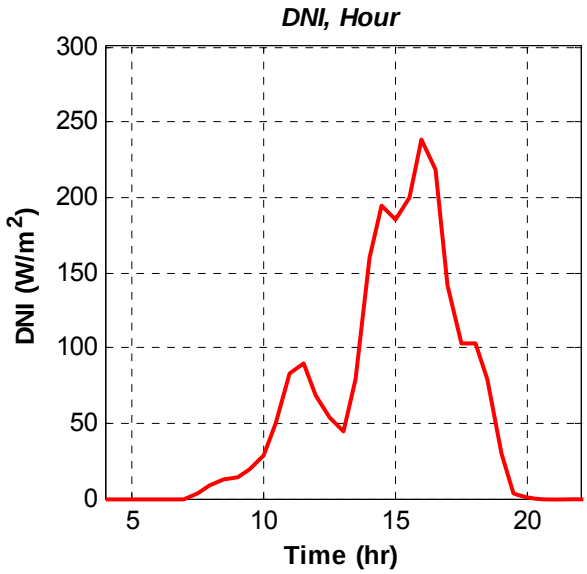
DNI, Hour
DNI (W/m2)
Time (hr)
300
250
200
150
100
50
0
5
10
15
20

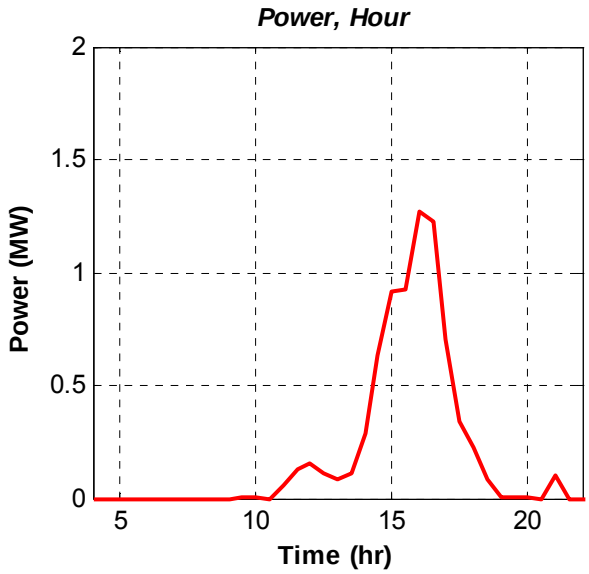
Power, Hour
Power (MW)
Time (hr)
2
1.5
1
0.5
0
5
10
15
20

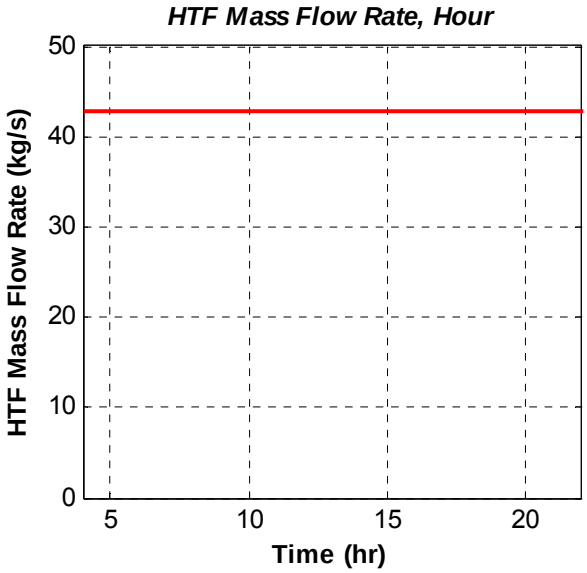
HTF Mass Flow Rate, Hour
HTF Mass Flow Rate (kg/s)
Time (hr)
50
40
30
20
10
0
5
10
15
20

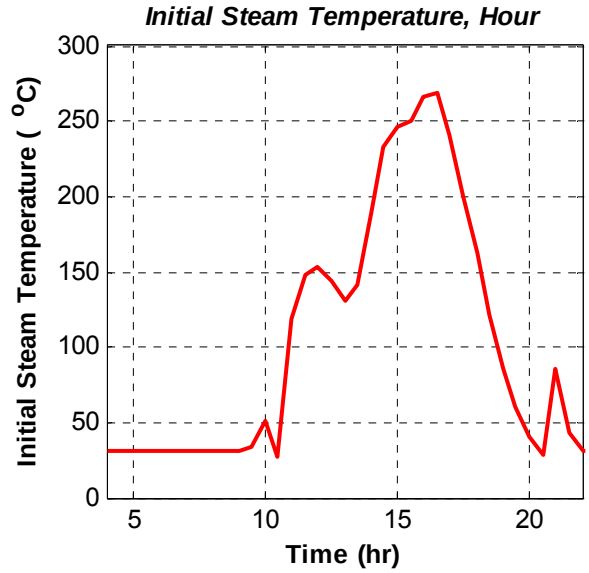
Initial Steam Temperature, Hour
Initial Steam Temperature (oC)
Time (hr)
300
250
200
150
100
50
0
5
10
15
20

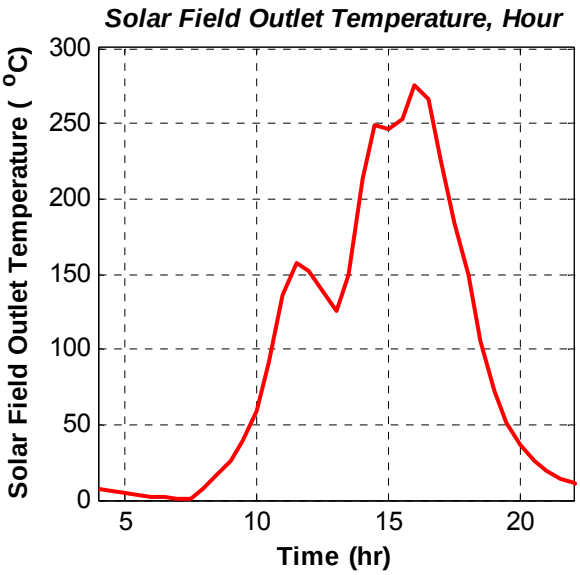
Solar Field Outlet Temperature, Hour
Solar Field Outlet Temperature (°C)
300
250
200
150
100
50
0
5
10
15
20
Time (hr)

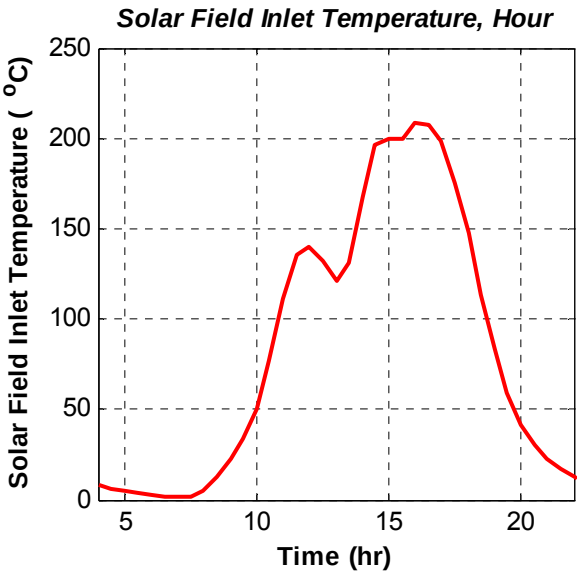
Solar Field Inlet Temperature, Hour
Solar Field Inlet Temperature (°C)
250
200
150
100
50
0
5
10
15
20
Time (hr)

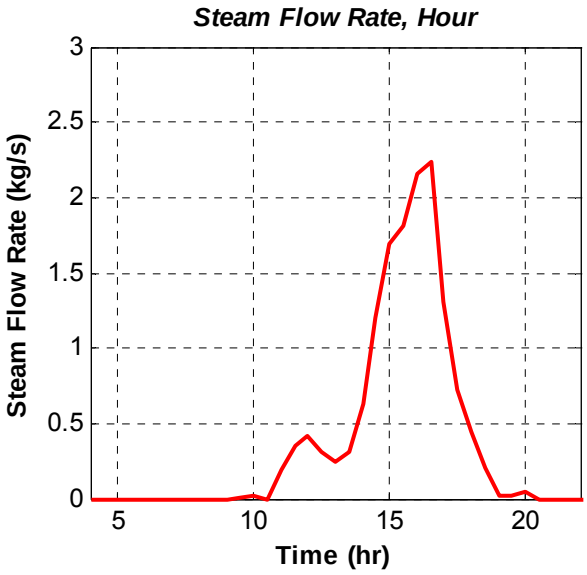
Steam Flow Rate, Hour
Steam Flow Rate (kg/s)
3
2.5
2
1.5
1
0.5
0
5
10
15
20
Time (hr)

B.7 September 15

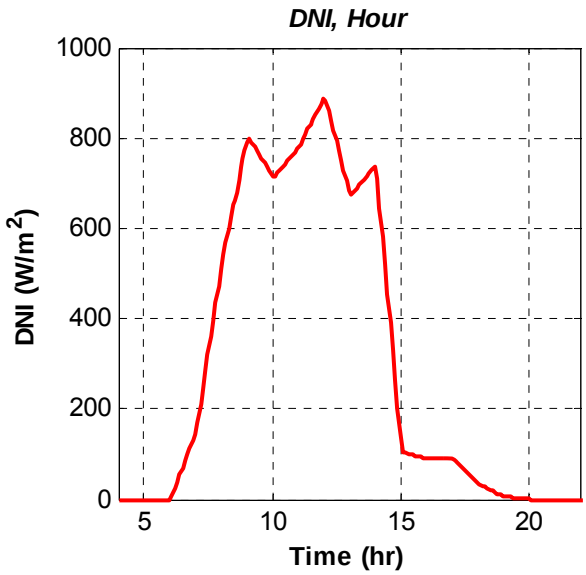

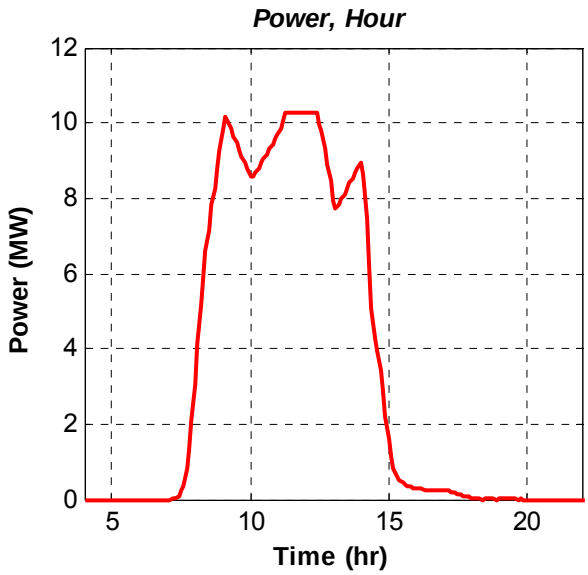

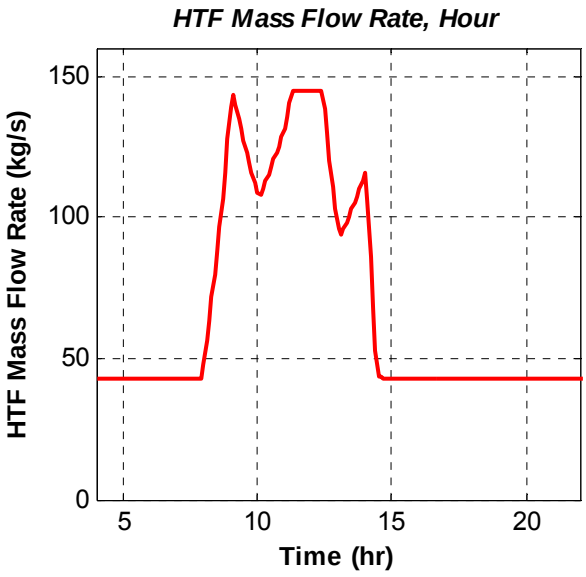

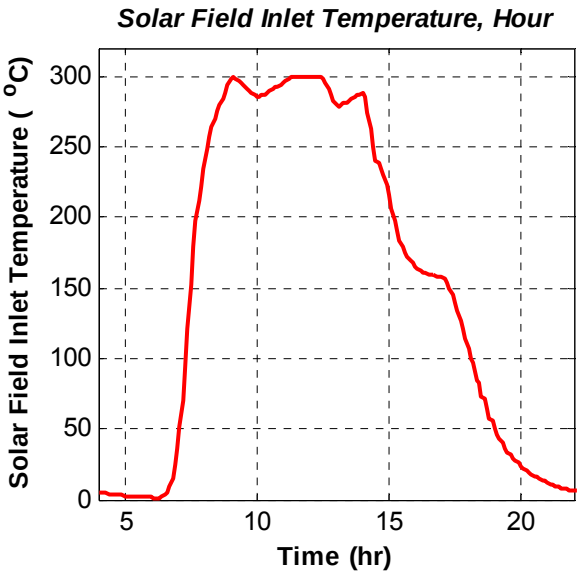

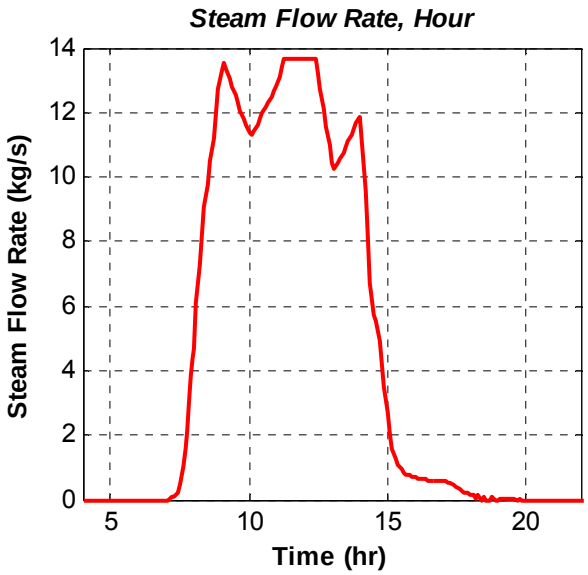
Steam Flow Rate, Hour
Steam Flow Rate (kg/s)
Time (hr)
0
2
4
6
8
10
12
14
5
10
15
20

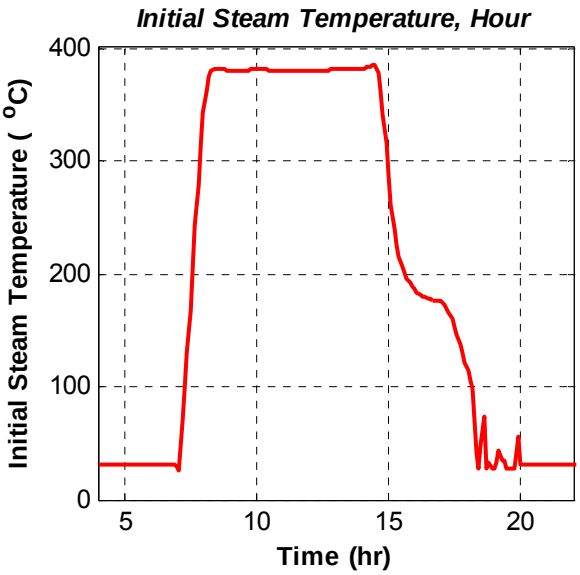
Initial Steam Temperature, Hour
Initial Steam Temperature (°C)
Time (hr)
0
100
200
300
400
5
10
15
20

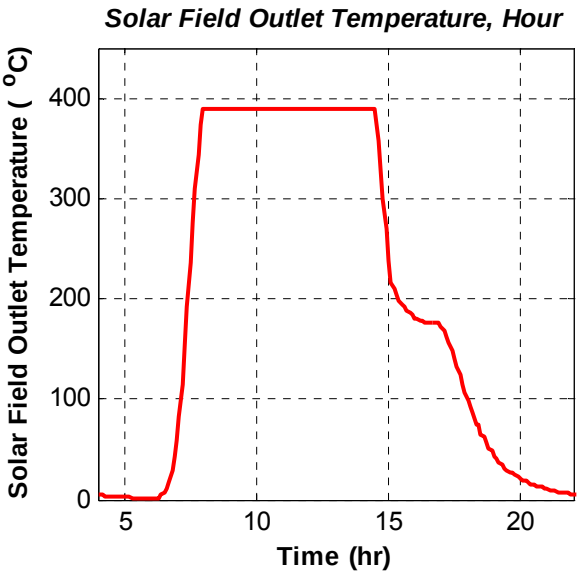
Solar Field Outlet Temperature, Hour
Solar Field Outlet Temperature (°C)
Time (hr)
0
100
200
300
400
5
10
15
20

B.8 October 15

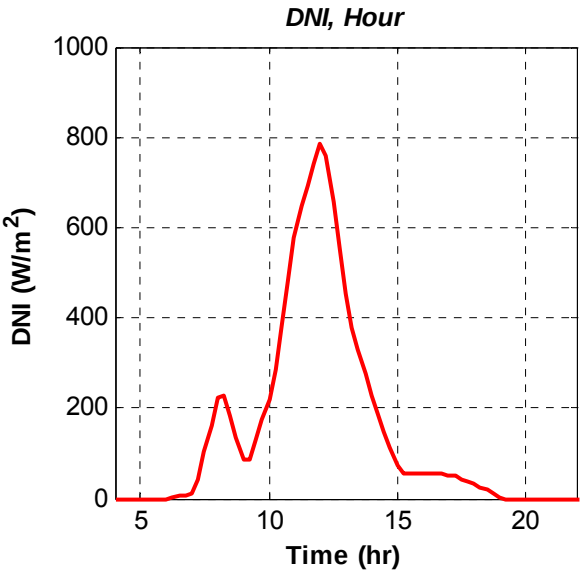

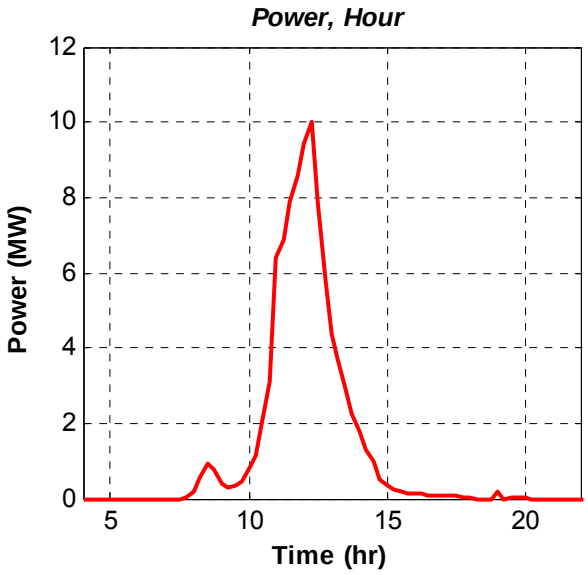

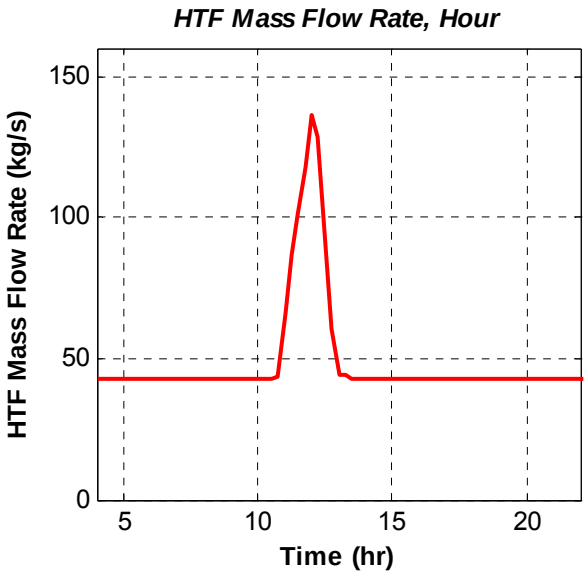

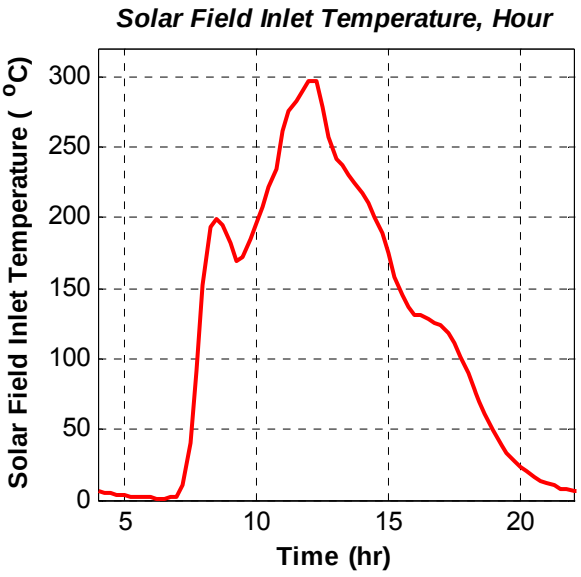

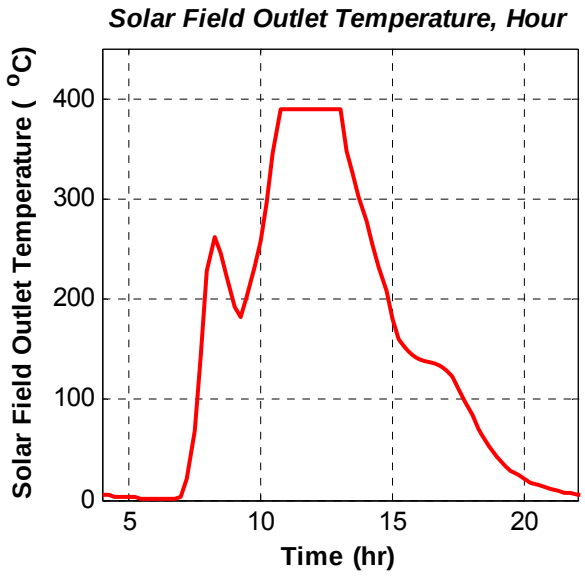
Solar Field Outlet Temperature, Hour
Solar Field Outlet Temperature (°C)
0
100
200
300
400
5
10
15
20
Time (hr)

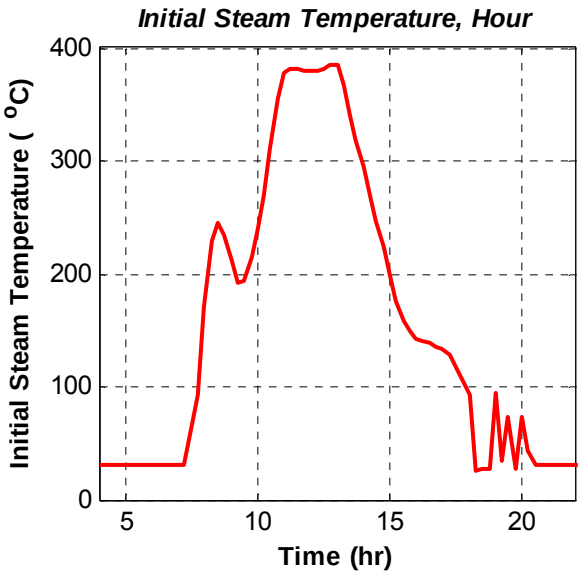
Initial Steam Temperature, Hour
Initial Steam Temperature (°C)
0
100
200
300
400
5
10
15
20
Time (hr)

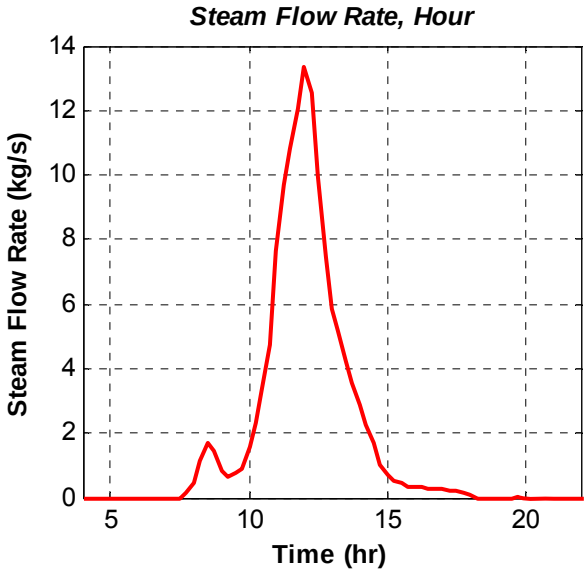
Steam Flow Rate, Hour
Steam Flow Rate (kg/s)
0
2
4
6
8
10
12
14
5
10
15
20
Time (hr)

B.9 November 15

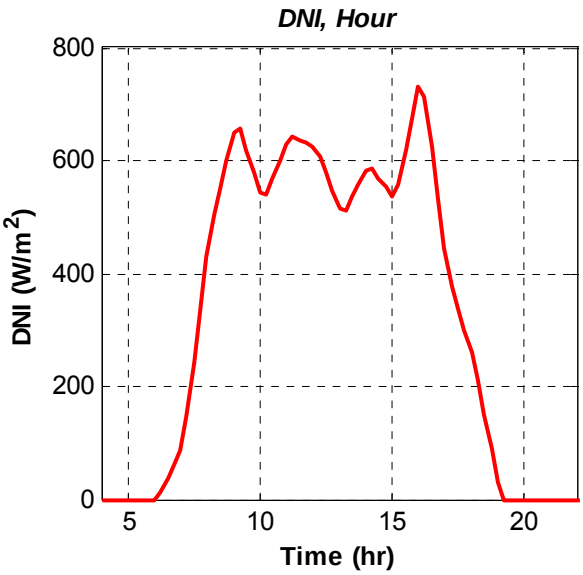

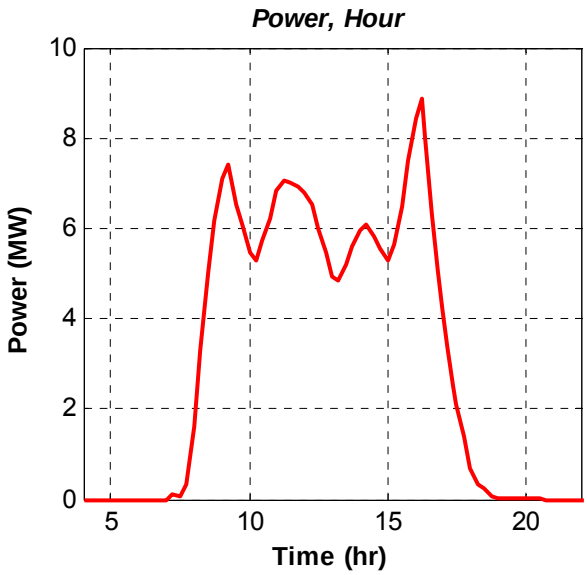

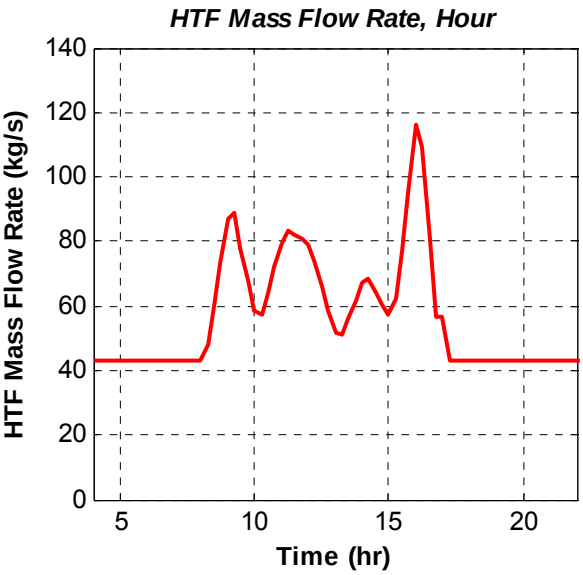

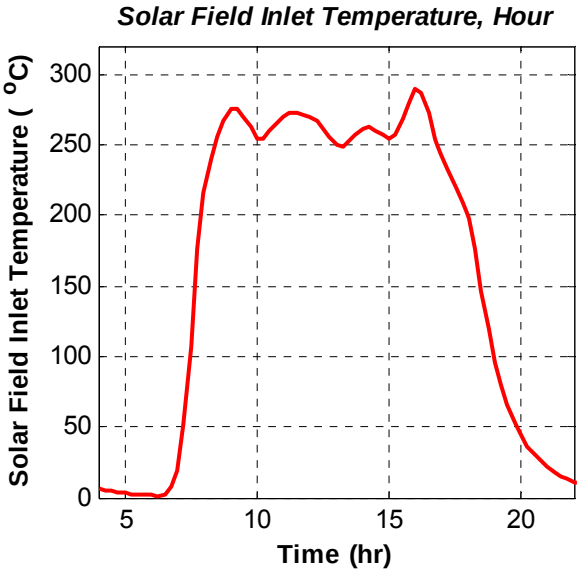

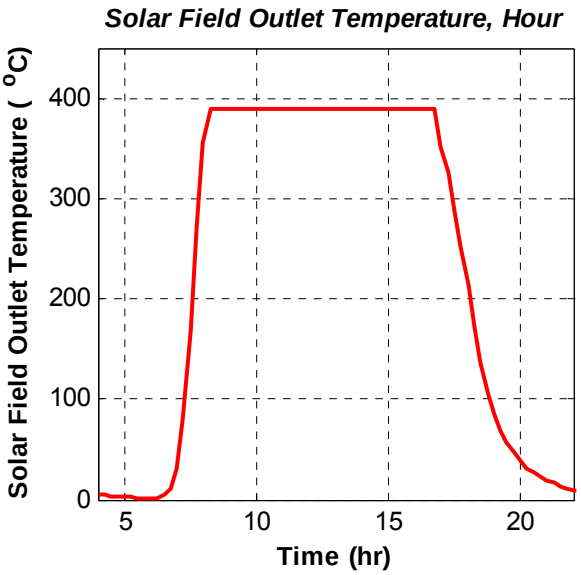
Solar Field Outlet Temperature, Hour
Solar Field Outlet Temperature (°C)
400
300
200
100
0
5
10
15
20
Time (hr)

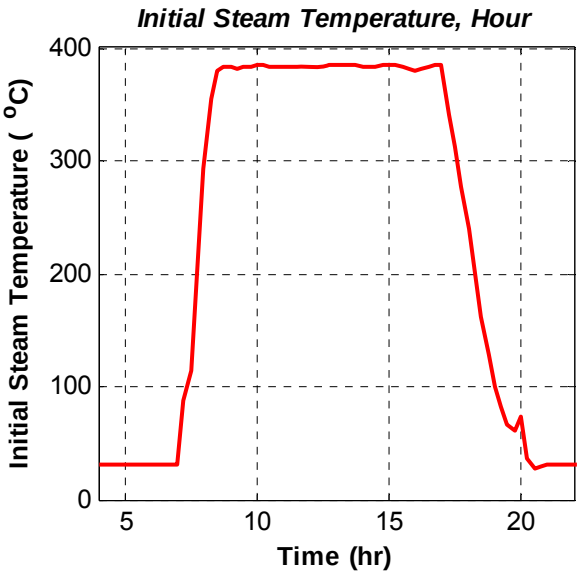
Initial Steam Temperature, Hour
Initial Steam Temperature (°C)
400
300
200
100
0
5
10
15
20
Time (hr)

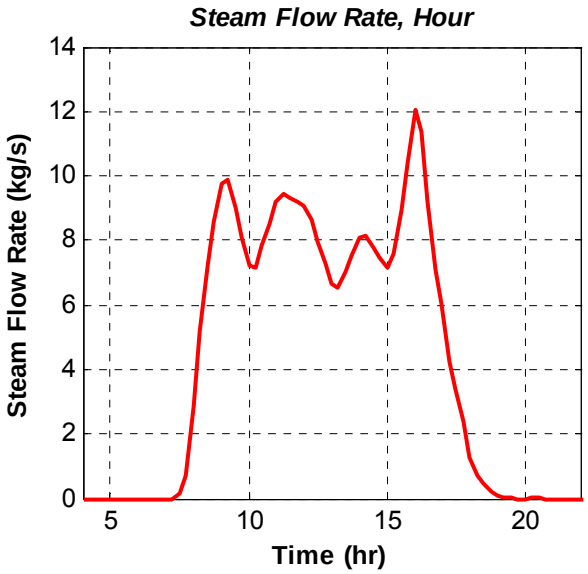
Steam Flow Rate, Hour
Steam Flow Rate (kg/s)
14
12
10
8
6
4
2
0
5
10
15
20
Time (hr)

B.10 December 10

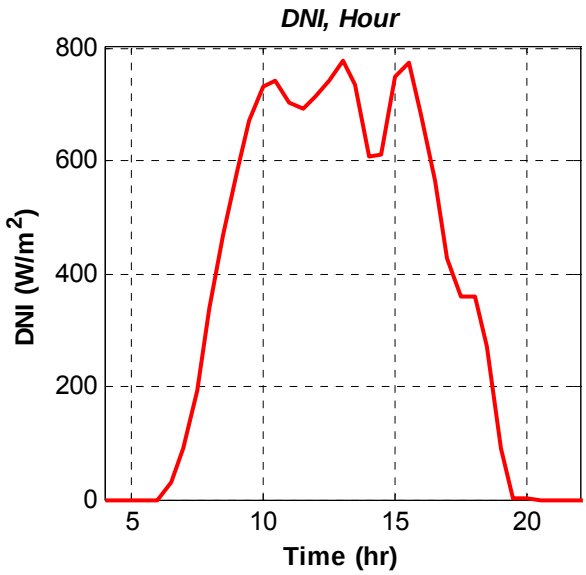

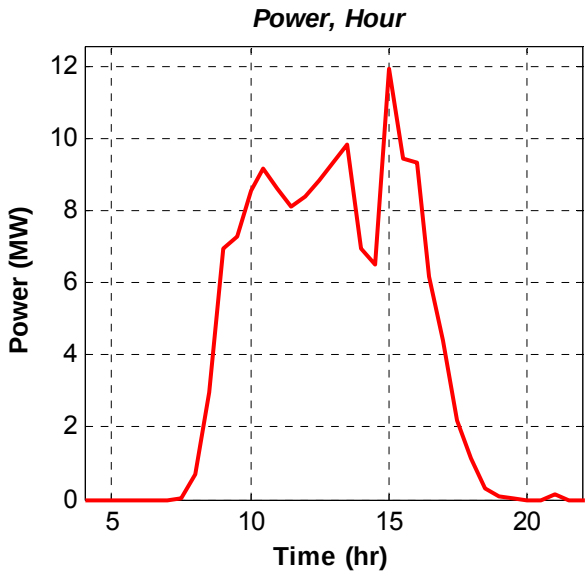

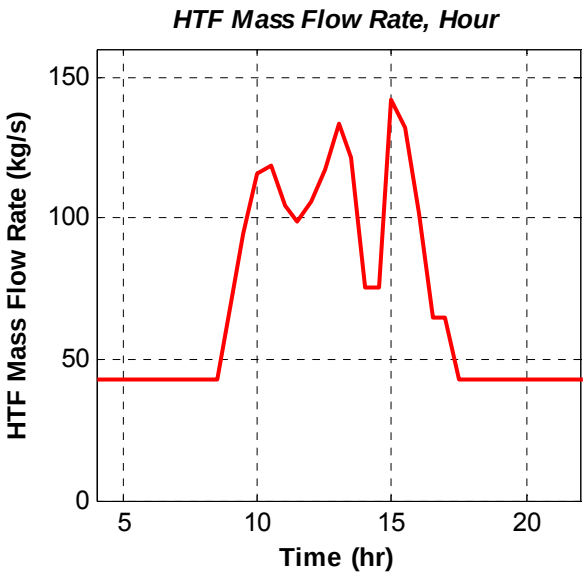

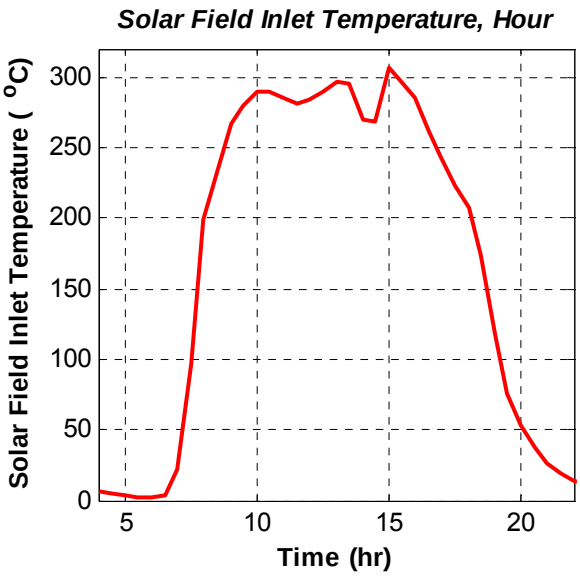

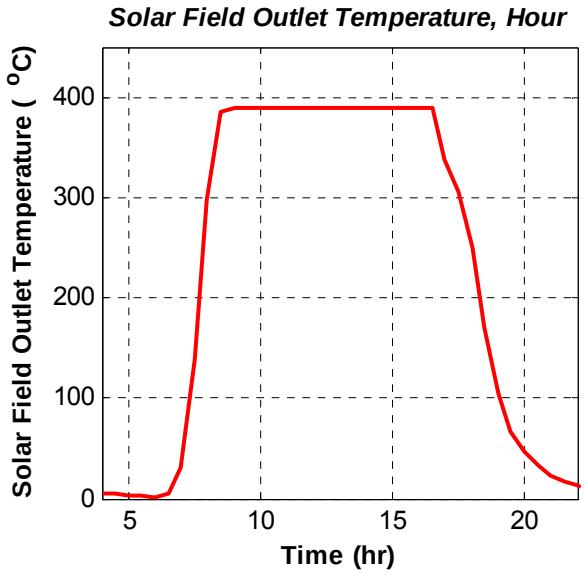
Solar Field Outlet Temperature, Hour
Solar Field Outlet Temperature (°C)
0
100
200
300
400
5
10
15
20
Time (hr)

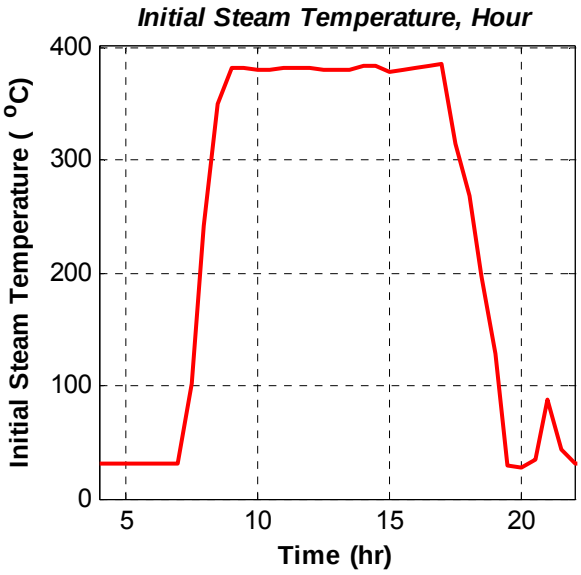
Initial Steam Temperature, Hour
Initial Steam Temperature (°C)
0
100
200
300
400
5
10
15
20
Time (hr)

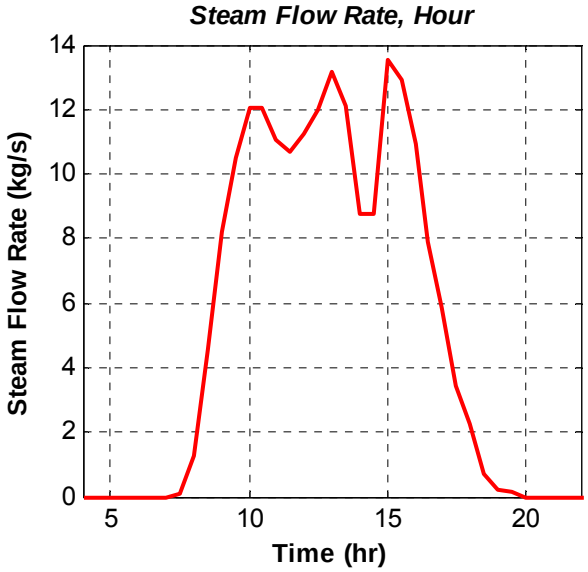
Steam Flow Rate, Hour
Steam Flow Rate (kg/s)
0
2
4
6
8
10
12
14
5
10
15
20
Time (hr)

REFERENCES

[1] Bejan, A. *Convection Heat Transfer.* 2nd edition, New York: NY, John Wiley & Sons, 1995

[2] Bialobrzeski, Robert W. *Optimization of a SEGS Solar Field for Cost Effective Power Output.* Georgia Institute of Technology: Master's Thesis, August, 2007.

[3] Çengel, Yunus A., and Boles, Michel A. *Thermodynamics an Engineering Approach.* 5th Edition, 2005.

[4] Dudley etal. *Test Results: SEGS LS-2 Solar Collector*. Sandia National Laboratories: SAND94-1884, December, 1994.

[5] Duffie, John A., and Beckman, William A. *Solar Engineering of Thermal Processes*. 2nd edition, New York: John Wiley and Sons, Inc., 1991.

[6] EEPCO (Website). *EEPCo in Brief.* Available at: http://www.eepco.gov.et. Last accessed: June 12, 2009.

[7] El-Wakil, M. M. *Power plant Technology*. New York: McGraw-Hill, Inc., 1984.

[8] *Engineering Equation Solver (EES)*. Middleton, WI: F-Chart Software, 2005, Available at http://www.fchart.com.

[9] *Energy Plus Weather (EPW)*. Available at: http://www.eere.energy.gov/buildings/energyplus/cfm/weather_data.cfm, Last accessed: June 25, 2009.

[10] Forristall, Russell. *Heat Transfer Analysis and Modeling of a Parabolic Trough Solar Receiver Implemented in Engineering Equation Solver*. National Renewable Energy Laboratory: NREL/TP-550-34169, October, 2003.

[11] *Therminol Information Bulletin No. 4*. Available at*:* twt.mpei.ac.ru/TTHB/HEDH/HTF-VP1.PDF, Last accessed: July 10, 2009.

[12] Incropera, Frank P., and DeWitt, David P. *Fundamentals of Heat and Mass Transfer.* 5th edition, New York: John Wiley and Sons, Inc., 2002.

[13] Jones, Scott A., Pitz-Paal, R., Schwarzboezl, P., Blair, N., and Cable, R. *TRNSYS Modeling of the SEGS VI Parabolic Trough Solar Electric Generating System***.** Washington D.C: Proceedings of Solar Forum 2001, April, 2001.

[14] Kau-Fui, Vincent Wong. *Thermodynamics for Engineers*. CRC press, 2000.

[15] Kehlhofer, Rolf. *Combined-Cycle Gas and Steam Turbine Power Plants*. PennWell Publishing Company, 1997.

[16] Lippke, Frank. *Simulation of the Part Load Behavior of a 30MWe SEGS Plant*. Prepared for Sandia National Laboratories, Albuquerque, NM, SAND95-1293, June 1995.

[17] Moran, Michael J, and Shapiro, Howard N. *Fundamentals of Engineering Thermodynamics*. 4th Edition, John Wiley and Sons, 2002.

[18] *Power from the Sun*. Available at: http://www.powerfromthesun.net/book.htm. Last accessed: March 25, 2009.

[19] *Sam User Guide*, SAM Software, Available at: https://www.nrel.gov/analysis/sam.

[20] Schwarzbözl, Peter and Zentrum, Deutsches. *A TRNSYS Model Library for Solar Thermal Electric Components (STEC)*. A Reference Manual, Release 3.0,2006.

[21] *Solar Field Image*. Available at: http://www.trec-uk.org.uk.

[22] Stuetzle, Thorsten A. *Automatic Control of the 30MWe SEGS VI Parabolic Trough Plant, Master's Thesis*. Department of Mechanical Engineering, University of Wisconsin – Madison. 2002.

[23] *TRNSYS – A Transient System Simulation Program*. Madison, WI: University of Wisconsin-Madison Solar Energy Laboratory. Available at: http://sel.me.wisc.edu/trnsys/

[24] U.S. Department of Energy and Electric Power Research Institute. *Renewable Energy Technology Characterizations***.** EPRI TR-109496, December, 1997.

[25] *Weather Data*. Available at: http://swera.unep.net. Last accessed: November 15, 2008.

[26] Wikipedia (Website). *SEGS*. Available at: http://en-wikipedia.org/wiki/SEGS. Last accessed: June 5, 2009**.**